BRNO UNIVERSITY OF TECHNOLOGY
VYSOKÉ UČENÍ TECHNICKÉ V BRNĚ

FACULTY OF CHEMISTRY
FAKULTA CHEMICKÁ

INSTITUTE OF MATERIALS SCIENCE
ÚSTAV CHEMIE MATERIÁLŮ

EFFECT OF BIOCERAMIC ADDITIVES ON MORPHOLOGY, PHYSICAL AND BIOLOGICAL PROPERTIES OF COLLAGEN SCAFFOLDS FOR BONE TISSUE ENGINEERING

VLIV BIOKERAMICKÝCH ADITIV NA MORFOLOGII, FYZIKÁLNÍ A BIOLOGICKÉ VLASTNOSTI KOLAGENOVÝCH NOSIČŮ PRO TKÁŇOVÉ INŽENÝRSTVÍ KOSTÍ

MASTER'S THESIS
DIPLOMOVÁ PRÁCE

AUTHOR — **Bc. Nikola Klieštiková**
AUTOR PRÁCE

SUPERVISOR — **Ing. Jana Brtníková, Ph.D.**
VEDOUCÍ PRÁCE

BRNO 2018

VYSOKÉ UČENÍ TECHNICKÉ V BRNĚ
FAKULTA CHEMICKÁ

Zadání diplomové práce

Číslo práce:	FCH-DIP1177/2017
Ústav:	Ústav chemie materiálů
Studentka:	**Bc. Nikola Klieštiková**
Studijní program:	Chemie, technologie a vlastnosti materiálů
Studijní obor:	Chemie, technologie a vlastnosti materiálů
Vedoucí práce:	**Ing. Jana Brtníková, Ph.D.**
Akademický rok:	2017/18

Název diplomové práce:

Vliv biokeramických aditiv na morfologii, fyzikální a biologické vlastnosti kolagenových nosičů pro tkáňové inženýrství kostí

Zadání diplomové práce:

1. Lit. rešerše – kolagenové nosiče a jeho modifikace biokeramikou
2. Příprava kolagen/biokeramických pěn, síťování
3. Testování různých kolagenových vzorků z hlediska morfologie, fyzikálních a biologických vlastností
4. Vyhodnocení, závěr

Termín odevzdání diplomové práce: 7.5.2018

Diplomová práce se odevzdává v děkanem stanoveném počtu exemplářů na sekretariát ústavu. Toto zadání je součástí diplomové práce.

Bc. Nikola Klieštiková student(ka)	Ing. Jana Brtníková, Ph.D. vedoucí práce	prof. RNDr. Josef Jančář, CSc. vedoucí ústavu

V Brně dne 31.1.2018

prof. Ing. Martin Weiter, Ph.D.
děkan

ABSTRACT

The diploma thesis deals with preparation of three-dimensional porous collagen composite scaffolds for bone tissue engineering and study of the effect of addition of bioceramic particles on morphological, biomechanical and biological properties. Theoretical part describes biomaterials and bioceramic particles used for scaffolds in bone tissue engineering and their fabrications method. As for experimental part, samples were prepared by the freeze-drying method. As tested material, type I collagen from porcine and bovine sources was combined with hydroxyapatite and mixture of β-tricalcium phosphate and α-tricalcium phosphate in ratios 1 : 1, 1 : 2 and 2 : 1. The effect of bioceramics solubility and particle sizes on scaffolds morphology, biomechanics and biocompatibility was evaluated. Addition of bioceramic particles changed the morphology of the samples. The pore size decreased, whereas the porosity was nearly the same in all tested samples. Bioceramic particles also made the collagen matrix of the scaffolds less hydrophilic, moreover they stabilized the scaffolds against the effect of enzymatic degradation. The biomechanical properties of the samples were tested in both dry and hydrated state. In dry state, the pure bovine collagen scaffolds reached the highest compressive strength, contrary in hydrated state, the samples containing bioceramic particles reached the highest value. None of the samples was cytotoxic and the most preferable environment for cell adhesion and proliferation was in the pure bovine collagen scaffolds and also in the composite scaffolds with ratio HAp : β-TCP : 1 : 1.

KEY WORDS

Tissue engineering, scaffold, collagen, hydroxyapatite, β-tricalcium phosphate, α-tricalcium phosphate, composite.

ABSTRAKT

Diplomová práce se zabývá přípravou trojrozměrných porézních kolagenových kompozitních nosičů pro tkáňové inženýrství kostí a studiem vlivu přídavku biokeramických částic na morfologické, biomechanické a biologické vlastnosti. Teoretická část popisuje biomateriály a biokeramické částice používané pro nosiče v tkáňové inženýrství kostí a jejich metody výroby. Pokud jde o experimentální část, byly vzorky připraveny metodou lyofilizace. Testovaným materiálem byl kolagen typu I z prasečího a hovězího zdroje, který byl kombinován s hydroxyapatitem a směsí β-fosforečnanu vápenatého s α-fosforečnanem vápenatým v poměrech 1 : 1, 1 : 2 a 2 : 1. Byl hodnocen vliv rozpustnosti a velikosti částic na morfologii, mechaniku a biokompatibilitu nosičů. Přidání biokeramických částic změnilo morfologii vzorků. Velikost pórů se snížila, zatímco pórovitost byla ve všech testovaných vzorcích téměř stejná. Biokeramické částice také způsobily, že kolagenová matrice nosičů byla méně hydrofilní, a navíc dokázaly stabilizovat nosiče proti působení enzymatické degradace. Biomechanické vlastnosti vzorků byly testovány v suchém i mokrém stavu. V suchém stavu dosáhl nejvyšší pevnosti v tlaku čistý bovinní kolagenový nosič, naopak v hydratovaném stavu, dosáhly nejvyšší hodnoty vzorky obsahující biokeramické částice. Žádný ze vzorků nebyl cytotoxický a nejvhodnější prostředí pro buněčnou adhezi a proliferaci bylo v čistém bovinním kolagenovém nosiči a také v kolagenovém kompozitním nosiči s poměrem HAp : β-TCP : 1 : 1.

KLÍČOVÁ SLOVA

Tkáňové inženýrství, skafold, kolagen, hydroxyapatit, β-fosforečnan vápenatý, α-fosforečnan vápenatý, kompozit.

KLIEŠTIKOVÁ, N. *Effect of bioceramic additives on morphology, physical and biological properties of collagen scaffolds for bone tissue engineering.* Brno: Brno University of Technology, Faculty of Chemistry, 2018. 86 s. Supervisor of diploma thesis Ing. Jana Brtníková, Ph.D..

DECLARATION

I declare that I have elaborated my diploma thesis independently and that the used references are correctly and completely quoted. The content of the thesis is considered as a property of the Faculty of Chemistry, Brno University of Technology and can only be used for commercial purposes with the consent of the supervisor of the diploma thesis and the dean of the Faculty of Chemistry, Brno University of Technology.

……...
author's signature

PROHLÁŠENÍ

Prohlašuji, že jsem diplomovou práci vypracovala samostatně a že všechny použité literární zdroje jsem správně a úplně citovala. Diplomová práce je z hlediska obsahu majetkem Fakulty chemické VUT v Brně a může být využita ke komerčním účelům jen se souhlasem vedoucího diplomové práce a děkana Fakulty chemické VUT v Brně.

……...
podpis diplomanta

Acknowledgements:

I would like to thank my supervisor Ing. Jana Brtníková, Ph.D. for helpful discussions, interest, thesis corrections and also SEM images, Doc. Ing. Lucy Vojtová, Ph.D. for helpful discussions and willingness, Ing. Petr Poláček, Ph.D. for patient help in testing mechanical properties, Mgr. Veronika Pavliňáková, Ph. D. for valuable advices on scaffolds preparation, Ing. Lenka Michlovská, Ph. D. for ATR-FTIR analysis, Institute of Experimental Medicine in Prague for testing biological properties and all colleagues involved in this work. This work was supported by the CEITEC 2020 (LQ1601) with financial support from the Ministry of Education, Youth and Sports of the Czech Republic under the National Sustainability Programme II.

CONTENT

1 INTRODUCTION

Currently, the whole world is experiencing an exceedingly high demand for functional bone grafts especially in populations where aging is coupled with increased obesity and poor physical activity. Unfortunately, reconstructive surgery (mostly due to trauma or tumour removal) is still limited by lack of the autologous material and donor site morbidity. Thus, materials that enhance bone regeneration get a very high potential in clinical applications. The use of porous material scaffolds from polymer and bioceramic components to support bone cells and tissue growth is longstanding area of interest.

Bone tissue engineering is based on the understanding of bone structure, bone mechanics, and tissue formation as it aims to induce new functional bone tissues. Thus, to successfully regenerate or repair bone, knowledge of the bone biology and its development is crucial. Challenges of bone tissue engineering include engineering of the materials that can match both the mechanical and biological properties of the real bone tissue matrix and support the vascularization of large bone tissue architectures. The goal is to mimic as much as possible the three-dimensional and a highly complex extracellular environment of the bone tissue which provides optimal conditions for cell adhesion, proliferation and finally differentiation. Engineering functional bone tissues using combinations of cells, collagen-based scaffolds with bioceramic components and signalling molecules are a promising approach and these techniques could lead to unbounded possibilities for tissue regeneration and repair.

The aim of the thesis is to get an overview of biomaterials and bioceramic particles used for scaffold in bone tissue engineering and their fabrications method in the form of a literary research. Then to follow up previous studies dealing with collagen-based scaffolds containing individual bioceramic particles and prepare pure collagen scaffolds and collagen composite scaffolds containing mixtures of bioceramic particles differing in particle size and solubility in water. Finally, to observe the effect of mixtures of bioceramic particles on morphological, biomechanical and biological properties of collagen-based scaffolds.

2 CURRENT STATE OF THE ART

2.1 Tissue Engineering

Tissue engineering (TE) is a rapidly advancing interdisciplinary field that combines the principles of life sciences, materials sciences, and engineering to construct tissue engineered grafts, which are transplanted to the body as replacements for the missing or severely damaged tissues and organs [1; 2]. TE holds promises of eliminating re-operations by using biodegradable substitutes, solving problems of immune rejections of implants and shortage of organ donations, initiating and supporting natural regeneration process, offering potential treatments for currently untreatable medical conditions [3].

Generally, strategies of TE (several TE strategies are schematically presented in Fig. 1) combines living cells with a natural/artificial support (carrier) or scaffold to develop three-dimensional (3D) living structure that is functional and structurally, mechanically is equivalent to the tissue to be replaced [4]. Effective mimicking of a tissue is highly complex process including many aspects associated with different features of each single tissue. There are three major components that must be considered to develop a tissue:

1. Cells
2. Signalling molecules
3. Scaffolds

They are commonly referred as tissue engineering triad [5].

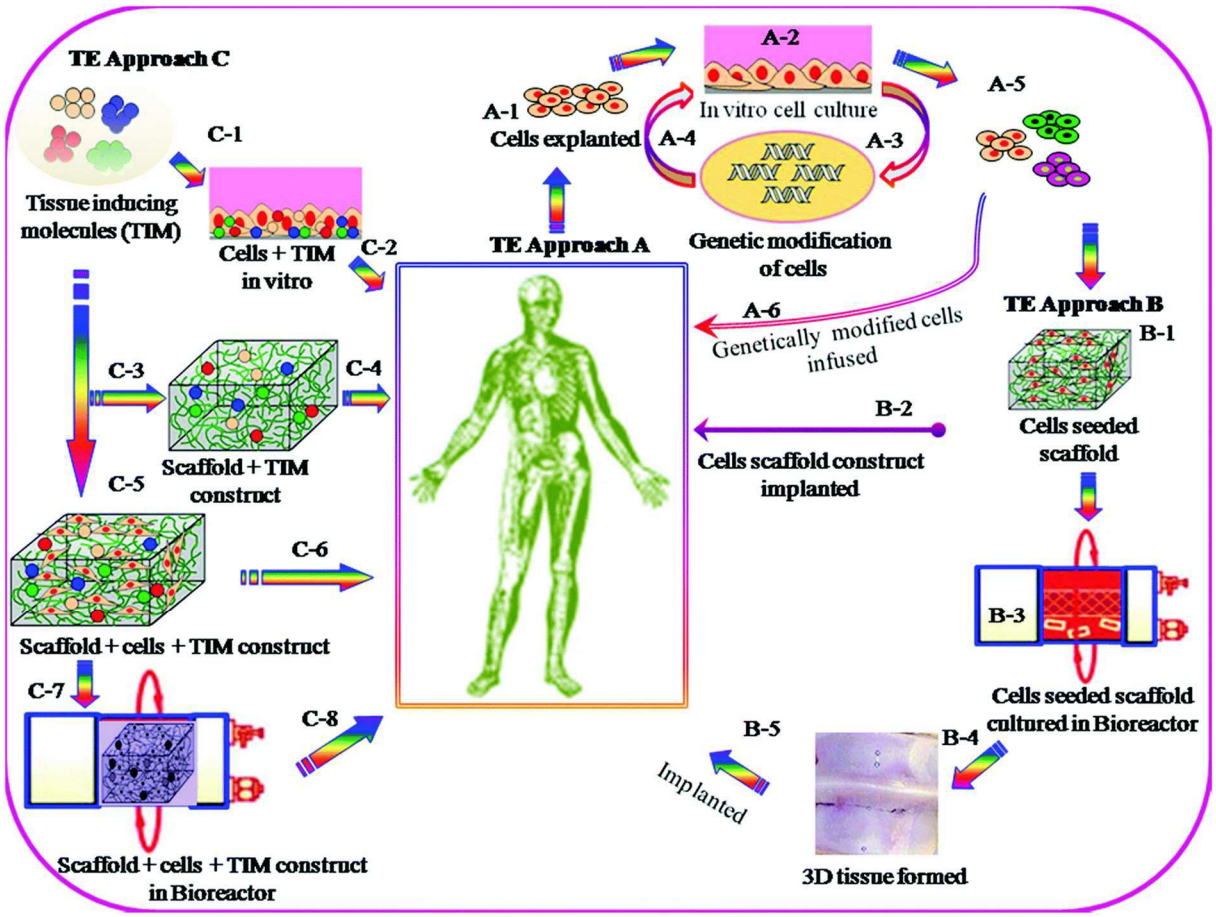

Fig. 1: Schematic representation showing different tissue engineering (TE) strategies. TE approach A: cells explanted from an individual (A-1), which can be cultivated in vitro (A-2) to differentiate, eventually modify them genetically (A-3 and A-4) and expand them (A-5) before to be reinfused, preferentially, in the same individual (A-6). TE approach B: explanted cells could be engineered before re-exposing them to all the signals (e.g., mechanical and molecular) of the human body. Cells encapsulated or seeded onto the hydrogel/scaffold (B-1) and implanted in the body (B-2) to act as an artificial organ, or cells seeded/encapsulated in scaffolds assembled in a bioreactor (B-3) to form 3D tissue (B-4) serving as an external artificial organ (i.e. artificial liver), and then implanted (B-5). TE approach C: using tissue-inducing substances that can be added in all types of in vitro cultivations (C-1) before to reinfusion to exposed cells in the body (C-2). TIM can be added to the scaffold prior to implantation (C-3 and C-4). The use of TIM in vitro and on cells that are growing onto a scaffold (C-5 and C-6) that will be implanted after a certain time, or that the whole construct can be cultured in a bioreactor to generate an artificial organ prior to implantation (C-7 and C-8). [6]

2.1.1 Cells

Cells for tissue engineering that can be obtained from the same individual to whom they will be re-implanted, are called autologous cells. Allogenic cells are isolated from body from the same species, but they are not immunologically identical. Xenogenic cells are obtained from donors of different species. For instance, animal cells like bovine, equine, and porcine tissues have been used extensively for cardiovascular implants [7]. Transplantation of autologous cells is optimal because of minimal immune complications like pathogen transmission and immune rejection. That makes them an ideal source for use in tissue engineering [8]. Nevertheless, in some cases, this type of cells might be unavailable like genetic diseases. Also, very ill patient,

severely burnt patient and even an elderly person may lack affordable quantities of cells to establish useful cell lines [7].

The cell types used in tissue engineering range from differentiated adult cells to undifferentiated progenitor cells and stem cells. Stem cells are undifferentiated, and they are found among differentiated cells in tissues or organs. They have ability to self-renewal and cell potency. Generally, there are three types of stem cells: embryonic stem cells (EMS), induce pluripotent cells (iPS) and adult stem cells [7].

EMS can be isolated from the inner cell mass of pre-implantation embryos during the blastocyst stage. They can differentiate into practically all specialized cell types and thus they are considered pluripotent [9]. They also can proliferate in an undifferentiated state, so they have the ability to self-renew. Nevertheless, its use has been limited due to ethical concerns regarding use of human embryonic stem cells, the potential tumorogenicity and immunological incompatibilities. iPS cells are the result of the transformation of an adult, somatic cell through reprogramming into a pluripotent stem cell. Although they are considered as pluripotent, these cells are not identical to EMS cells, but they are similar. That is caused by the way of reprogramming. Like EMS, iPS cells can cause tumours [10]. Adult stem cells are multipotent stem cells found in specific niches or tissue compartments [9]. They are available in various sources like trabecular bone, muscle, blood, bone marrow, liver, skin, cornea, and retina of the eye, dental pulp. Recently some evidence proves that adult stem cells have greater plasticity than was thought before [11].

According the plasticity or development versatility of stem cell, they can be classified into three groups: totipotent cells, pluripotent cells and multipotent cells. Totipotent stem cells are early embryonic cells of 1–3 days from oocyte fertilization. It has the potential to form all cell types in a body, also extra embryonic or placental cells. An entire functional organism is possible to create by this type of cell. Pluripotent stem cells can differentiate into any of the three germ layers: endoderm, mesoderm, and ectoderm but like totipotent stem cells cannot create entire organism. Multipotent stem cells are specialized further from the pluripotent stem cell division. Multipotent stem cells can differentiate into multiple cell types, but usually specific to one germ layer [7].

2.1.2 Signals

Signalling molecules provide stimuli for cell adhesion, growth, differentiation, vascularization and other functions. There are several kinds of signalling molecules used such as growth factors, cytokines, hormones, small molecules like neurotransmitters, proteins, morphogenes, mRNA etc. [12]. Among these signalling molecules, multifunctional proteins like growth factors and cytokines have studied more for tissue engineering application [13; 14].

Growth factors (GFs) are signalling diffusible proteins made by body itself that regulate many aspects of cellular functions. GFs play a crucial role in information transfer between different cell populations and their microenvironment, the extracellular matrix (ECM), and throughout the processes of wound healing, morphogenesis, and tissue regeneration [15]. As members of a large group of polypeptide regulatory molecules, GFs are normally released by healthy cell lines in the body whose primary role is to direct the maturation of cells during normal turnover and in the post-injury tissue repair response. In the latter case, these cells provide key instructions for tissue formation and repair because they are involved in cell

infiltration, cell proliferation, and matrix synthesis, deposition and organisation, which lead to angiogenesis and finally scar/tissue formation [16].

However, there are still several concerns that GFs may have even negative effects, especially for using high levels of doses. Exposure of the myocardium to high local levels of GFs can cause hemangioma-like tumours, vascular malformations, and neointimal development [17].

Cytokines are small secreted proteins released by cells that have a specific effect on the interactions and communications between cells. They are often produced in a cascade, as one cytokine stimulates its target cells to make additional cytokines. Cytokines can also act synergistically or antagonistically. Cytokines are made by many cell populations, but the predominant producers are helper T-lymphocytes and macrophages [18]. Cytokines (BMP2, TGFβ and WNT ligands) play an important role in osteogenic differentiation of mesenchymal stem cells and bone remodelling. Ideally, cytokines can be released by programmed way into the micro-environments of the bone graft and then direct desired bone remodelling [13; 19].

2.1.3 Scaffolds

Scaffolds play a significant role in tissue engineering. They are explained as 3D porous solid biomaterials that mimic natural environment for cell behaviour such as migration, proliferation, differentiation, and ECM deposition [4]. Scaffolds are generally considered as essential elements of tissue engineering; therefore, they should have these key properties:

- Have interconnected pores with a proper pore size in order to provide tissue integration and vascularization [20; 21].
- Be biocompatible to avoid unwanted tissue responses to the implant [22].
- Be biodegradable with proper degradation rate to match with the rate of formation of new tissue [23].
- Have good mechanical properties to supply suitable environment for cells, distribute inductive materials or cells to the renovate location and offer cues to manage the composition and function of recently created tissue [21; 24].
- Have appropriate surface chemistry to allow cellular attachment, differentiation and proliferation [25; 26].
- Simulate the composition and biological role of the extracellular matrix [27].

Macrostructure of the scaffold reflects the external geometry of the issue. A 3D scaffold that mimic the external geometry of the tissue is more desired for scaffold placement and fixation in clinical applications. A direct contact between defect line of tissues and the scaffold enhance the interaction between fabricated construct and the host site [20; 21].

Scaffolds can be constituted of bulk materials or they have a pore or tube geometry. Pores or tubes can be introduced in scaffolds as isolated formations or they can be interconnected. Huge advantage of interconnected porous or tubular system is the improved nutritional supply in deeper areas, thereby cells can survive in these regions. A high interconnectivity of pores or tubes facilitates hydrodynamic microenvironment, but at the same time reduces mechanical strength [28; 29].

Tissue regeneration in vivo may be achieved by using scaffolds with optimal hollow structures (tube/pore combinations). The size of these pore structures not only improves the fluid flow through the scaffold but may also allow vascular ingrowth. Bone formation critically depends on vascularization. Indicated pore size is ranging from 200 μm to 500 μm for vascular

ingrowth [30]. The influence of pore size distribution in bone tissue scaffold on biological interactions is noted in Table 1.

Table 1: Pore size distribution for an ideal scaffold in bone tissue engineering application [30].

Pore size (µm)	**Biological relevance**
< 1	Protein interaction and adsorption
1–20	Initial cell attachment and directed cell growth
20–100	Cell proliferation, migration
100–1000	Cell growth and collateral bone growth
> 1000	Important for maintaining and programming the shape and functionality of implant

High ratio surface/volume is highly advantageous for cell attachment and migration in porous scaffold. Since pore diameter and internal surface area are related linearly, mechanical stability decreases with increasing surface area. Scaffold should ideally have sufficient mechanical strength during in vitro culturing as well as the mechanical endurance while is regenerating in physiological environment [20; 31].

The ideal rate of scaffold degradation must be adjusted to be parallel the rate of new tissue formation. At the same time retains sufficient structural integrity until the newly grown tissue replaced the scaffold [32]. Moreover, during degradation of the scaffold should not be changing the physiological pH or releasing of toxic degradation products.

A scaffold should ideally be used as carrier for proteins which can easily bound to scaffold material. They should be biologically active and should be released as it is predetermined [31].

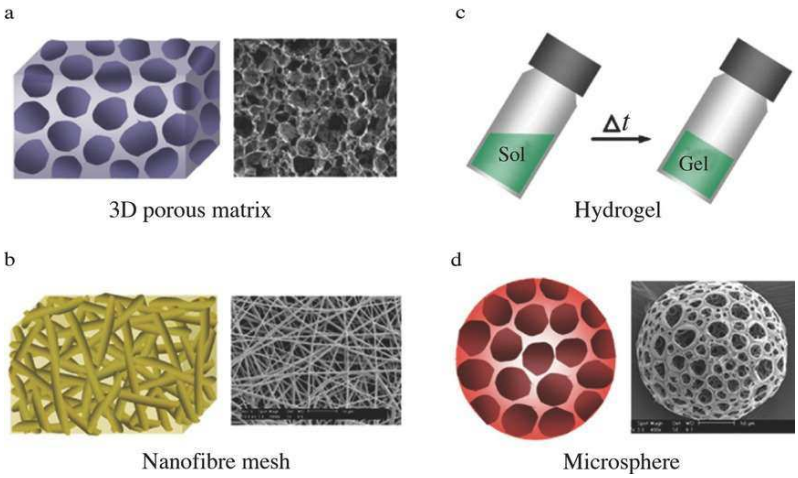

Fig. 2: Representative cartoons and images of four different forms of polymeric scaffold used in tissue engineering [33].

There are four different forms of polymeric scaffold used in tissue engineering (Fig. 2):

1. A typical 3D highly porous matrix that allows high cell seeding density and tissue ingrowth.
2. A microfibrous or nanofibrous matrix that provides better resemblance of physiological ECM.
3. A Thermosensitive sol-gel transition hydrogel.
4. A porous microsphere.

Of the polymeric scaffolds listed above, a typical 3D porous matrix and nanofibrous matrix are surgical implantable forms and a thermosensitive sol-gel transition hydrogel and porous microsphere are the injectable forms [34].

2.1.4 Extracellular Matrix

The extracellular matrix (ECM) is non-cellular 3D macromolecular network present within all tissues and organs. The ECM consists of a large variety of matrix macromolecules whose precise composition and specific structures vary from tissue to tissue. The major components of ECM (Fig. 3) are fibrous forming protein (collagen and elastin), cell binding glycoproteins (fibronectin and laminin), proteoglycans and glycosaminoglycans [35; 36].

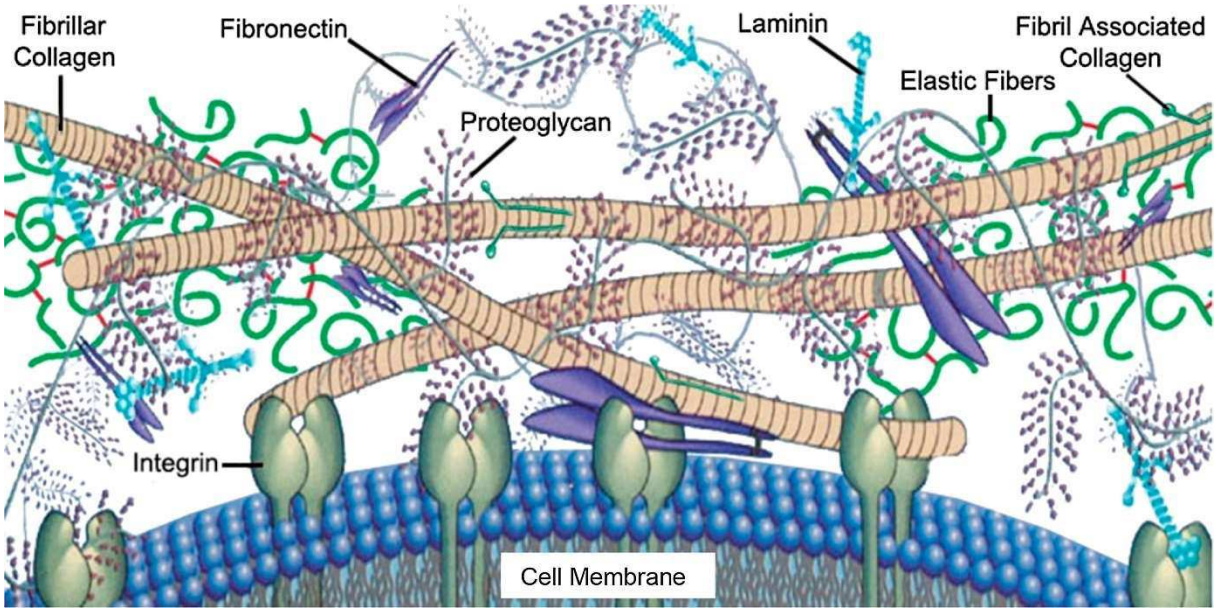

Fig. 3: Representative cartoon of ECM composition [37].

The ECM generates the essential scaffold for the cellular constituents. The ECM determines biochemical and mechanical properties of each organ, such as its tensile and compressive strength and elasticity, and also provides protection by maintaining extracellular homeostasis and water retention. Moreover, the ECM directs morphological organization and physiological functions by binding growth factors and interacting with cell-surface receptors to initiate signal transductions and regulate gene transcription [35].

Components of the ECM can be produced intracellularly by all cells and secreted into the ECM via exocytosis. However certain cells produce a specific type of ECM: fibroblasts secrete connective tissue ECM, osteoblasts secrete bone-forming ECM, chondroblasts secrete cartilage-forming ECM, fibroblasts and epithelial cells together make basement membrane [38].

Collagen is the most abundant fibrous protein in the interstitial ECM and constitutes the main structural element which provides tensile strength, regulates cell adhesion, supports chemotaxis and migration of cells and directs tissue development. Collagen is synthesized and secreted in the ECM mainly by fibroblasts [39]. Depending on the amount of tension on the matrix fibroblasts can organize collagen fibrils into sheets or cables which significantly influences the alignment of collagen fibres [35].

Elastic fibres are very complex ECM structure that provides recoil to tissues which undergo repeating stretching forces, such as large elastic blood vessels, lungs, heart, skin, bladder and elastic cartilage. Elastic fibres are composed of two discrete components, elastin being the major constituent and microfibrils. Tropoelastins, the monomeric precursors of elastin with unique composition and tendency to self-associate, are secreted and cross-linked one to another via their lysine-containing domains by members of the lysyl oxidase enzyme family [40; 41]. Polymer also contains the hydrophobic domains that are responsible for the elastic properties of the network. However, elastin stretch is crucially limited by tight association with collagen fibrils [40]. Microfibrils are composed of number of different glycoproteins including the large fibrillin which is situated in the periphery of the fibre [42]. It is suggested that microfibrils provide a scaffold that helps the alignment and cross-linking of the elastin molecules [43].

Fibronectin is critical for attachment and migration of cells, functioning as "biological glue". It is a large glycoprotein that can be found in all vertebrates. Fibronectin is secreted as dimer which is composed of two very large subunits joined by disulphide bonds at one end. Each subunit is folded into a series of functionally different domains that are intermitted by flexible polypeptide chain [44]. Unlike fibrillar collagen, fibronectin cannot self-assemble into fibrils because additional proteins, especially integrins, are needed for fibril formation. Fibronectin matrix is mainly produced at times of dynamic tissue remodelling, formation or repair, and is essential during embryonic development [45; 46].

Laminins are large heterotrimeric cross-shaped glycoproteins that are assembled along with collagen type IV, about 20 glycoproteins (nidogens, agrin, perlecan, etc.) and proteoglycan heparan sulphate in basement membranes. Each laminin heterotrimer consists of one α, one β, and one γ chain, each of which is encoded by individual genes. Many laminins self-assemble to form highly complex networks that remain in close association with cells through interactions with cell surface receptors. Laminins are essential for early embryonic development and organogenesis [35; 47].

Proteoglycans consists of core protein to which one or more glycosaminoglycan (GAG) side chains are covalently attached. GAGs are very long highly negatively charged heteropolysaccharides that contain repeating disaccharides composed mainly of N-acetylated hexosamines (N-acetyl-D-galactosamine or N-acetyl-D-glucosamine) and D-/L-hexuronic acid (D-glucuronic acid or L-iduronic acid). There are six types of glycosaminoglycans: the galactosaminoglycans chondroitin sulphate (CS) and dermatan sulphate (DS), and the glucosaminoglycans heparan sulphate (HS), heparin (Hep), keratan sulphate (KS), and hyaluronic acid (HA) [48]. HA is the only GAG which is biosynthesized at the cell membrane and not at the Golgi apparatus and which is not substituted with sulphate groups unlike the others. Large variability in structure of GAG chains provides proteoglycans extreme molecular diversity and huge structural basis for biological functions. Proteoglycans can be found in intracellular compartments as well as in the ECM. They interact with numerous growth factors, cytokines and chemokines, cell surface receptors and ECM molecules either via their core proteins or, mainly, through their GAG side chains participating for example in cell signalling, proliferation, migration, differentiation, apoptosis, and adhesion [35]. Thanks, their extreme hydrophilicity they are essential for hydrogel formation that enable matrices to bear high compression or to have lubrication functions [49].

2.2 Fabrication Techniques of Scaffolds

Most of the scaffolds were conventionally developed with an objective of drug delivery but later explored for 3D cell culture in the context of tissue engineering. Just like constituting materials, the methods and techniques for creating 3D scaffold are numerous though each one has its own limitations and rewards.

Based on the target architecture of ECM, scaffold properties such material strength, pore density, pore size, their distribution and connectivity need to be controlled. At the same time the technique of should not alter or change the biocompatibility and inherent cell-interactive characteristics of the biomaterial at any stage. The methods of fabrication of biocompatible 3D scaffolds with appropriate architectures can be divided into two classes: conventional and advanced [30].

2.2.1 Conventional Techniques

Conventional fabrication techniques are defined as processes that create scaffolds having a bulk or porous structure (interconnected or non-interconnected) which lacks any long-range channelling microstructure [50]. Most of the scaffolds were conventionally developed with an objective of drug delivery but later explored for 3D cell culture in the context of tissue engineering.

Conventional scaffold fabrication techniques include [51]:

- Fibre bonding
- Phase separation
- Solvent casting/particulate leaching
- Membrane lamination
- Melt molding
- Gas foaming/high pressure processing
- Hydrocarbon templating
- Freeze drying
- Combinations of these techniques

Despite the fact conventionally produced scaffolds are used to construct a great variety of tissues, most are limited by some flaws which restrict their applications in TE. Among the main limitations belong:

- Manual intervention: All conventional techniques are manual based processes that mostly require multi-stage processing to get appropriate scaffold. Dependence on user skills and experiences can result in inconsistent outcomes and poor repeatability [51].
- Inconsistent and flexible processing procedures: Conventionally fabricated scaffolds usually possess inconsistent pore sizes, pore morphologies, porosities and internal surface areas over their entire volumes [51].
- Shape limitations: Three-dimensional scaffolds is often limited by the complexity in the design and construction of the mold [51].
- Use of porogens: The use of porogens limits dimensions of scaffolds to thin membranes with thickness of 2 mm to facilitate complete porogen removal. Porogen particles entrapped by the matrix will remain in the scaffold. Moreover, it is difficult to prevent the agglomeration of porogen particles and achieve uniform porogen dispersion [52].

- Use of toxic organic solvents: Most of conventional techniques involve extensive use of toxic organic solvents in order to convert the raw materials (granules, pellets or powders) into the final scaffolds. Incomplete removal of solvents from the fabricated scaffolds especially in thicker constructs will result in harmful residues that have negative effects on adherent cells, incorporated biological active agents or nearby tissues [53].

Specific advantages and disadvantages of individual conventional techniques are summarized in Table 2.

Table 2: Summarization of advantages and disadvantages of conventional techniques [50; 51; 52; 54].

Technique	Advantages	Disadvantages
Fibre bonding	Easy process High porosity High surface area to volume ratio	High processing temperature for non-amorphous polymer Limit range of polymers Lack of mechanical strength Problems with residual solvent Lack of control over micro-architecture
Phase separation	Allows incorporation of bioactive agents Highly porous structures	Lack of control over micro-architecture Problems with residual solvent Limited range of pore sizes
Solvent casting and particulate leaching	Highly porous structures Large range of pore sizes Independent control of porosity and pore size Crystallinity can be tailored	Limited membrane thickness Lack of mechanical strength Problems with residual solvent Residual porogens
Membrane lamination	Macro shape control Independent control of porosity and pore size	Lack of mechanical strength Problems with residual solvent Tedious and time-consuming Limited interconnected pores
Melt moulding	Independent control of porosity and pore size Macro shape control	High processing temperature for non-amorphous polymer Residual porogens
Polymer/ceramic fibre composite-foam	Good compressive strength Independent control of porosity and pore size	Problems with residual solvent Residual porogens
High-pressure processing	Organic solvent free Allows incorporation of bioactive agents	Nonporous external surface Closed pore structure
High-pressure processing and particulate leaching	Organic solvent free Allows incorporation of bioactive agents	Limited interconnected pores Lack of mechanical strength Residual porogens

	Highly porous structures Large range of pore sizes Independent control of porosity and pore size	
Freeze drying	Highly porous structures High pore interconnectivity	Limited to small pore sizes
Hydrocarbon templating	No thickness limitation Independent control of porosity and pore size	Problems with residual solvent Residual porogens

2.2.2 Advanced Techniques

Advanced fabrication techniques are developed particularly to solve the versatility, reproducibility and scale-up issues of designing the scaffold for TE. Advanced scaffold fabrication techniques include [30]:

- Rapid prototyping (solid free form fabrication) – 3D plotting, 3D printing, stereolithography, selective laser sintering, fused deposition modelling, etc.
- Electrospinning
- In situ photopolymerization
- High internal phase emulsion
- Self-assembling peptides

Also, advanced scaffold fabrication techniques have their limitations, especially high processing temperatures, limited material range and use of toxic organic solvents. On the other hand, there are some significant advantages that draw attention of researchers to future perspectives [51]:

- Customized design: Direct utilization of CAD (computed-aided design) models as inputs for scaffold fabrication allows complex scaffold designs to be realized. Then, patient specific data and scaffold structural properties required for regenerating specific tissues can be incorporated into the scaffold design [51].
- Computer-controlled fabrication: The use of automated computerized fabrication will result in high quality production with minimal manpower requirements. The high-resolution devices with the ability to define and control individual process parameters will be able to create highly accurate and consistent pore morphologies. The ability to optimize scaffold designs will facilitate cell attachment, colonization and proper ECM formation [51].
- Anisotrophic scaffold microstructures: The use of CAD and advanced scaffold fabrication techniques will allow user control localized pore morphologies and porosities to suit the requirements of different cell types in the same scaffold volume. This can be achieved by incorporating different controllable macroscopic and microscopic designs on different regions of the same scaffold. Having an anisotrophic scaffold microstructure is great advantage in TE applications where multiple cell types are arranged in hierarchical structures [55].
- Processing conditions: Advanced techniques provide a diverse range of processing conditions which include solvent and/or porogen free processes and room temperature

processing. Some techniques also allow pharmaceutical and biological agents to be incorporated into the scaffolds during fabrication [56; 57].

2.3 Biomaterials for Scaffold Matrices

Biomaterials for scaffold matrices can divided into three individual groups: ceramics, synthetic polymers and natural polymers. Ceramics are not generally used for soft tissue engineering.

Ceramic scaffolds have many advantageous aspects like being bioactive, biocompatible, biodegradable, mechanically stiff (Young's modulus). On the other hand, they are less elastic and more brittle. They also exhibit shaping difficulties. Bioceramics can be classified into the following three groups [58]:

- Bioinert groups e.g. alumina and zirconia
- Surface bioactive groups e.g. high temperature sintered hydroxyapatite (s-HA), bioglass
- Bioresorbable groups e.g. low temperature sintered hydroxyapatite (u-HA), α-tricalcium phosphate (α-TCP), β-tricalcium phosphate (β-TCP), octacalcium phosphate (OCP), tetracalcium phosphate (TTCP)

Natural polymers have an advantage in the inherent bioactivities that can promote excellent cell adhesion, attachment, proliferation and tissue recovery. Furthermore, they are also biodegradable and so allow host cells, over time, to produce their own extracellular matrix and replace the degraded scaffold. However, there are still some limitations, such as, difficult to purify, potential risk for disease transmission, batch to batch difference, and lack enough mechanical properties and thermal stability [59]. Several mostly used natural polymers for scaffolds and their biomedical applications are listed in Table 3.

Numerous synthetic polymers have been tried to produce scaffolds because of their several advantages as a scaffold material and also due to their availability. Synthetic polymers can be biodegradable and non-biodegradable. Synthetic polymeric materials can be fabricated with a tailored architecture and properties (e.g. porosity, degradability and mechanical properties), according to their applications. That means they can be produced under controlled conditions with large uniform quantities and long shelf life. However, there is a risk of rejection of these polymeric scaffolds because of their reduced bioactivity. During the degradation process, formation of acidic products and consequently lowering the local pH is a common problem with synthetic polymers which can result in cell-tissue necrosis [60]. Several mostly used synthetic polymers for scaffolds and their biomedical applications are listed in Table 4.

Each of these individual biomaterial groups has specific advantages and, needless to say, disadvantages so the use of composite scaffolds comprised of different phases is becoming increasingly common.

Table 3: Several kinds of natural polymers for scaffolds and related applications [61].

Natural polymers	Chemical structure	Biomedical applications
Agarose	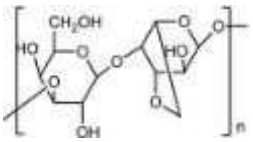	Cell encapsulation and proliferation

Chitosan	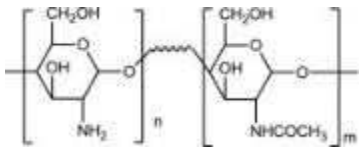	Encapsulate hepatocytes, orthopaedic scaffold
Collagen	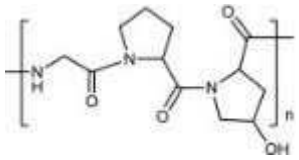	Wound healing, promote blood coagulation, scaffold for cells
Gelatin	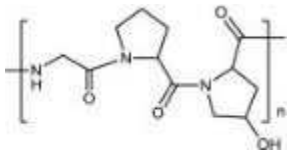	Support cells for orthopaedic applications
Silk	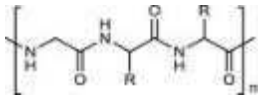	Cell attachment, bone growth

Table 4: Several kinds of synthetic polymers for scaffolds and related applications [61].

Synthetic polymers	**Structural units**	**Biomedical applications**
Poly(glycolic acid)		Heart valve engineering, support for muscle and endothelial cell growth
Poly(D,L-lactic acid-co-glycolic acid)	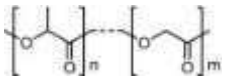	Regenerate an extracellular matrix
Poly(ε-caprolactone)		Support of cell viability
Polyorthoester		Bone reconstruction
Polyanhydride	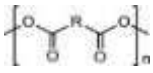	Weight-bearing orthopaedic
Polycarbonate(tyrosine derived)	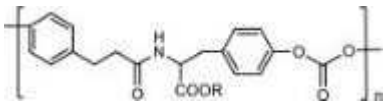	Bone scaffolds
Poly(ethylene glycol)	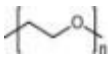	Forming scaffolds copolymerized with other polymers
Polyurethane	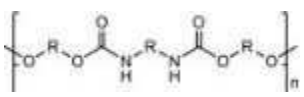	Support cell attachment

2.4 Collagen

Collagen is the most abundant structural protein in all animals, forms up to 35 % of all proteins, and is a major component of the ECM and connective tissues. Collagen has been long on the top list of preferred materials for tissue engineering scaffolds thanks the fact that is well tolerated, it promotes cell adhesion and proliferation, and it provides biodegradable scaffolds with good mechanical properties [62; 63]. To date, some 30 various types of collagen have been identified in collagen family [64]. According to its compositional and structural characteristics they are grouped as fibril and network forming, fibril-associated collagens with interrupted triple helices (FACITs), membrane-associated collagens with interrupted triple helices (MACITs), multiple triple-helix domains and interruptions (MULTIPLEXINs) [63]. Most collagens consist of fibril-forming collagens (up to 90% of all human collagens) with their characteristic quarter-staggered fibril-array [65]. The most abundant collagens are type I which is present mainly in bone, tendons, skin, dentin, etc., type II mostly in cartilage and type III in skin. The other minor collagen types are rather organ-specific [64].

2.4.1 Structure of Collagen

Among the different collagen types are rather high structural diversities, but all members of collagen family have one characteristic feature: a right-handed triple helix composed of three α-chains [66]. These might be formed by three identical chains (homotrimers) as in collagens II, III, VII, VIII, X, and others or by two or more different chains (heterotrimers) as in collagen types I, IV, V, VI, IX, and XI. Each of the three α-chains within the molecule forms an extended left-handed helix with a pitch of 18 amino acids per turn [67]. The three chains, staggered by one residue relative to each other, are supercoiled around a central axis in a right-handed manner to form the triple helix [68]. Structure and organization of collagen is shown in Fig. 4.

A structural prerequisite for the assembly into a triple helix is a glycine residue in every third position of the polypeptide chains resulting in a $(Gly\text{-}X\text{-}Y)_n$ repeat structure which characterizes the “collagenous” domains of all collagens. The α-chains assemble around a central axis in a way that all glycine residues are positioned in the center of the triple helix, while the more “volume” side chains of the other amino acids occupy the outer positions. This allows a close packaging along the central axis of the molecule. The X and Y position is often occupied by proline and hydroxyproline. Depending on the collagen type, specific proline and lysine residues are modified by post-translational enzymatic hydroxylation. The content of 4-hydroxyproline is essential for the formation of intramolecular hydrogen bonds and contributes to the stability of the triple helical conformation [69].

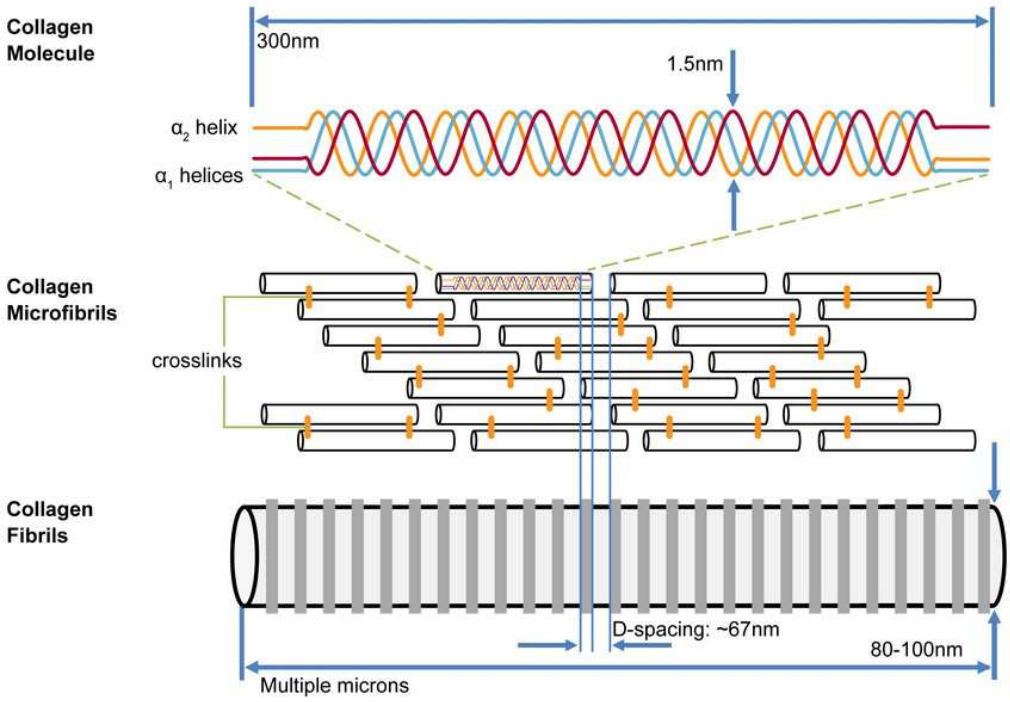

Fig. 4: Scheme of collagen structure and organization [70].

The helix-forming (Gly-X-Y) repeat is the predominating motif in fibril-forming collagens (I, II, III) resulting in triple helical domains of 300 nm in length which corresponds to about 1000 amino acids [71; 72]. Although the triple helix is a key characteristic of all collagens and represents the major part in fibril-forming collagens, non-collagenous domains neighbouring the central helical part are also important structural components. Thus, the C-propeptide is thought to play a fundamental role in the initiation of triple helix formation, whereas the N-propeptide is thought to be involved in the regulation of primary fibril diameters. The short non-helical telopeptides of the processed collagen monomers are involved in the covalent cross-linking of the collagen molecules as well as linking to other molecular structures of the surrounding matrix [71].

Fibroblasts are the major producer of collagen in connective tissue. Collagen pro-α chain is synthesized from a unique mRNA on the rough endoplasmic reticulum and then is transferred to the Golgi apparatus of the cell. During this transfer, some prolines and lysines residues are hydroxylated by the lysyl oxydase enzyme. Specific lysines are glycosylated and then pro-α chains self-assemble into procollagen prior and pass to excretory vesicles. During passage through the plasma membrane, the propeptides are cleaved outside the cell to allow for the auto-polymerisation by telopeptides. This step is the initiation of tropocollagen self-assembly into 10 to 300 nm sized fibril and the agglomeration of fibril into 0.5 to 3 µm collagen fibers [73].

2.4.2 Physical and Chemical Properties of Collagen

The fibrillar structure of collagen is stabilized by several posttranslational modifications that allow the formation of intermolecular and interfibrillar cross-links. There are two main types of intermolecular cross-links: enzymatic and advanced glycation end-products (AGEs). Enzymatic cross-links are essential in the formation of functional collagen fibrils, whereas AGEs accumulate with age and diabetes and may impair normal function [74]. Cross-linking

directly affects the mechanical function of connective tissues [75; 76] and also affects tissue biochemistry, making collagen less susceptible to proteolytic degradation [77; 78].

Enzymatic cross-link formation is initiated by the enzyme lysyl oxidase acting on specific lysines in the telopeptides [76]. The resulting allysine reacts rapidly with a specific lysine in the helical region of a neighbouring molecule to form an immature divalent intermolecular bond [79]. Over time, immature cross-links can react with an additional telopeptide allysine to form a trivalent mature bond. AGE cross-links are formed by reactions with reducing sugars, such as glucose. This type of reaction is largely unspecific, producing both cross-linking and noncross-linking compounds along the protein. The amount of AGEs formed on a protein increases with time until it is degraded. This allows large amounts of AGEs to accumulate due to the extensive half-life of collagen [76; 80].

Covalent crosslinks between collagen molecules are the major obstacles for dissolution. Collagen is insoluble in organic solvents. Water-soluble collagen represents only a small fraction of total collagen and the amount depends on the age of the animal and type of tissue extracted. The most commonly used solvents are neutral salt solution (0.5–2 M NaCl) or dilute acetic acid. Neutral salt solutions can extract freshly synthesized and negligibly crosslinked collagen molecules present in the tissue. Modifications in temperature, shaking rate and volume of extractant to tissue ratio can irreversibly change the composition of the collagen [81]. Dilute acidic solvents, e.g. 0.5 M acetic acid, citrate buffer or hydrochloric acid pH 2–3 are more efficient than neutral salt solutions. The intermolecular crosslinks of the aldimine type are dissociated by the dilute acids and the repulsive repelling charges on the triple-helices lead to swelling of fibrillar structures [82]. It is possible to solubilize approximately 2% of the tissue collagen with dilute salt or acid solutions. The remaining 98% is referred to as insoluble collagen although this dominant collagen material is not absolutely insoluble and can be further disintegrated without major damage to the triple-helical structures. There two possibilities how to continue dissolution, either solution of strong alkali or using enzymes to cleave remaining crosslinks [83; 84].

2.4.3 Immunogenicity and Biocompatibility

Collagen is an animal-derived biomaterial, so there is a potential to evoke an immune response which should be considered. Implantation of collagen may initiate an acute inflammatory response which can sometimes provoke a chronic inflammatory response. The inflammation cause secretion of a large number of antibodies, cytokines or pathogens. Therefore, the determination of immunological response following in vivo implantation is based on assessment of pro-inflammatory cytokine and antibody secretions and monitoring the population changes of immune cells. Complete immunogenic purification is difficult. Although collagen extracted from animal sources may exhibit a small degree of antigenicity, it is generally considered acceptable for tissue engineering applications on humans [64; 85].

An immune response against collagen mainly targets to epitopes in the telopeptide region at each end of the tropocollagen molecule [86; 87]. However, the conformation of the helical part and the amino acid sequence on the surface of the polymerized collagen fibril, also influence the immunologic profile of the collagen molecule [88; 89]. Thus, the difference of immunogenicity between polymerized collagen and their smaller counterpart lies on the accessibility of the antigenic determinants that decrease during the polymerisation process [90].

2.4.4 Degradation of Collagen

Native collagen has the poor solubility qualities, therefore often happens a slow metabolic turnover [91]. Water and enzymes are needed to digest collagen linkages and to start a degradation [64]. The rate of the degradation process often needs to be regulated using diverse methods such as crosslinking techniques or a structural modification agent [92]. Biodegradation of collagen-based biomaterials for TE could potentially lead to the restoration of tissue structure and functionality [93]. In addition, the degradation product of collagen type I to III have also been shown to induce a chemotactic attraction of human fibroblasts [94]. On the other hand, collagen degradation products can induce an undesirable immunological response leading to inflammation and tissue destruction [95].

Hydrolytic degradation is slower under neutral pH conditions where the cleavage of covalent bonds (such as ester and peptide bonds) together dominates. Under alkaline pH conditions, the splitting of the peptide bonds progresses in a bit faster way than neutral pH [85].

Native collagens are highly resistant and, they are completely digested only by specific collagenases and pepsin-cleaving enzymes which can cleave collagen in its undenatured helical regions under physiological pH and body temperature [96]. Degradation of collagen in vivo is more complex than in vitro. Collagen can be degraded by endopeptidases, such as metalloproteinases (collagenases, gelatinases, etc.) and serine-, cysteine- and aspartic-proteases. The mechanism relies on three abilities: binding collagen molecules, unwinding the three α-chains and cleaving each strand of the triple helix [64].

2.4.5 Crosslinking of Collagen

Naturally collagen tissue possesses significant strength, this strength is lost when collagen products are made from soluble collagen or after electrospinning, then material is even more soluble in pure water due to the loss of the quaternary structure [97]. Therefore, collagen must be crosslinked to provide greater stability in solutions, reduce enzymatic sensitivity and increase the mechanical strength of the fibres and resistance to the denaturation temperature. In addition, crosslinking allows reduction in the antigenicity of collagen and sometimes decreases its calcification [85; 98].

There are three types of crosslinking techniques: physical, chemical and enzymatic. Physical crosslinking relies on irradiation by ultra-violet wavelengths (UV) and dehydrothermal treatment (DHT). Both techniques produce similar results in crosslinking collagen scaffolds, tensile strength is increased, and collagen molecular structure is partially fragmented. However, UV irradiation is more time-effective when compared to DHT treatment as it takes only 15 minutes instead of 3 to 5 days for the DHT treatment. UV crosslinked collagen scaffolds also result in a more suitable biomaterial for load-bearing applications due to its enhanced enzymatic resistance. However, UV irradiation is only effective for thin and transparent scaffolds, allowing UV to go through the structure [99].

Chemical crosslinking in collagen scaffold can be achieved via:

- Covalent amine/imine linkage, mainly with the ε-amino group of lysine residue (e.g., glutaraldehyde [100], isocyanate crosslinking [101]).
- The carboxyl group in collagen (e.g., 1-ethyl-3-(3-dimethylaminopropyl)-1-carbodiimide hydrochloride (EDC) crosslinking [64]).

- The H-bond between the polyphenolic OH group and different amino acids (e.g., genipin crosslinking [102]).
- Metal-protein complex formation (e.g., chromium crosslinking) [103].

The use of aldehydes such as formaldehyde and glutaraldehyde were extensively used in the past decade. Glutaraldehyde was the most employed and studied chemical method used to crosslink collagen-based biomaterials [73]. Nowadays it is the most commonly used N-ethyl-N′-[3–dimethylaminopropyl] carbodiimide chloride/N-hydroxy succinimide (EDC/NHS) as a non-toxic cross-linker which crosslinks without incorporation of the crosslinking reagent. The reaction is based on the formation of an amidic bond from lysine or hydroxylysine NH_2 and C=O from glutamic or aspartic acid [64]. EDC is not included in the new crosslink bond (thus so-called the zero-length crosslink) but is simply transformed into water-soluble urea-derivatives. EDC is known as a low cytotoxic crosslinker since it is not itself incorporated into the crosslinked structure, however, the urea derivates formed as by-products have been reported to exhibit some degree of cytotoxicity [104].

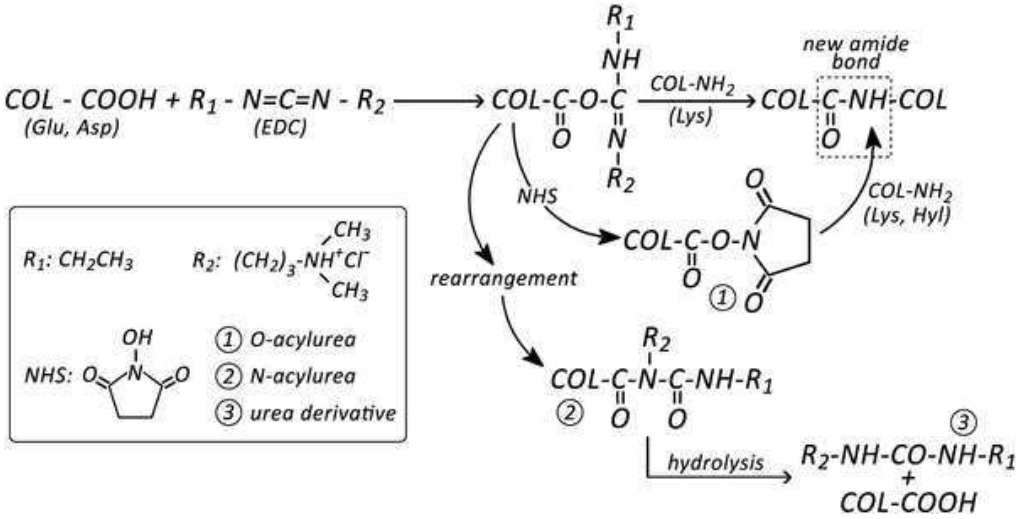

Fig. 5: A representative crosslinking scheme of collagen either with EDC or in combination with NHS in order to modify number of intermediates and side-by products [85].

Combination of EDC/NHS, where the NHS acts as a competitor, slows crosslinking, by competing with EDC in the reaction, thus adding additional reaction step (Fig. 5). Furthermore, it inhibits the hydrolysis and reduces formation of by-products and intermediates (N-acylurea and O-acylurea derivates). The rate of crosslinking can be controlled via the EDC/NHS ratio. Evidently the reaction also depends on moisture levels in the environment and alcohol vapours (which accelerate dissolution) [64]. It is proved that EDC and EDC/NHS crosslinked collagen scaffolds are structurally stable and maintain fibre structure for up to 3 months and they are also cytocompatible. Thus, EDC and EDC/NHS seem to be more appropriate crosslinker than commonly used genipin or glutaraldehyde [105].

Finally, enzymatic crosslinking agents like transglutaminase can be used to enhance tensile strength and enzymatic resistance of collagen-based biomaterial. The major advantage with the approach of using a biologic polymerization technique is that no chemical residues or by-products remain in the scaffold structure, and therefore eliminate the risk of inducing cytotoxic effects [106].

2.4.6 Fabrication Techniques of Collagen Based Scaffolds

Collagen is an excellent candidate material for many biomedical applications, although its low shape-controllability remains as important limitation. Particularly, the processability of collagen using solid-freeform techniques is limited by its hydrophilic nature and low viscosity at room temperature [107; 108; 109]. There are various methods to fabricate 3D collagen scaffold, mostly used include a freeze drying [110] , electrospinning [111], three-dimensional printing (3DP) [112] and self-assembly [113].

In the freeze-drying process, also known as lyophilization, a polymer is firstly dissolved into a suitable solvent (water). Then, the polymer solution is cooled down below its freezing point, leading to the solidification of the solvent that is evaporated via sublimation, leaving a dry scaffold with. For this process, vacuum with high power is needed in order to come out with a scaffold which has numerous and interconnected pores [114]. The polymer solution characteristics like concentration, viscosity and the amount of aqueous phase dispersed in the system affect the porosity and pore size. By increasing the polymer concentration in the continuous phase, the dispersed aqueous phase is subjected to superior shear forces and this decreases the size of water domains and leads to the production of materials with lower porosity and smaller pores. Whereas, a decrease in the amount of water decreases average pore size [115; 116]. A main advantage of the technique is the possibility to avoid high temperatures that could reduce the activity of incorporated biological factors. Moreover, pore size can be easily controlled by tuning the freezing regime. The drawback of this technique is smaller pore size and long processing time [117].

Electrospinning uses electrical charges to draw fine fibres up to the nanometer scale and create a nanofibrous structure with high surface areas able to adsorb proteins and binding sites to cell membrane receptors. A standard system requires four major components: a spinner with a metallic needle, a syringe pump, a high-voltage power supply and a grounded collector. The electric field strength overcomes the surface tension of the droplet and generates a charged liquid jet that is then elongated and whipped continuously by electrostatic repulsion until it is deposited on the grounded collector. The solvent evaporates in the process and the jet solidifies to form a nonwoven fibrous membrane [118; 119]. The electrospinning technique can process a wide range of materials in order to produce scaffolds with required morphology and porosity, including fibres with diameters from few microns to nanometres [120]. Another important feature of this technique is that the nanofibers can be functionalized via incorporation of bioactive species [121]. The diameter of each fibre can be controlled by altering the concentration and flow rate of the polymer solution and varying the distance between the needle and collector. A main disadvantage of electrospinning is the use of organic solvents.

3DP technique invented at the Massachusetts Institute of Technology can ink-jet a liquid binder solution onto a powder bed at room temperature conditions. The process begins with a binder jetting machine distributing a layer of powder onto a platform. Liquid droplets of a bonding agent are deposited onto the powder layer through inkjet print heads, bonding the particles together. The platform is then lowered, and a next layer of powder is laid out on top. By repeating the process of laying out powder and bonding, the parts are built up in the powder bed. Removal of the unbound powder reveals the fabricated part [122; 123]. The 3DP process can be direct or indirect. And the indirect 3DP technique at room temperature allows to fabricate

porous collagen scaffolds. In the indirect technique, molds are printed using plaster powder and biodegradable polymers are cast into the printed molds. That technique involves the fabrication of a simple 3D sacrificial primary template that works as a mold for a secondary one. This template is then removed by physical, chemical or thermal way. The limitation is restriction on shape or design due to demolding difficulty [124; 125].

Self-assembly is defined as the autonomous organization of components into patterns or structures without human intervention [126]. Self-assembly of biological molecules can be induced by noncovalent bonds or weak covalent interactions, including electrostatic, van der Waals, hydrophobic interactions, ionic, hydrogen, and coordination bonds. Various nanofilaments of proteins can be assembled into nanofibers with a high aspect ratio, which can mimic the physical microenvironment of cells in vivo [127]. In the body, these nanofibers could wrap around cells covering long distances over their surfaces and act as cables that connect neighbour cells and mechanically support them by creating 3D network [128]. Despite the fact the self-assembly nanofibers and nanoscale network can be easily adjusted by changing pH of aqueous solution, fabricated 3D structures have poor mechanical properties and they are unstable [129]. Another limitation is the high production cost and complicated processing. On the other hand, self-assembly produces much thinner nanofibers than electrospinning and avoids the use of organic solvent thus reduce the cytotoxicity because it is carried out in aqueous salt solution or physiological media [130].

2.5 Bioceramic Components

Pure collagen scaffolds achieve poor mechanical strength therefore bioceramics with the similar constituent to the intrinsic inorganic components of bone are mostly used component. In addition to the strength enhancement, bioceramics can also improve osteoconductive ability, dimensional ability and increase the surface area for cell attachment on the composite scaffold [131; 132]. The inorganic nature and mechanical rigidity determine bioceramics to application related to hard tissue repair, such as bone and teeth. However, several studies have also demonstrated the potential of bioceramics as an innovative way to regenerate soft tissues including muscle and nerve tissue regeneration, treatment of diseases affecting sense organs (eye and ear), embolization of neoplastic tissues, cancer radiotherapy via injectable microspheres and wound dressing [133; 134].

2.5.1 Hydroxyapatite

Hydroxyapatite (HAp, $Ca_{10}(PO_4)_6(OH)_2$) is a naturally occurring mineral form of calcium apatite that crystallizes in the hexagonal crystal system (Fig. 6). It is the most commonly used calcium phosphate with the molar ratio of Ca/P = 1.67 which is very close to bone apatite. It has excellent biocompatibility, bone-bonding ability and osteoconductive properties. Moreover, HAp is thermodynamically the most stable calcium phosphate ceramic compound under physiological conditions as pH, temperature and composition of the body fluids [135; 136].

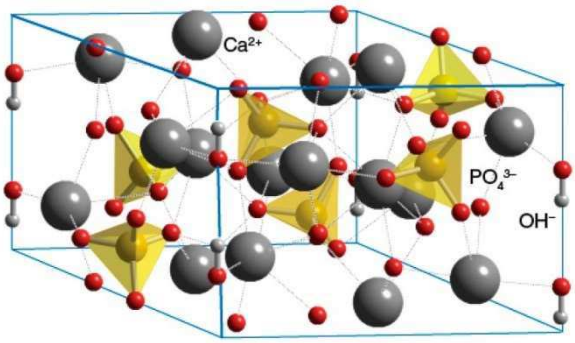

Fig. 6: Representative cartoon of unit cell of hexagonal HAp [137].

The biology bone is mainly constructed by the inorganic (HAp) and organic components (especially by collagen). HAp represents 65–75 wt.% depending on the specific type of the bone. Apart from the bone tissue, HAp is also the main inorganic mineral constituent of enamel, dentine and pathologically calcified tissues [138].

Nano-hydroxyapatite (nano-HAp) is attracting interests as a biomaterial for use in prosthetic applications due its high similarity in size, crystallography and chemical composition with naturally occurring HAp in hard tissues [139].

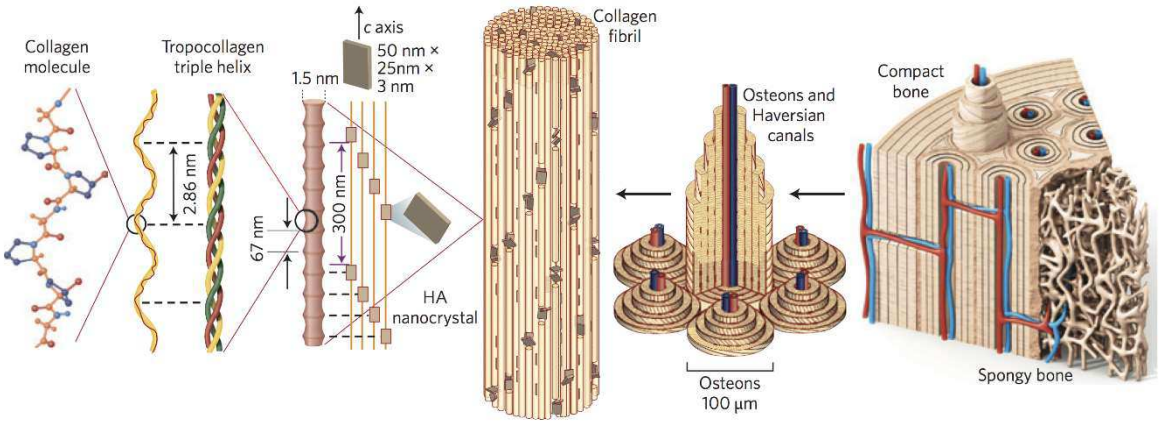

Fig. 7: Scheme of hierarchical structure of bone [140].

In the microstructure of cortical bone, mineralized collagen fibres form into planar arrangements called lamellae (3–7 µm wide). As seen in Fig. 7, in a cortical bone the lamellae wrap in concentric layers (3–8 lamellae) around a central canal, to form an osteon. The osteons have shapes of cylinders, and they are roughly parallel to the long axis of the bone [141]. The microstructure of trabecular bone has different fibre-like texture. HAp plates are arranged parallel to a common direction. In the nanostructure crystals of HAp occur at regular intervals along the collage fibrils, with an approximate repeat distance of 67 nm, which corresponds to the distance by which adjacent collagen molecules are staggered [142]. This arrangement in the nanometre scale enhances the isotropic properties found in bone, prevents crack propagation and increase toughness [143]. The formation of the apatite in the extracellular space of the collagen is called “biomineralization”. That process depends on different factors such as stage (e.g., development and fracture healing), region, age, etc. HAp nucleation is possible thanks to

stereochemical orientation of negatively charged groups formed by anionic proteins and type I collagen [135].

HAp can sufficiently simulate the mineralogical structure of bone. Therefore, the collagen/HAp composite scaffolds have been extensively investigated and used for bone tissue engineering [144; 145]. Addition of HAp crystals improves compressive modulus of collagen scaffold that is related to the concentration of collagen, the amount of HAp, the fabrication method of composite and crosslinking method [146]. HAp can form direct chemical bonds with bone tissue and that leads to faster and better bone-bonding. Cells therefore proliferate better and show enhanced bioactivity on rough surfaces [147].

Nano-sized HAp particles are more effective because of their immense surface area. Composite scaffolds nano-HAp/collagen achieve highly porous, interconnected structure and the higher compressive modulus than composite scaffolds containing micro-HAp crystals [136]. Evenly, micro-HAp crystals can make composite scaffold brittle and hardly biodegradable [147]. HAp crystals can be deposited to form thin HAp coatings on the scaffold after soaking in simulated body fluid (SBF). This way is more like a biomimetic process which can mimic the biochemical and biophysical properties of bone matrix. The "biomimetic" scaffolds are expected to take the place of the missing bone [148].

2.5.2 β-Tricalcium Phosphate

β-tricalcium phosphate (β-TCP, β-$Ca_3(PO_4)_2$) is another representative of calcium phosphate bioceramics that crystalizes in the rhombohedral crystal system. The Ca/P ratio of β-TCP is 1.5. It is osteoinductive and resorbable material that offers superior biochemical activity for bone regeneration therapies [149]. Although, β-TCP itself possessed neither intrinsic osteogenic nor osteoconductive properties. To promote osteogenic activity β-TCP particles must be combined with marrow-derived osteoprogenitor cells. Then β-TCP can activate the differentiation of mesenchymal stem cells (MSCs) into osteoblasts and ECM formation such as collagen type I and the following mineralization [150]. Moreover, incorporation of β-TCP into collagen has a synergistic effect on bone healing. Composite material supports better contact to surrounding bone tissue by swelling of the collagen component [151].

Distribution of β-TCP powders in a collagen matrix effectively improves the structural and biological stability of the composite scaffold. Firstly, the compressive modulus of the composite scaffold tends to increase due to cell proliferation and the following formation of network structure. Then, the compressive modulus starts to decrease because of the material degradation. Finally, active calcification by formation and growth of mineralized nodules results in the recovery of modulus [152].

It is observed that the promotion of cell and tissue ingrowth into the scaffold is facilitated by β-TCP nanoparticle modification. Scaffolds modified with β-TCP nanoparticles and basic fibroblast growth factor (FGF-2) can induce the formation bone structures. An important role in final biocompatibility plays the applied dose of nanomaterial. A high dose of β-TCP nanoparticles promotes high cell proliferation and vessel ingrowth. In contrast, when concentration of calcium ions is increased, it stimulates chemotactic responses in monocytes associated with macrophage differentiation and an inflammatory reaction. Therefore, overdoses of Ca^{2+} ions suppress the proliferation of cells and limit formation of the new bone tissue [153].

Compared to HAp, β-TCP has a faster degradation rate and can be completely replaced by newly formed bone tissues. β-TCP is generally resorbed within 6 weeks after implantation, whereas commercially available hydroxyapatite is almost nonresorbable. Biphasic calcium phosphate (BCP) is the mixture of different proportions of HAp and β-TCP. It combines the stability of HAp with biodegradability of β-TCP. Different biodegradation rates can be achieved by changing the proportion of the composition phases [152; 153].

2.5.3 α-Tricalcium Phosphate

Tricalcium phosphate (TCP) has three polymorphic forms: β, α and α'. The last one transforms into the α form during cooling. It crystalizes in the monoclinic crystal system. β-TCP is stable at room temperature and reconstructively transforms to 1 125 °C into α-tricalcium phosphate (α-$Ca_3(PO_4)_2$, α-TCP), which is metastable, and it is retained until room temperature [154; 155]. α-TCP, as well as β-TCP, is used in clinical applications in dentistry, maxilla-facial surgery and orthopaedics. α-TCP is the main constituent of the powder component of various hydraulic bone cements [156].

Despite the fact that TCPs have the same chemical composition, α and β form differ considerably in their structure, density and solubility, which determine their biological properties and clinical applications. For example, α-TCP is highly more soluble and reactive than β-TCP therefore α-TCP is used mainly as a fine powder in the preparation of calcium phosphate cements. It promotes osteogenesis by increasing collagen synthesis and mineralization of the extracellular matrix [157]. Remains from both α-TCP and β-TCP are completely integrated into newly formed bone after a degradation process. Although, it is proven that α-TCP bone filler powder increases bone density and probably HAp created by hydrolysis of α-TCP play the role in enhancing osteoconducting ability [158].

α-TCP is also osteoconductive and bioactive, both in vitro and in vivo. Although the content of α-TCP relatively make material more cytotoxic than with addition of HAp or β-TCP because of the phosphoric acid generated during its hydrolysis [159]. On the other hand, it is more bioreabsorbable than HAp, β-TCP and biphasic (HAp/β-TCP) bioceramics used in clinical practice. That can be used in controlling the rate of scaffold degradation as well as developing biodegradable carriers for controlled release of drugs, macromolecules or cells [160; 161].

3 MAIN GOALS OF THE WORK

The thesis follows up previous studies dealing with the collagen-based composite scaffolds containing individual bioceramic particles [144; 145].The main goals of the work are to prepare the three-dimensional porous collagen composite scaffolds for bone tissue engineering, then to compare bioceramic mixtures due their solubility and particle sizes and to study the effect of addition of bioceramic mixtures on the scaffolds:

- Morphology – homogeneity and inner structure, porosity, pore size and its distribution.
- Swelling behaviour.
- Enzymatic degradation.
- Chemical properties – chemical interactions between bioceramic particles and the pure collagen matrix.
- Mechanical properties in dry state and hydrate state that simulate physiological body conditions.
- Biocompatibility – cytotoxicity, cell proliferation and osteoconductivity.

4 EXPERIMENTAL PART

4.1 Chemicals

- Collagen – Type I collagen, 0.5 wt% aqueous suspension, was derived from a bovine skin (Collado, Czech Republic) and a porcine tendon (CEITEC, Czech Republic)
- Hydroxyapatite (HAp) calcined at 1000°C for 1 h of mean particle size 130 nm, (Riedel-de Haën, Germany)
- β-tricalcium phosphate (β-TCP) of mean particle size 4.21 μm which contained 89 wt% of β-TCP and 11 wt% of calcium pyrophosphate, (Fluka, Swiss)
- α-tricalcium phosphate (α-TCP) of mean particle size 11.01 μm which contained 92 wt% of α-TCP and 8 wt% of HAp, (Premier Biomaterials, Ireland)
- N-(3-Dimethylaminopropyl)-N′-ethylcarbodiimide hydrochloride (EDC) was diluted to obtain 0.03M solution in 98% ethanol (w/w), (Sigma-Aldrich, Germany)
- N-hydroxysuccinimide (NHC) was diluted to obtain 0.01M solution in 98% ethanol (w/w), (Sigma-Aldrich, Germany)
- 98% ethanol (PENTA, Czech Republic)
- Sodium phosphate dibasic (Na_2HPO_4), (Sigma-Aldrich, Germany)
- Isopropanol (PENTA, Czech Republic)
- Normal saline solution (NS), (B. Braun, Inc., Germany
- Clostridium histolyticum for general use (Type I; 0.25–1.0 FALGPA units/mg solid, ≥125 CDU/mg solid), (Sigma-Aldrich, Germany)
- Sodium chloride (NaCl), (Lach-Ner, Czech Republic)
- Potassium chloride (KCl), (Lach-Ner, Czech Republic)
- Dipotassium phosphate (KH_2PO_4), (Lach-Ner, Czech Republic)
- Hydrochloric acid (HCl), (PENTA, Czech Republic)
- Ultrapure water (type 1) was prepared on Direct-Q® 3UV Water Purification System, (Merck, Germany)

4.2 Equipment

- Disintegrator – Ultra Turrax T18 basic, (IKA, Germany)
- Centrifuge – 5804 R, (Eppendorf, Germany)
- Freeze-dryer – Epsilon 2-10D LSCplus, (Martin Christ, Germany)
- Scanning electron microscope – Mira3 XMU, (TESCAN, Czech Republic)
- Sputter coater – EM ACE600, (Leica, Germany)
- Solids analyser – RSA-G2, (TA Instruments, USA)
- FTIR-ATR analyser – VERTEX 70V, (Bruker, USA)

4.3 Fabrication of Scaffolds

An aqueous collagen suspension was used to fabricate highly porous collagen scaffold by the freeze-drying method. The concentration of the aqueous collagen suspension was 0.5 wt% and it was prepared by means of swelling of collagen in refrigerated ultrapure water and homogenised using a disintegrator (5 000 rpm for 10 min). Samples were centrifuged for 1 min at 2 000 rpm to remove air bubbles. Then the aqueous collagen suspension was poured into the well-plates (48 wells) and put into a freezer overnight. Afterward, they were lyophilized for

two days (temperature of ice condenser and shelf temperature was -80 °C and -50°C, respectively).

The highly porous collagen/HAp/β-TCP/α-TCP composite scaffolds were also fabricated by the freeze-drying method. The concentration of the aqueous collagen suspension was 0.5 wt% and it was prepared by means of swelling of collagen in refrigerated ultrapure water and homogenised using disintegrator (5 000 rpm for 10 min). Bioceramics components were stirred in small volume of the refrigerated ultrapure water let it swell (for 15 min). Then, small amounts of bioceramic suspension were gradually added to the homogenised collagen suspension, while the mixture was homogenised again using a disintegrator (5 000 rpm for 5 min) to prevent a precipitation. Then the collagen/bioceramic suspension was poured into the well-plates (48 wells) and put into a freezer overnight. Finally, they were lyophilized for two days (temperature of ice condenser and shelf temperature was -80°C and -50 °C, respectively).

5 types of highly porous collagen and collagen/HAp/β-TCP/α-TCP composite scaffolds were prepared. The composition of each type is listed in Table 5. Samples had the cylindrical shape with an average diameter of 8 mm and an average length of 10 mm except samples 1B which have an average diameter of 6 mm and average length of 7 mm.

Table 5: Composition of the scaffolds.

Full sample name	Abbreviated sample name	Bovine collagen [wt%]	Porcine collagen [wt%]	Bioceramic components [wt%]	Weight ratio HAp : β-TCP : α-TCP
1A col bov	1A	100	0	0	-
1B col pig	1B	0	100	0	-
2A HAP TCP	2A	50	0	50	50 : 45 : 5
3A HAP TCP	3A	50	0	50	25 : 70 : 5
4A HAP TCP	4A	50	0	50	75 : 20 : 5

Both, the porous collagen and collagen/HAp/β-TCP/α-TCP composite scaffolds were cross-linked by using the crosslinking agent with carbodiimides – N-(3-Dimethylaminopropyl)-N′-ethylcarbodiimide hydrochloride/ N-hydroxysuccimide (EDC/NHS) in ethanol as a solvent according to Sloviková [162]. Briefly, the cross-linking solution was added directly to the scaffolds in well-plates and stayed there for next 2 h at room temperature. After that, the scaffolds were washed with 0.1 M Na_2HPO_4 two times for 30 min and with ultrapure water three times for 30 min. Finally, the scaffolds were poured with ultrapure water and put into a freezer overnight. Then they were lyophilized for two days to eliminate water content without loss of structural integrity

4.4 Characterization of the Scaffolds

4.4.1 Morphology

The morphology and microstructure of lyophilized scaffolds were investigated by means of scanning electron microscopy (SEM). Prior the SEM analysis, the prepared scaffolds (one from each group) were frozen in liquid nitrogen for few minutes to get stiffer samples. Then they were carefully cut into 3 mm slices with a scalpel to expose the internal structure. They were attached to aluminium pin stubs using a carbon tape (Fig. 8). After that, samples were sputter

coated with 10 nm of Au/Pd layer and imaged by SEM in the secondary electron emission mode at a voltage of 10 kV acceleration voltages and working distance 20–30 mm.

Fig. 8: Image of scaffolds on aluminium pin stubs prepared for SEM analysis.

The pore size of the scaffolds was determined from SEM images in which the applied magnification was 52× and resolution of 4 mm. Data was imported to ImageJ software and then at least 20 pores were measured in a perpendicular direction through the long axis and minor axis.

4.4.2 Porosity

The porosity value of the scaffolds was evaluated by two methods:

1. Liquid displacement method (using Archimedes principle).
2. Using pictures from the SEM analysis and software ImageJ.

Results from both methods were then compared.

When the porosity of the scaffolds was measured by liquid displacement method, each sample was thoroughly immersed into glass bottle filled with isopropanol that was not a solvent of the scaffold, penetrated into pores easily and did not cause swelling of the material. The scaffold with the isopropanol soaked into the pores was removed from the bottle (Fig. 9). Three cylindrical samples with an average diameter of 8 mm and an average length of 10 mm were tested in each group except samples 1B which have an average diameter of 6 mm and average length of 7 mm. The porosity was then determined by using equation (1):

$$\text{Porosity (\%)} = \frac{\frac{w_2 - w_3 - w_s}{\rho_i}}{\frac{w_1 - w_3}{\rho_i}} \cdot 100, \qquad (1)$$

where w_1 is the weight of the glass bottle filled with isopropanol, w_2 is the weight of the glass bottle after the immersion of the scaffold, w_3 is the weight of the glass bottle with isopropanol after removal of the scaffold, w_s is the weight of the dry scaffold and ρ_i is the density of isopropanol [152].

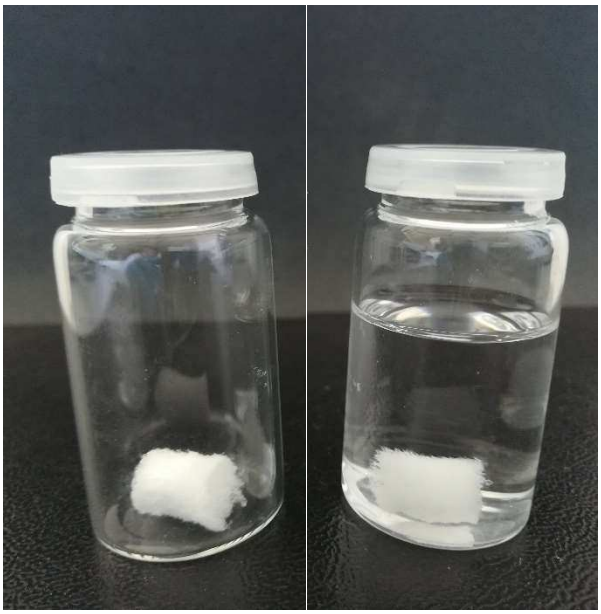

Fig. 9: The representative images of the dry scaffold (left) and the scaffold immersed in isopropanol (right).

The second method used greyscale images from SEM analysis in which the applied magnification was 52× and used resolution of 4 mm. Binary images were created using software ImageJ and the function thresholding. Then area fraction was calculated.

4.4.3 Swelling Behaviour

The swelling behaviour of each scaffold was quantitively evaluated based on the swelling ratio. The porous scaffolds were immersed in normal saline solution at 37 °C (for 5, 10, 15, 20, 30, 45, 60, 90 and 120 min) until a stable mass was obtained. Three cylindrical samples with an average diameter of 8 mm and an average length of 10 mm were tested in each group except samples 1B which have an average diameter of 6 mm and average length of 7 mm.

At each sampling time the scaffolds were moved from NS and the excess of NS was removed using the filter paper and then they were weighed. The swelling ratio was then calculated using the following equation (2):

$$\text{Swelling Ratio} = \frac{w_{\text{wet}} - w_{\text{dry}}}{w_{\text{dry}}}, \tag{2}$$

where w_{dry} is the initial weight of the dried scaffold and w_{wet} is the weight of the scaffold with soaked NS [163].

4.4.4 Enzymatic Degradation

The enzymatic in vitro degradation of the scaffolds was performed using bacterial collagenase from Clostridium histolyticum in phosphate-buffered saline (PBS) that was prepared according recipe in Table 6 by dissolving reagents in ultrapure water and adjusting pH to physiological value of 7.4 with HCl [164]. Three cylindrical samples with an average diameter of 8 mm and an average length of 10 mm were tested in each group except samples 1B which have an average diameter of 6 mm and average length of 7 mm.

Table 6: PBS recipe.

Reagent	c_m [g·dm^{-3}]
NaCl	8.0266
KCl	0.2212
Na_2HPO_4·12 H_2O	3.6618
KH_2PO_4	0.2334

Firstly, the scaffolds were placed in PBS solution for 1 h, incubated at 37 °C and then they were taken from the solution, the excess of PBS was removed using the filter paper and they were weighed. Subsequently, the scaffolds were immersed in PBS solution with the added collagenase (2.2 mg/ml) and again they were incubated at 37 °C. The selected concentration of the collagenase approximately corresponded to the physiological concentration found in the skin or synovial fluid [165; 166].

At the given times (1, 2, 4, 8, 24, 48 and 72 h), the scaffolds were removed from the medium, squeezed between filter papers and they were weighed. Finally, the enzymatic in vitro degradation of the scaffolds was evaluated by means of the determination of weight loss according the following equation (3):

$$\text{Weight Loss (\%)} = \frac{w_i - w_t}{w_i} \cdot 100, \tag{3}$$

where w_i is the initial weight of the scaffold which was immersed 1 h in PBS solution at 37 °C and then the excess of PBS was removed using the filter paper, w_t is the weight of the scaffold after time t [167].

4.4.5 Attenuated Total Reflection Infrared Spectrometry

In order to notice the chemical interaction of HAp, β-TCP, α-TCP and collagen infrared analysis was performed using attenuated total reflection spectrometry (ATR-FTIR). Scaffolds were cut into 3 mm slices that were placed directly onto the diamond crystal for data acquisition. Small amount of bioceramic powders used in composite scaffolds were measured analogously to the scaffolds. All spectra were recorded in transmittance mode by collecting 32 scans in a spectral range of 4 000–600 cm^{-1} with a resolution of 4 cm^{-1} using software OPUS (Bruker, USA). A sample compartment and optic ways of the device were evacuated during whole recording.

4.4.6 Mechanical Properties

In order to describe the mechanical behaviour of the scaffolds in dry and hydrated states, compression tests were performed by means of the adaption of the ISO 13314 standard [168] which refers to the mechanical testing of porous and cellular metals. The mechanical properties of the scaffolds were measured on both dry samples and samples hydrated in NS conditioned at 37 °C for 5 min. Five cylindrical samples with an average diameter of 8 mm and an average length of 10 mm were tested in each group except samples 1B which have an average diameter of 6 mm and average length of 7 mm.

Plateau stress and energy absorption were determined using RSA-G2 Solids Analyzer in the compression mode (Fig. 10). The measurements were carried out at a constant linear rate of 0,05 mm·s^{-1} and at an axial force of 0.05 N for dry state and 0.01 N for hydrated state. The maximum gap change was chosen so that compressive strain was 50 %.

The stress-strain curves obtained were used to determine mechanical properties as follows: plateau stress (σ_{pl}) was defined as the arithmetical mean of the stresses between 20 % and 30 % of compressive strain. Energy of absorption (W) was calculated as the area under the stress-strain curve up to 50 % of strain. Finally, energy absorption efficiency (W_e) was calculated as energy absorption divided by upper limit of the compressive strain (ε_0) and the compressive stress at the upper limit of the compressive strain (σ_0). The upper limit of the compressive strain was 50 %.

In this context, plateau stress represents the closest concept to that of yield stress respectively, which is employed for solid materials. In order to simplify the comparison of sample's results and the results of other studies, it was assumed that plateau stress represents compressive strength [169; 170].

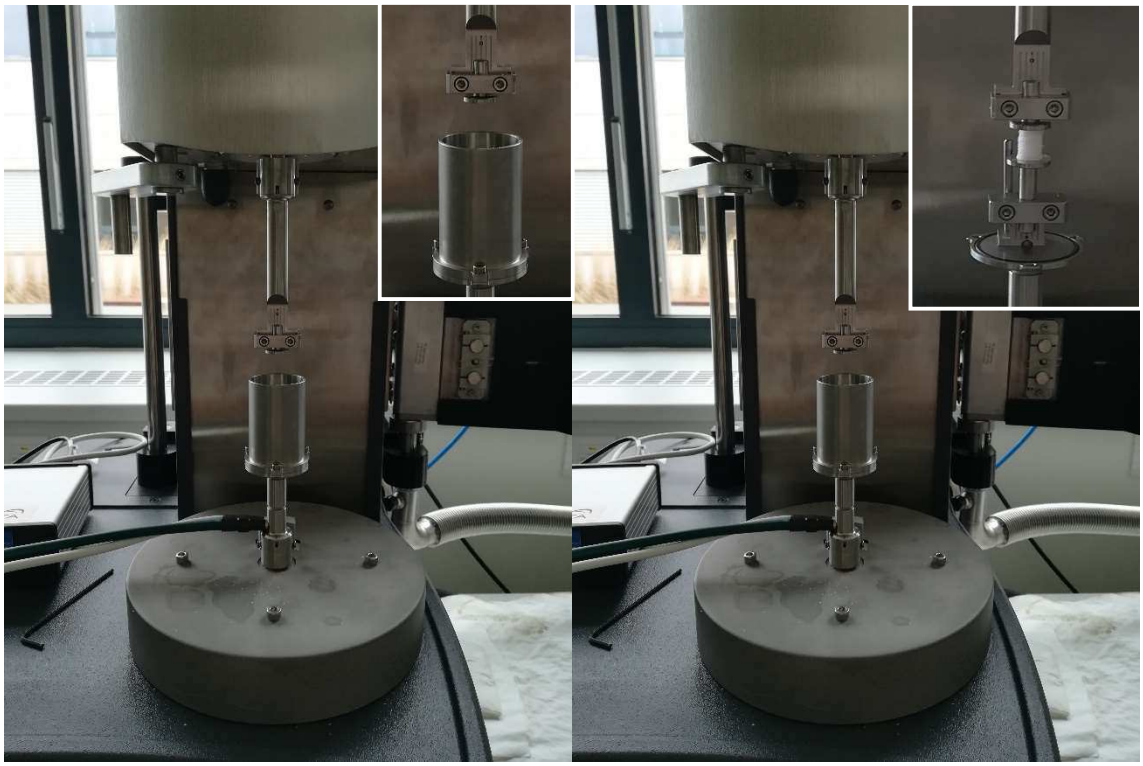

Fig. 10: Image of the geometry of RSA-G2 Solids Analyzer in the compression mode; left – measurement of hydrated scaffold where the geometry is immersed in NS, right – measurement of dry scaffold.

4.4.7 Biological Properties

The ability of the scaffolds to induce the osteogenic differentiation of human mesenchymal stem cells derived from bone marrow was evaluated by cell experiment that was performed by the Institute of Experimental Medicine, Prague. Each scaffold was seeded with 7 000 cells which were pre-cultured in a tissue culture flask with cell growth medium consisting of alpha-minimal essential medium (α-MEM) supplemented with 10% fetal bovine serum (FBS), 1% penicillin-streptomycin, calcium ascorbate-2-monophosphate (50 $\mu g \cdot ml^{-1}$), 10 mM of glycerol-2-monophosphate and 100 nM of dexamethasone. The experiment lasted 35 days and data were collected after 1, 7, 14, 21, 24 and 35 days.

The cell viability was monitored by the double stranded deoxyribonucleic acid (dsDNA) quantification test that was based on increasing fluorescent intensity that is observed when

PicoGreen binds to dsDNA. The fluorescent intensity of the PicoGreen dye was measured with a spectrofluorometer capable of producing the excitation wavelength of ~480 nm and recording at the emission wavelength of ~520 nm. The DNA was then quantified by comparison of the sample fluorescence to the fluorescence of a set of standards that were included in every sample run. Nuclea and cytoplasm were also visualized by dyeing DiOC/PI. Moreover, it was observed how deep into the scaffold cells penetrated. The rate of induction of osteogenic differentiation was assessed by the relative expression of mRNA (qPCR) of specific osteogenic marker – the transcription factor RunX2 (Runt-related transcription factor 2).

5 Results and Discussion

5.1 Morphology

The cross-section morphologies of the pure collagen scaffolds and the collagen/HAp/β-TCP/α-TCP composites were evaluated through SEM imaging. The micrographs of the pure collagen scaffolds (1A and 1B) are reported in
Fig. 11 and the micrographs of the collagen/HAp/β-TCP/α-TCP composite scaffolds (2A, 3A and 4A) are shown in Fig. 12. All scaffolds showed relatively similar highly porous 3D structure with high degree of interconnectivity, very similarly with the spongious bone.

The pore shape of the bovine collagen scaffold (1A) appeared relatively more regular and round-shaped compared to them of the porcine collagen scaffold (1B) in which the pores looked rather oval-shaped, elongated in one axis. Mineral phase in collagen/HAp/β-TCP/α-TCP composite scaffolds (2A, 3A and 4A) also made them irregular with elongated pores, but still they had more regular and complex architecture than samples of the porcine collagen scaffolds.

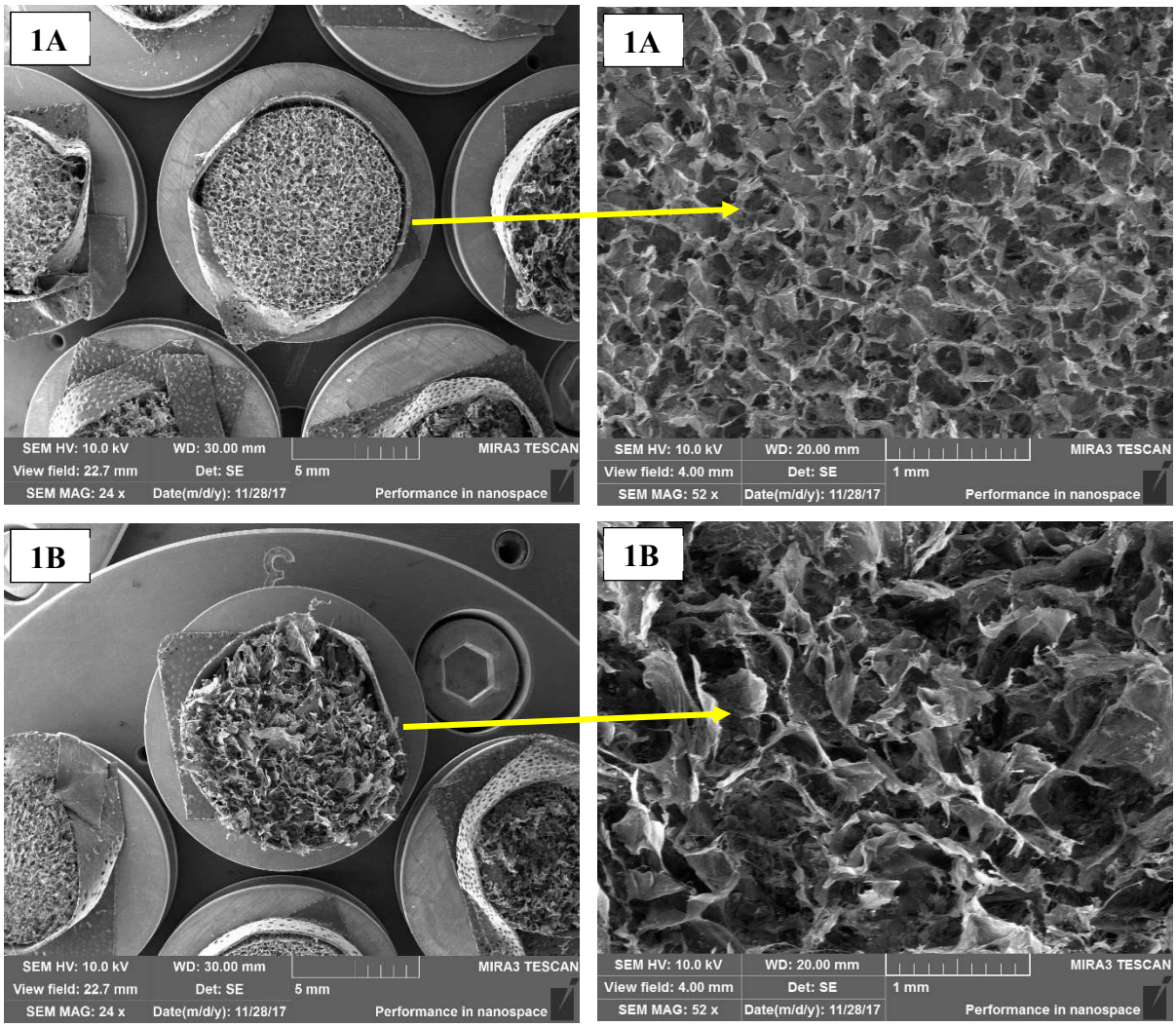

Fig. 11: SEM images of pure collagen scaffolds; overall view on the sample (left) and magnification of the inner structure (right).

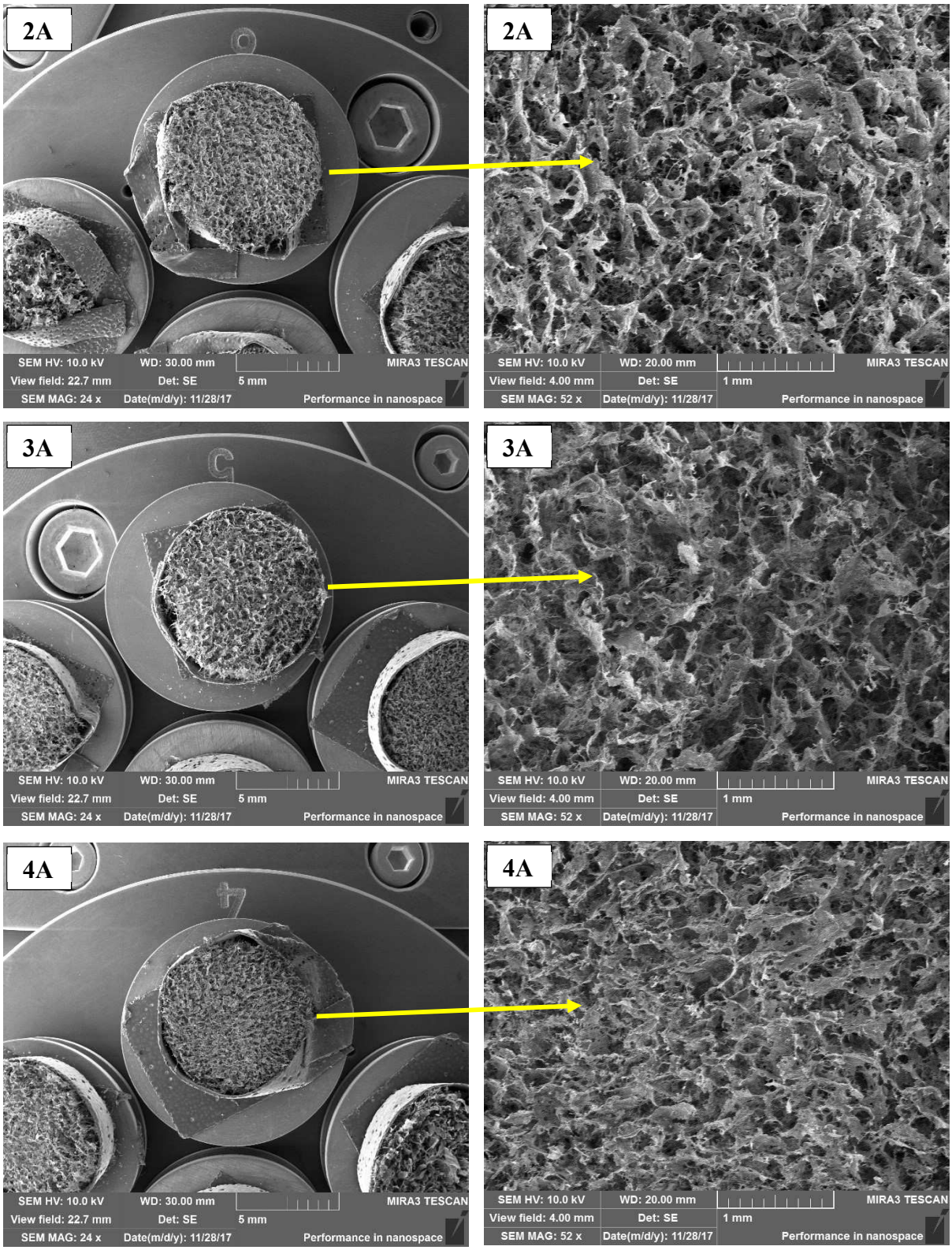

Fig. 12: SEM images of the collagen/HAp/β-TCP/α-TCP composite scaffolds; overall view on the sample (left) and magnification of the inner structure (right).

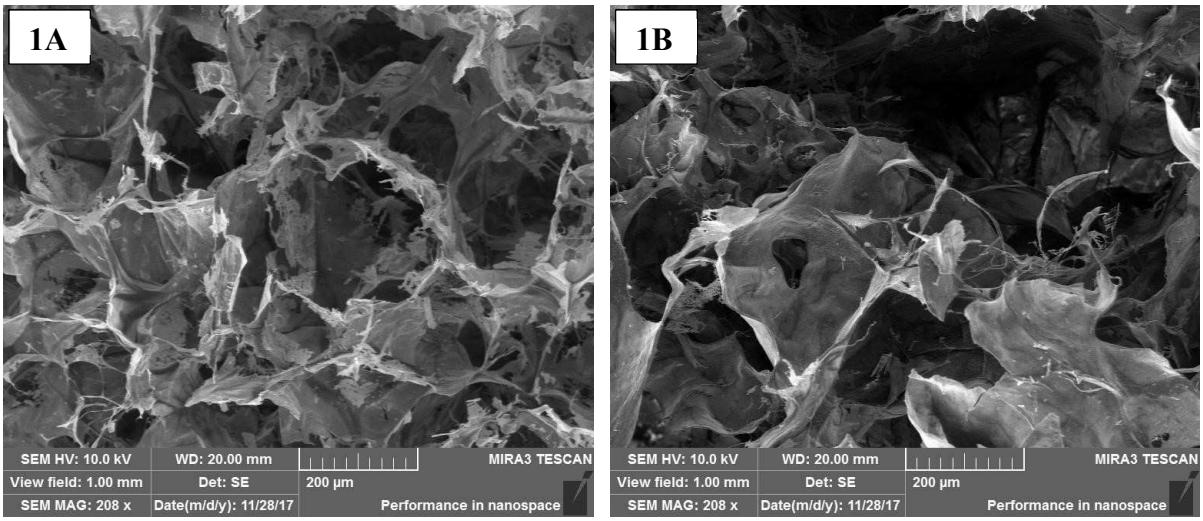

Fig. 13: SEM images of the pore walls of the pure collagen scaffolds

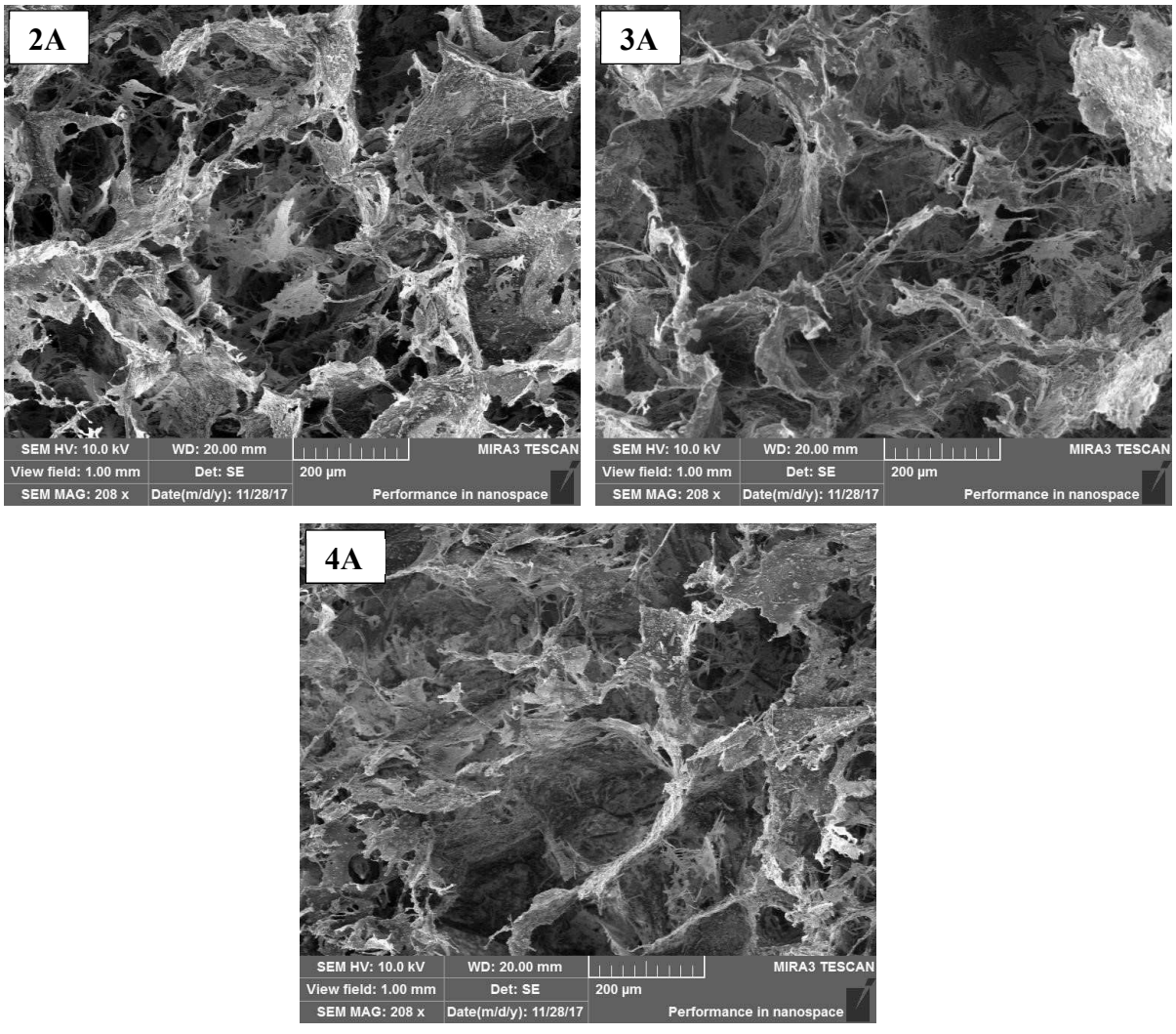

Fig. 14: SEM images of the pore walls of the collagen/HAp/β-TCP/α-TCP composite scaffolds

The morphology of the pore walls of the pure collagen scaffolds and the collagen/HAp/β-TCP/α-TCP composite scaffolds is illustrated in Fig. 13 and Fig. 14. Pores of the pure collagen scaffolds (1A and 1B) were defined by the walls with smooth surface. The pore formation during freeze-drying and crosslinking were related to the reduction of the collagen fibres in between pores which were accompanied with a formation of more sheet-like structures and condensed walls. On the contrary, particles of HAp, β-TCP and α-TCP that were well adhered on collagen matrix (samples 2A, 3A and 4A) as shown in Fig. 15, made the surface of the pore walls much rougher. They were also defined by sheet-like structures and condensed walls, although the sample 2A, 4A and especially 3A (sample with the predominance of TCPs particles) contained more collagen fibres in between pores unlike the pure collagen scaffolds (1A and 1B). It could be caused by TCPs particles and as shown in Fig. 14, the higher was content, the more fibrillar and relaxed was structure of the walls.

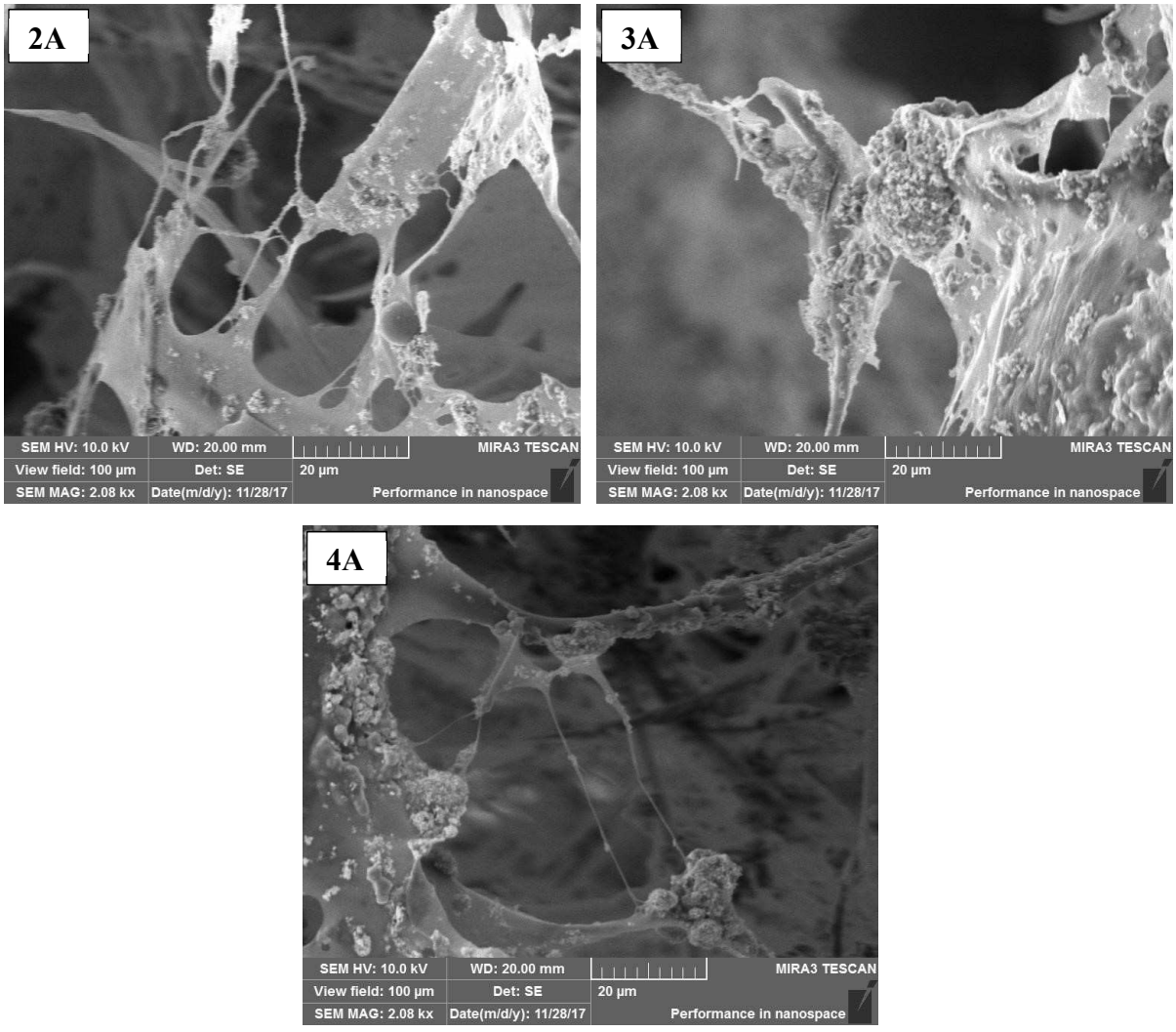

Fig. 15: SEM images of the detail of bioceramic particles adhered on collagen.

The pore size was measured by using software ImageJ. The pore size average and its standard deviation of the pure collagen scaffolds and the collagen/HAp/β-TCP/α-TCP composite scaffolds are reported in Table 7. The pore size distribution of the pure collagen scaffolds and the collagen/HAp/β-TCP/α-TCP composite scaffolds is illustrated in Fig. 16. The largest pores and at the same time the widest distribution of pore size of all samples had the porcine collagen scaffolds (1B). Contrary, the bovine collagen scaffolds (1A) had the narrowest distribution of pore size. The average pore size decreased by 20 % compared to the porcine collagen samples (1B). This difference in pore size and size distribution could be explained on molecular difference between collagens from each source. Previously published amino acid sequencing data for type I collagen showed differences between bovine and porcine collagens, eventually resulting in source-dependant variations [171]. Although, the fabrication method of these two collagen types could be further optimized by modifying the freeze-drying procedure in order to achieve the desired pore size.

The addition of bioceramics to the collagen matrix decreased mean pore size approx. by 20 % (about 100 μm). The width distribution of the pore size was almost identical to each other and wider than by the bovine collagen scaffolds (1A) and narrower than by the porcine collagen scaffolds (1B). The average pore size was increasing with higher ratio of TCPs in samples that could be explained by the influence of bioceramic on hydrophilicity of collagen. Insoluble HAp particles made scaffold less hydrophilic than in case of TCPs particles therefore they allow the aqua-porogen create smaller pores.

Table 7: The pore size average and its standard deviation of pure collagen scaffolds and collagen/HAp/β-TCP/α-TCP composite scaffolds.

Sample	**Pore size average [μm]**
1A	471 ± 127
1B	568 ± 252
2A	388 ± 151
3A	407 ± 142
4A	356 ± 137

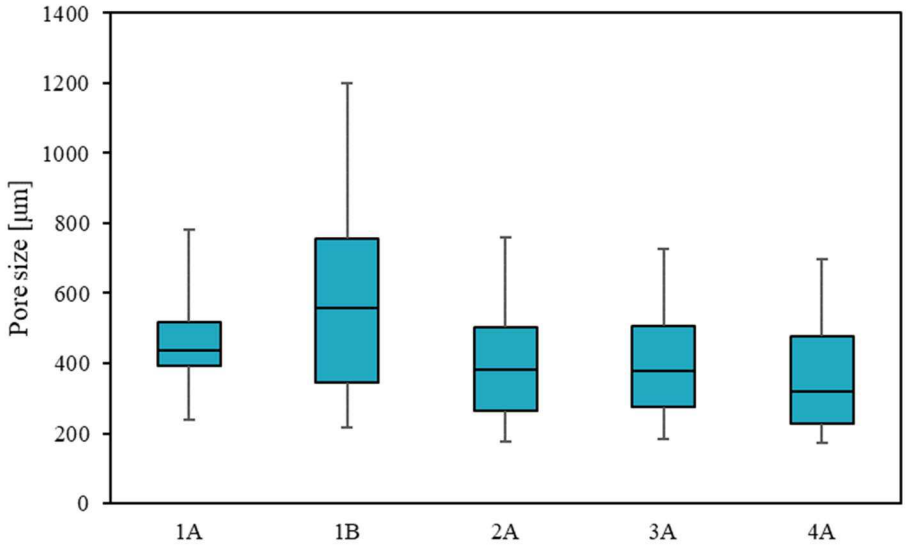

Fig. 16: The pore size average of the pure collagen scaffolds and the collagen/HAp/β-TCP/α-TCP composite scaffolds.

The pore size remained in a range of 170–500 µm except the porcine collagen scaffolds (1B) that remained in a range of 200–750 µm. It was reported that the optimum pore size to promote cell proliferation and migration in a bone tissue engineering was 325 µm. Larger pores then should provide an environment in which cells are not too tight and had good spreading, and multiple layers of cells could grow in multiple directions [172]. Thus, the bovine collagen scaffolds (1A) and collagen/HAp/β-TCP/α-TCP composite scaffolds (2A, 3A and 4A) should provide a superior substrate for the cell attachment and cell growth.

5.2 Porosity

As already mentioned above the microstructure such as pore size and its distribution, pore shape as well as porosity has the prominent influence on the cell intrusion, proliferation and function in tissue engineering. Therefore, the porosity of the pure collagen scaffolds and the collagen/HAp/β-TCP/α-TCP composite scaffolds was determined by two methods, which one of them was based on Archimedes principle and the second one was based on processing a binary image from a SEM image by ImageJ. Results of both methods are shown in Fig. 17 and the comparison of values from both methods is reported in Table 8. Using Archimedes principle, it was found that all samples were highly porous, and the porosity remained in a narrow range 96–98 % that was a close approximation to trabecular bone with 50–90% porosity [173].

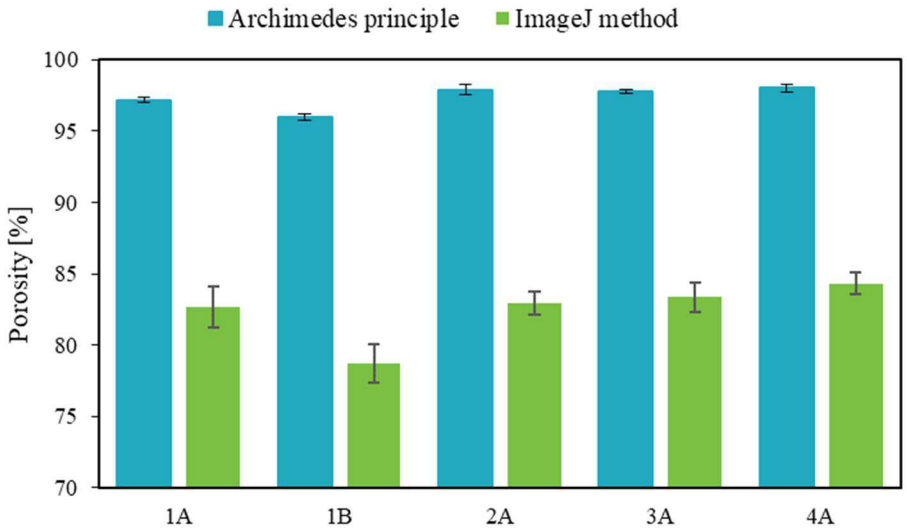

Fig. 17: The comparison of the porosity of the pure collagen scaffolds and the collagen/HAp/β-TCP/α-TCP composite scaffolds determined by using Archimedes principle and ImageJ method.

Using Archimedes principle, it was found that slightly more porous than the pure collagen scaffolds (1A and 1B) were collagen/HAp/β-TCP/α-TCP composite scaffolds (2A, 3A and 4A). The porosity of the individual samples 2A, 3A and 4A was nearly the same. Interactions between the bioceramic phase and the collagen could limit the collagen in self-assembly process which resulted in a higher porosity. It was not observed any effect of specific bioceramic particles on porosity, they functioned as a mixture.

The porcine collagen scaffolds (1B) were the least porous and that could be explained again on molecular difference between collagens from each source. From the perspective of the porosity that ensures the transport of nutrients, metabolites and cell proliferation, the porcine collagen scaffolds were not as suitable as other tested scaffolds for using in tissue engineering.

Table 8: The comparison of the average porosity and the standard deviation of the pure collagen scaffolds and the collagen/HAp/β-TCP/α-TCP composite scaffolds determined by using Archimedes principle and software ImageJ.

	Archimedes principle	**ImageJ software**
Sample	Average porosity [%]	Average porosity [%]
1A	97.2 ± 0.2	82.7 ± 1.4
1B	96.0 ± 0.2	78.7 ± 1.4
2A	97.9 ± 0.3	82.9 ± 0.8
3A	97.7 ± 0.2	83.4 ± 1.0
4A	98.0 ± 0.2	84.3 ± 0.7

Using ImageJ software was found that the porosity of all samples remained in a lower range 78–84 %. The trend of porosity among tested samples was almost identical with samples measured by using Archimedes principle, but values were decreased by 15 % (as seen in Fig. 17). Such a difference probably arose by converting a 3D SEM image into a 2D binary image

using threshold. When SEM images of very thin cuts of samples were used to reduce a distortion by 3D structures as much as possible, it could be achieved similar values which were measured by using Archimedes principle. On the other hand, processing of very thin cuts of the collagen scaffolds could be problematic to get under the condition that the pore shape was not deformed anyway.

5.3 Swelling Behaviour

The water absorption capacity of pure collagen scaffolds and collagen/HAp/β-TCP/α-TCP composite scaffolds was determined by equilibrium swelling studies and results are demonstrated in Fig. 18 by a swelling ratio dependence on time. Swelling was very closely related to pore size and porosity of the samples. All samples were swollen for 15 minutes at the constant weight. The pure collagen scaffolds achieved the highest swelling ratio, especially the porcine collagen scaffolds (1B) which had the largest mean pore size from all scaffolds. The swelling ratio of the bovine collagen scaffolds (1A), with higher degree of porosity but a smaller mean pore size, was close to the porcine collagen scaffolds (1B).

The content of bioceramic particles decreased significantly hydrophilic characteristics of the collagen/HAp/β-TCP/α-TCP composite scaffolds (2A, 3A and 4A). Water-insoluble HAp particles made the scaffolds the least hydrophilic, but quite stable. Therefore, the sample 4A with a high content of HAp got swollen after 15 min and stayed weight stable over the entire length of the experiment. Water-soluble TCPs particles made the scaffolds still hydrophilic but not as much as HAp particles. The sample 3A with a high content of soluble TCPs got swollen after 15 min and then the weight decreased. It was probably caused by washing out of TCPs particles from the scaffold.

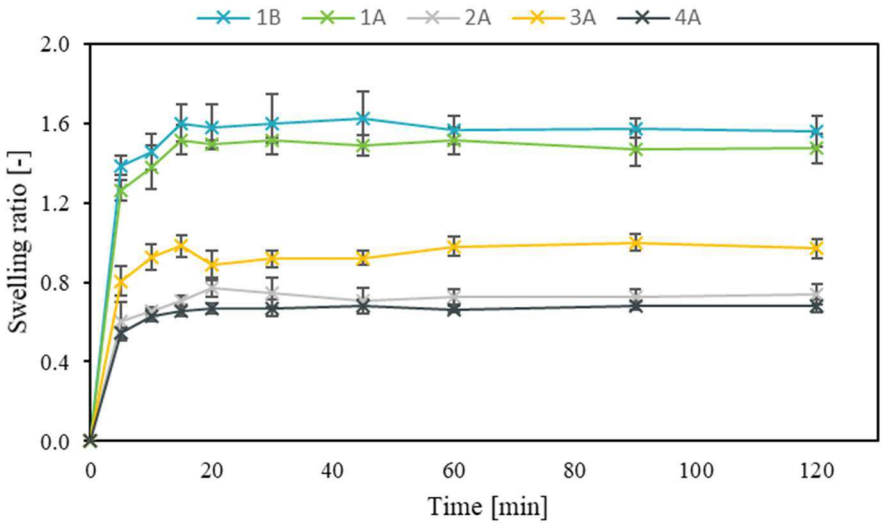

Fig. 18: The swelling ratio of the pure collagen scaffolds and the collagen/HAp/β-TCP/α-TCP composite scaffolds.

5.4 Enzymatic Degradation

The in vitro degradation test of the pure collagen scaffolds and the collagen/HAp/β-TCP/α-TCP composite scaffolds was investigated by monitoring the mass loss depending on the exposure time to the collagenase solution. The biodegradation results of the pure collagen scaffolds and the collagen/HAp/β-TCP/α-TCP composite scaffolds are demonstrated in Fig. 19.

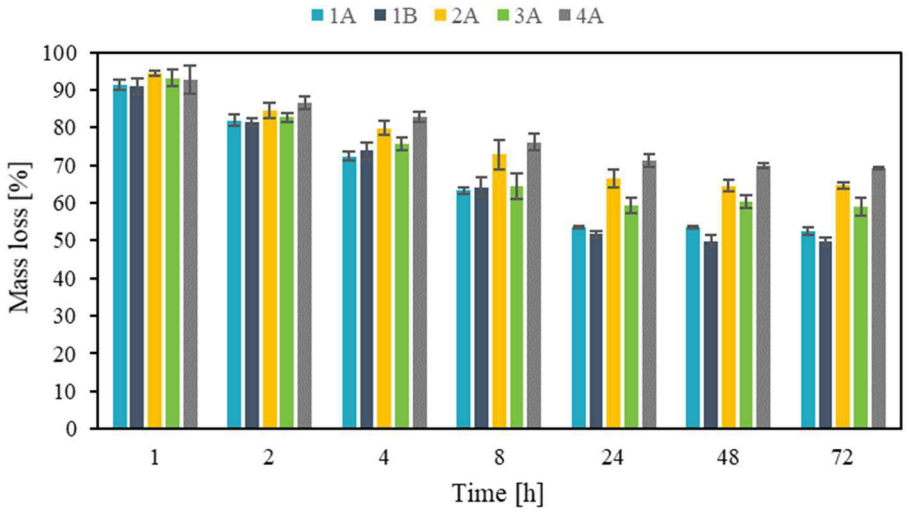

Fig. 19: The mass loss of the pure collagen scaffolds and the collagen/HAp/β-TCP/α-TCP composite scaffolds during enzymatic degradation after 1, 2, 4, 8, 24, 48 and 72 hours of degradation.

Pure collagen scaffolds achieved after 72 hours the greatest mass loss when only 52 % remained of the bovine collagen scaffolds (1A) and 50 % remained of the porcine collagen scaffolds (1B). At beginning, their degradation rate was slightly higher, although, after 24 hours their weights significantly decreased compared to the collagen/HAp/β-TCP/α-TCP composite scaffolds (2A, 3A and 4A). Also, there were visible changes in the structure of pure collagen scaffolds. They became softer and tended to fall apart, especially the porcine collagen scaffolds (1B). The irregular morphology of the porcine collagen enhanced the accessibility of collagenase to the peptide bonds, thus the degradation occurred easier.

Bioceramic particles apparently stabilized the collagen scaffolds against the collagenase activity. Their mass loss was 30–40 % after 72 hours of degradation and there were not visible changes in the structure compared to the pure collagen scaffolds (1A and 1B). Their addition made the collagen/HAp/β-TCP/α-TCP composite scaffolds (2A, 3A and 4A) less hydrophilic, so that the collagenase in PBS solution could not get to the collagen matrix so easily as in pure collagen scaffolds. The sample with predominance of HAp (4A) was the most stable as the hydrophilicity of composite scaffold was the lowest. On the contrary, the sample with predominance of β-TCP (3A) was the least stable against degradation. Surely, the mass loss was also influenced by washing out of unbounded bioceramic particles from scaffold and by dissolution of TCPs as was observed in sample with predominance of β-TCP (3A).

The weight of both, the pure collagen scaffolds and the collagen/HAp/β-TCP/α-TCP composite scaffolds did not change much after 24-hour degradation that could be caused by the exhaustion of an enzyme activity of the collagenase.

5.5 Attenuated Total Reflection Infrared Spectrometry

The pure collagen scaffolds (1A and 1B), the bioceramic particles and the collagen/HAp/β-TCP/α-TCP composite scaffolds (2A, 3A and 4A) were characterized by ATR-FTIR spectrometry and recorded infrared spectra are demonstrated in Fig. 20–Fig. 22. Assignments of the observed vibrational frequencies and their referenced range of wavenumber for the pure collagen scaffolds, the bioceramic particles and the collagen/HAp/β-TCP/α-TCP composite scaffolds are noted in Table 9–Table 11. These studies were performed to ensure that the cross-linking with bioceramics has not affected the chemistry of collagen. This could be important considering that cells are more prone to attach surfaces containing natural binding sites [174].

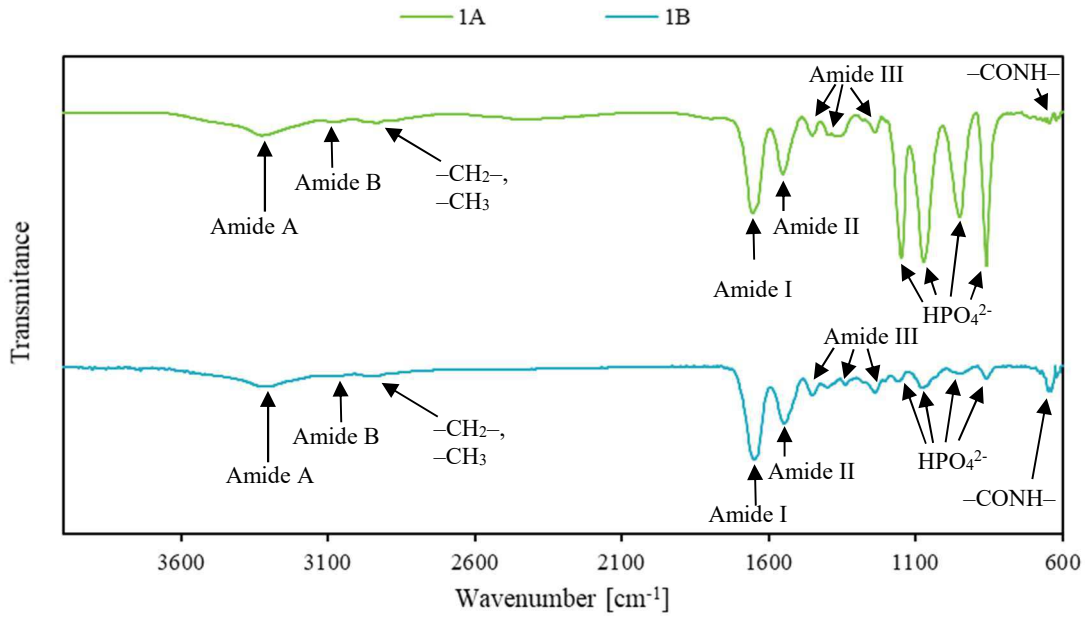

Fig. 20: ATR-FTIR spectra of the pure bovine collagen scaffolds (1A) and the pure porcine collagen scaffolds (1B).

ATR-FTIR spectra of both pure collagen scaffolds (1A and 1B) were quite similar and showed typical bands of type I collagen (as seen in Fig. 20 and in Table 9). These included the main absorption bands of amide A (little intense), amide B (little intense), amide I, amide II and amide III. The amide A band was a result of a free N–H stretching vibration and should occurred in the range of 3440–3400 cm^{-1} but the peak was found at ~3300 cm^{-1}. The band position was shifted because of the NH group of a peptide that was involved in hydrogen bonding, probably with a carbonyl group of the peptide chain [175]. The amide B band that was found at wavenumbers of ~3080 cm^{-1} represented the asymmetrical stretching of C–H group. The amide I peak at ~1650 cm^{-1} was associated with stretching vibrations of carbonyl groups (C=O bond), along polypeptide backbone. The amide II peaks at ~1450 cm^{-1} and ~1550 cm^{-1} were resulting from N–H bending vibration coupled with the stretching vibration C–N bond. The amide III peaks at ~1240 cm^{-1}, ~1340 cm^{-1} and ~1400 cm^{-1} were related to CN stretching [176]. The amide A and amide II peaks that were related to NH stretching and N–H bending

also indicated that these functional groups could be still available to promote cell attachment to collagen [177].

The spectra contained little intense bands in the range of 2940–2850 cm^{-1} that corresponded to asymmetrical stretching of CH_2 and symmetrical stretching of CH_3 groups in chain and bands in the range of 710–640 cm^{-1} that were related to out of plane bending of N–H. Moreover, the spectra showed non-typical bands at the range 1150–850 cm^{-1}. Especially in the spectrum of the bovine collagen scaffolds (1A), these bands were very intensive. This range corresponded to asymmetric and symmetric stretching of PO. It could be related to improperly washed out hydrogen phosphate which was used for washing the scaffolds after crosslinking.

Table 9: Assignments of the observed vibrational frequencies and their referenced range of the wavenumber for the pure bovine collagen scaffolds (1A) and the pure porcine collagen scaffolds (1B).

Sample	Absorption band [cm^{-1}]	Ref. range of wavenumber [cm^{-1}]	Assignment	Functional group	Ref.
1A	3323	3370–3270	Amide A	–CONH–	[178; 179; 180; 181]
	3082	3100–3070	Amide B	–CONH–	
	2933	2995–2915	$\nu_{as}(CH_2)$	$–CH_2–$	
	2878	2895–2840	$\nu_s(CH_3)$	$–CH_3$	
	1655	1720–1600	Amide I	–CONH–	
	1553, 1452	1600–1450	Amide II	$–CONH_2$	
	1396	1420–1400	Amide III	$–CONH_2$	
	1336	1350–1310	Amide III	–CONH–	
	1280, 1238	1305–1200	Amide III	–CONH–	
	1147	1250–1100	$\nu_s(PO)$	HPO_4^{2-}	
	1072, 950	1100–900	$\nu_{as}(PO)$	HPO_4^{2-}	
	858	880–850	$\nu(PO)$	HPO_4^{2-}	
	711, 682, 646, 621	770–620	$\gamma(NH)$	–CONH–	
1B	3313	3370–3270	Amide A	–CONH–	[178; 179; 180; 181]
	3078	3100–3070	Amide B	–CONH–	
	2937	2995–2915	$\nu_{as}(CH_2)$	$–CH_2–$	
	2877	2895–2840	$\nu_s(CH_3)$	$–CH_3$	
	1650	1680–1630	Amide I	–CONH–	
	1546, 1452	1600–1450	Amide II	$–CONH_2$	
	1398	1420–1400	Amide III	$–CONH_2$	
	1338	1350–1310	Amide III	–CONH–	
	1238, 1205	1305–1200	Amide III	–CONH–	
	1159	1250–1100	$\nu_s(PO)$	HPO_4^{2-}	
	1080, 943	1100–900	$\nu_{as}(PO)$	HPO_4^{2-}	
	860	880–850	$\nu(PO)$	HPO_4^{2-}	
	705,676,648	770–620	$\gamma(NH)$	–CONH–	

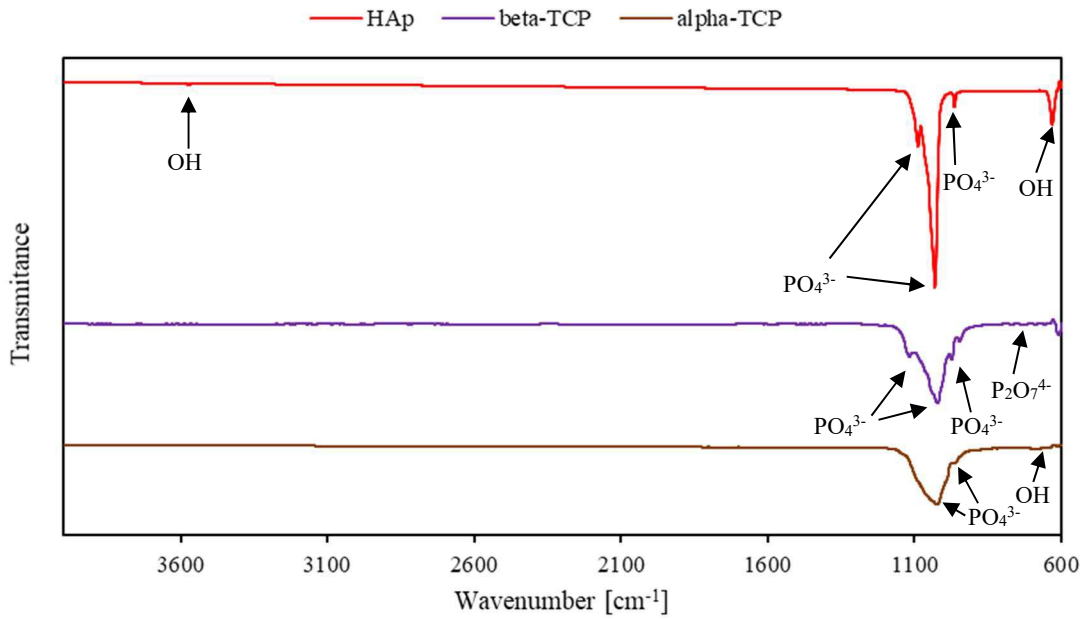

Fig. 21: ATR-FTIR spectra of the bioceramic particles used in the samples.

Table 10: Assignments of the observed vibrational frequencies and their referenced range of the wavenumber for HAp, β-TCP, α-TCP particles.

Sample	Absorption band [cm^{-1}]	Ref. range of wavenumber [cm^{-1}]	Assignment	Functional group	Ref.
HAp	3572	3670–3400	ν(OH)	–OH	[178; 179]
	1087, 1031,962	1100–900	ν_{as}(PO)	PO_4^{3-}	
	630	770–600	γ(OH)	–OH	
β-TCP	1217, 1119	1250–1100	ν_s(PO)	PO_4^{3-}	[178; 179; 182]
	1022, 973, 946	1100–900	ν_{as}(PO)	PO_4^{3-}	
	726	750–700	ν_s(POP)	$P_2O_7^{4-}$	
	605	600–500	δ(PO)	PO_4^{3-}	
α-TCP	1024, 964	1100–900	ν_{as}(PO)	PO_4^{3-}	[178; 179]
	686	770–600	γ(OH)	–OH	

Bioceramic particles content was mainly determined by bands located between 1200–900 cm^{-1} in spectra of collagen/HAp/β-TCP/α-TCP composite scaffolds. The all spectra of collagen/HAp/β-TCP/α-TCP composite scaffolds contained intensive vibrational bands of HAp (as shown in Fig. 21 and Table 10) which were results of asymmetric stretching of PO (1087, 1031, 962 cm^{-1}) and out of plane bending of O–H (630 cm^{-1}). The spectrum of the sample 3A also showed some of specific bands of β-TCP (Fig. 21 and Table 10) which were results of asymmetric stretching of PO (973, 946 cm^{-1}) and symmetric stretching of POP (723 cm^{-1}) from calcium pyrophosphate.

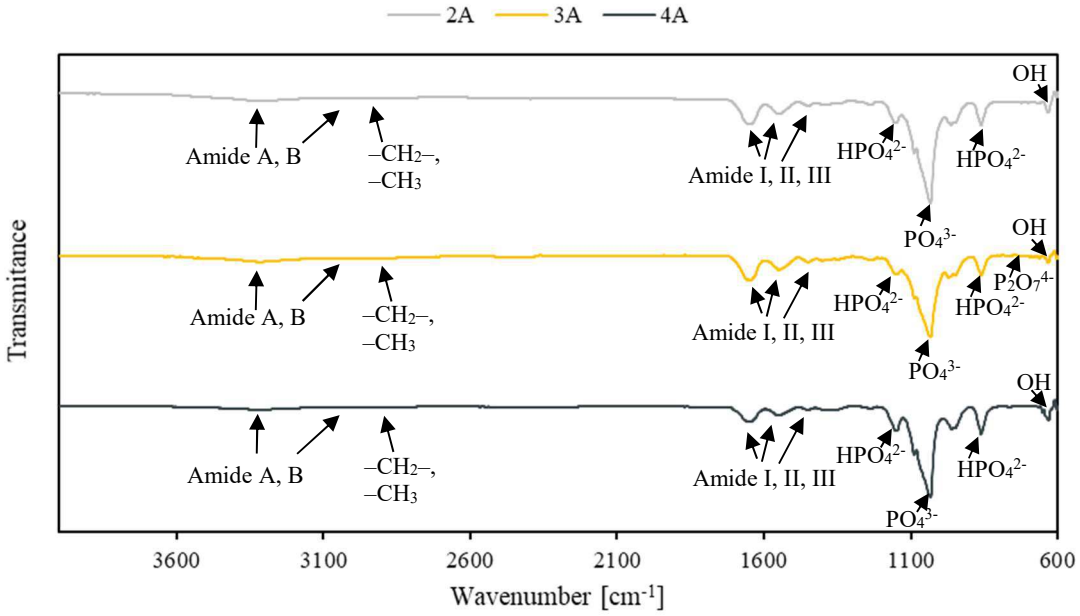

Fig. 22: ATR-FTIR spectra of the collagen/HAp/β-TCP/α-TCP composite scaffolds (2A, 3A and 4A).

ATR-FTIR spectra of the collagen/HAp/β-TCP/α-TCP composite scaffolds (Fig. 22 and Table 11) were also quite the same and showed typical bands of type I collagen which were approximately at similar wavenumbers as in the spectrum of the bovine collagen scaffold. The amide A and the amide B band position shifted towards lower wavenumbers (from 3323 cm^{-1} up to 3313 cm^{-1}) indicated the formation of bonds between bioceramic particles and the collagen matrix. The shift of amide A to lower wavenumbers was more significant in the samples with HAp predominance (4A) than in the samples with β-TCP predominance (3A) that could mean that bonds between HAp and collagen were stronger than between β-TCP and collagen. Another small shift towards lower wavenumbers occurred with the band of amide I. That could be related to new chelate bonds between Ca^{2+} and C=O bond. As the spectra of pure collagen scaffolds, the spectra of composite scaffolds also contained little intense bands in the range of 2940–2850 cm^{-1} that corresponded to asymmetrical stretching of CH_2 and symmetrical stretching of CH_3 groups in chain. Again, there was a presence of non-typical bands (of lower intensity compared to the bovine collagen scaffold) at the range 1150–850 cm^{-1} related to unproperly washed out hydrogen phosphate which was used for washing the scaffolds after crosslinking.

Table 11: Assignments of the observed vibrational frequencies and their referenced range of wavenumber for the collagen/HAp/β-TCP/α-TCP composite scaffolds.

Sample	Absorption band [cm^{-1}]	Ref. range of wavenumber [cm^{-1}]	Assignment	Functional group	Ref.
2A	3315	3370–3270	Amide A	–CONH–	[178; 179; 180; 181]
	3076	3100–3070	Amide B	–CONH–	
	2935	2995–2915	$\nu_{as}(CH_2)$	$–CH_2–$	
	2875	2895–2840	$\nu_s(CH_3)$	$–CH_3$	

	1649	1680–1630	Amide I	–CONH–	
	1550, 1452	1600–1450	Amide II	$–CONH_2$	
	1398	1420–1400	Amide III	$–CONH_2$	
	1350	1350–1310	Amide III	–CONH–	
	1238	1305–1200	Amide III	–CONH–	
	1149	1200–900	$\nu_{as}(PO)$	HPO_4^{2-}	
	1087, 1032, 962	1100–900	$\nu_{as}(PO)$	PO_4^{3-}	
	860	880–850	ν(PO)	HPO_4^{2-}	
	723	750–700	$\nu_s(POP)$	$P_2O_7^{4-}$	
	632	770–600	γ(OH)	–OH	
3A	3317	3370–3270	Amide A	–CONH–	[178; 179; 180; 181]
	3074	3100–3070	Amide B	–CONH–	
	2933	2995–2915	$\nu_{as}(CH_2)$	$–CH_2–$	
	2879	2895–2840	$\nu_s(CH_3)$	$–CH_3$	
	1649	1680–1630	Amide I	–CONH–	
	1549, 1450	1600–1450	Amide II	$–CONH_2$	
	1400	1420–1400	Amide III	$–CONH_2$	
	1344	1350–1310	Amide III	–CONH–	
	1236	1305–1200	Amide III	–CONH–	
	1148	1200–900	$\nu_{as}(PO)$	HPO_4^{2-}	
	1086, 1032, 972, 946	1100–900	$\nu_{as}(PO)$	PO_4^{3-}	
	860	880–850	ν(PO)	HPO_4^{2-}	
	723	750–700	$\nu_s(POP)$	$P_2O_7^{4-}$	
	632	770–600	γ(OH)	–OH	
4A	3313	3370–3270	Amide A	–CONH–	[178; 179; 180; 181]
	3074	3100–3070	Amide B	–CONH–	
	2933	2995–2915	$\nu_{as}(CH_2)$	$–CH_2–$	
	2879	2895–2840	$\nu_s(CH_3)$	$–CH_3$	
	1649	1680–1630	Amide I	–CONH–	
	1550, 1456	1600–1450	Amide II	$–CONH_2$	
	1396	1420–1400	Amide III	$–CONH_2$	
	1238	1305–1200	Amide III	–CONH–	
	1149	1200–900	$\nu_{as}(PO)$	HPO_4^{2-}	
	1087, 1033, 962	1100–900	$\nu_{as}(PO)$	PO_4^{3-}	
	860	880–850	ν(PO)	HPO_4^{2-}	
	631	770–600	γ(OH)	–OH	

5.6 Mechanical Properties

The mechanical properties of the scaffolds in dry and hydrated states obtained in the study are illustrated in Fig. 23 (dry state) and in Fig. 24 (hydrated state), results and their standard deviations are noted to Table 12. The mechanical properties of the scaffolds in dry state were mainly influenced by inner morphology of the scaffolds and in hydrated state (in simulated body conditions) by their composition.

The bovine collagen scaffolds (1A) with the most regular inner morphology achieved the highest compressive stress represented by plateau stress. A quite regular architecture of the sample could work as a reinforcing component. The scaffolds containing bioceramic particles (2A, 3A and 4A) reached slightly lower compressive stresses. Composite collagen scaffolds were prepared by freeze-drying and cross-linking always with a content of bioceramic phase, because of this, particles were well adhered to the collagen matrix whereas made it more brittle. The porcine collagen scaffolds (1B) achieved the lowest value of compressive stress due to the irregular inner structure with large and highly elongated pores in one axis.

A different trend was observed by compressive strength of all the samples following hydration. The compressive strength of the all samples significantly decreased (by 100×). The lowest compressive stress was achieved by bovine collagen scaffolds (1A). Contrary, bioceramic particles demonstrated as reinforcing component of the scaffolds and also, they decreased hydrophilicity of the scaffold, so they prevent the normal saline solution to weak the collagen matrix. The porcine collagen scaffolds (1B) reached the highest value of compressive stress, although that was caused by the geometry and structure of the samples. The results of compressive stress of the samples 1B that were obtained during the compression test in the hydrated state did not match values of the porous sample. The pore structure of 1B absolutely collapsed after the hydration, and the response of the bulk material was measured instead.

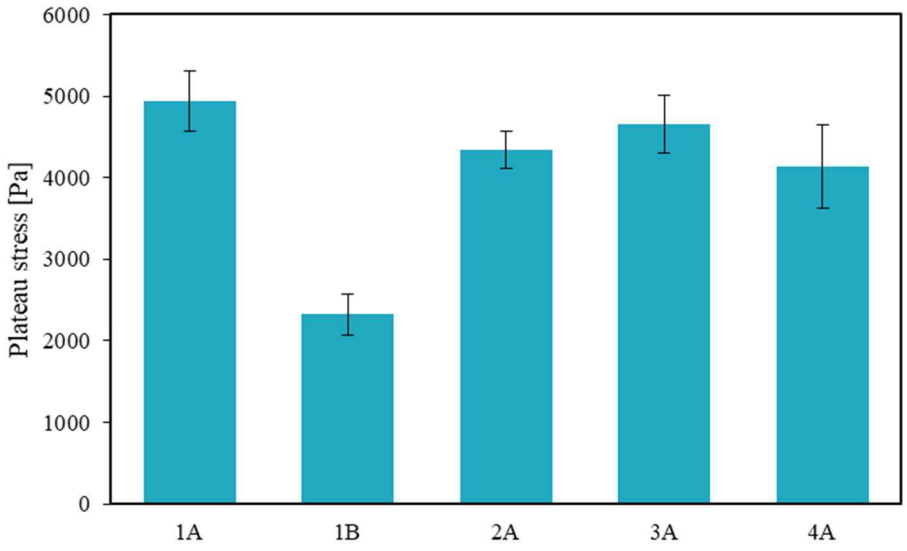

Fig. 23: Plateau stress (compressive strength) of the pure collagen scaffolds and the collagen/HAp/β-TCP/α-TCP composite scaffolds in dry state.

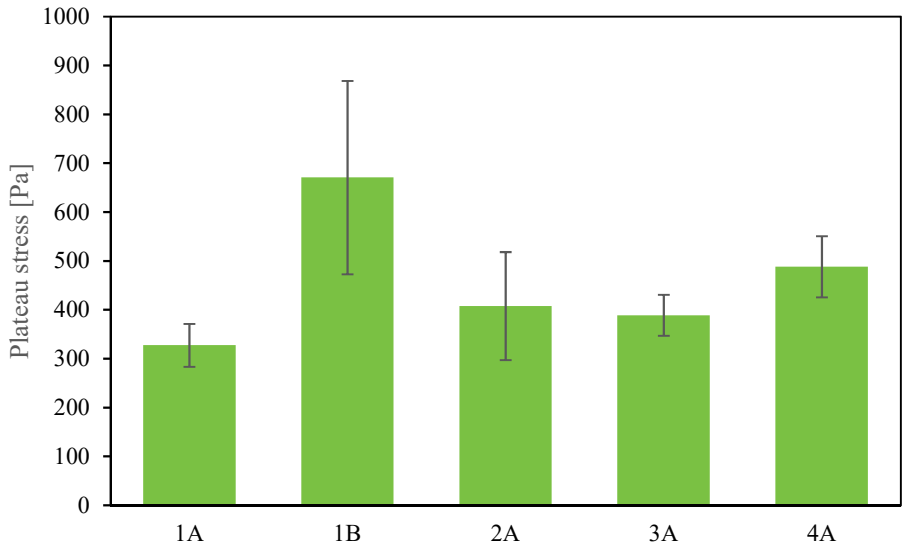

Fig. 24: Plateau stress (compressive strength) of the pure collagen scaffolds and the collagen/HAp/β-TCP/α-TCP composite scaffolds in hydrated state.

In contrast to previous findings, energy absorption efficiency in hydrated state significantly decreased only in the bovine collagen scaffolds (1A; by 26 %) compared to collagen/HAp/β-TCP/α-TCP composite scaffolds (2A, 3A and 4A) where the decrease was very small, almost insignificant. This parameter represented the ability of the material to effectively absorb deformation energy. A comparison of energy absorption efficiency in the dry state and hydrated state indicated relatively small changes in the inner structures of the bovine collagen scaffolds (1A) and collagen/HAp/β-TCP/α-TCP composite scaffolds (2A, 3A and 4A) following hydration.

The pure porcine collagen scaffolds (1B) showed even increase of energy absorption efficiency following hydration, although that was related the geometry and structure of the samples as reported previously. The measured values of energy absorption efficiency did not match to the porous samples 1B but the bulk material of the samples 1B.

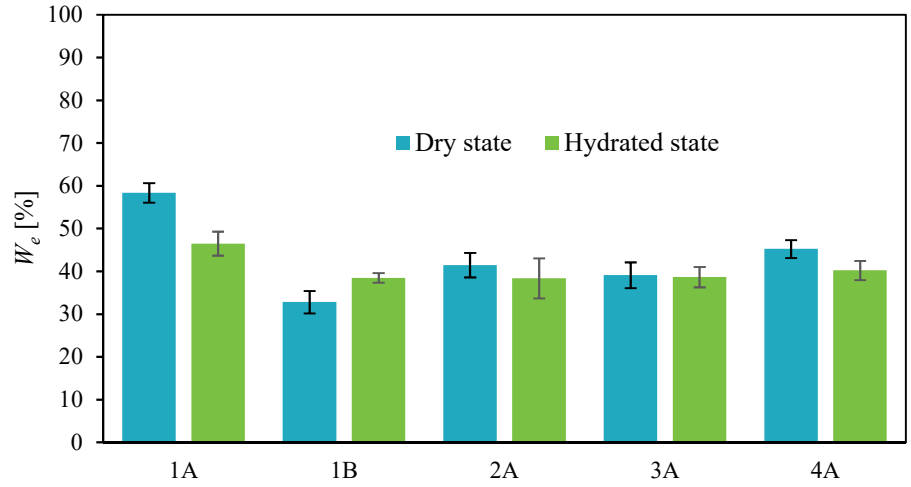

Fig. 25: Energy absorption efficiency of the pure collagen scaffolds and the collagen/HAp/β-TCP/α-TCP composite scaffolds in dry and hydrated states.

Table 12: Results and their standard deviations of mechanical testing of the pure collagen scaffolds and the collagen/HAp/β-TCP/α-TCP composite scaffolds.

Sample	Plateau stress in dry state [Pa]	Plateau stress in hydrated state [Pa]	Energy absorption efficiency in dry state [%]	Energy absorption efficiency in hydrated state [%]
1A	4931 ± 368	327 ± 44	58 ± 2	46 ± 3
1B	2327 ± 252	671 ± 198	33 ± 3	38 ± 1
2A	4339 ± 224	408 ± 111	41 ± 3	38 ± 5
3A	4658 ± 355	389 ± 42	39 ± 3	39 ± 2
4A	4139 ± 515	488 ± 63	45 ± 2	40 ± 2

5.7 Biological Properties

Number of cells living on the pure collagen scaffolds (1A and 1B) and collagen/HAp/β-TCP/α-TCP composite scaffolds (2A, 3A and 4A) were quantified using dsDNA test and the results are demonstrated in Fig. 26. The visualisation of the number of cells on scaffolds is shown in Fig. 27 and the depth penetration of cells is shown in Fig. 28. None of the tested scaffolds were cytotoxic. Cells in all samples proliferated during whole experiment, indicating sufficient mechanical stimulation by their environment.

The most preferable environment for cell adhesion and proliferation was after 21 days in the bovine collagen scaffolds (1A). The collagen itself promoted high cell adhesion and cell proliferation as seen in Fig. 26–Fig. 28. The porcine collagen scaffolds (1B) also provided environment for cell adhesion and proliferation especially thanks his largest mean pore size, although cells did not have appropriate stimuli to proliferate more and differentiate, then they probably started to die.

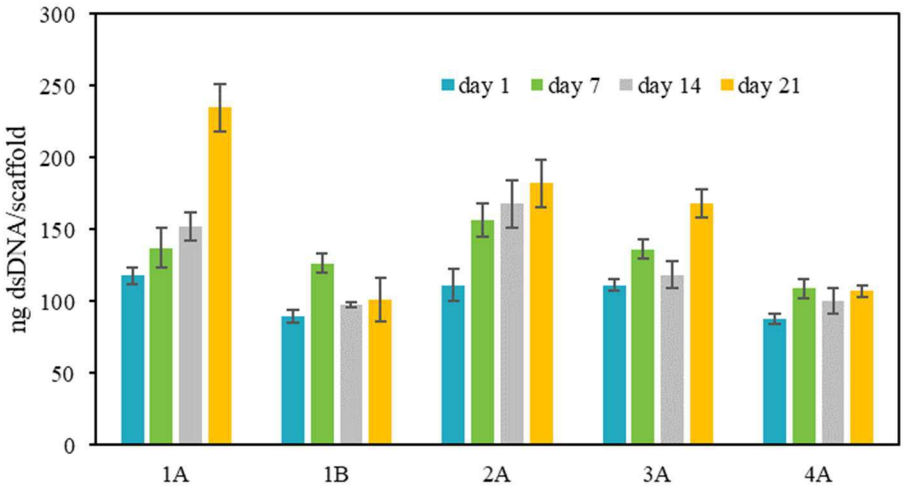

Fig. 26: Amount of cellular dsDNA on the pure collagen scaffolds and the collagen/HAp/β-TCP/α-TCP composite scaffolds after 1, 7, 14 and 21 days.

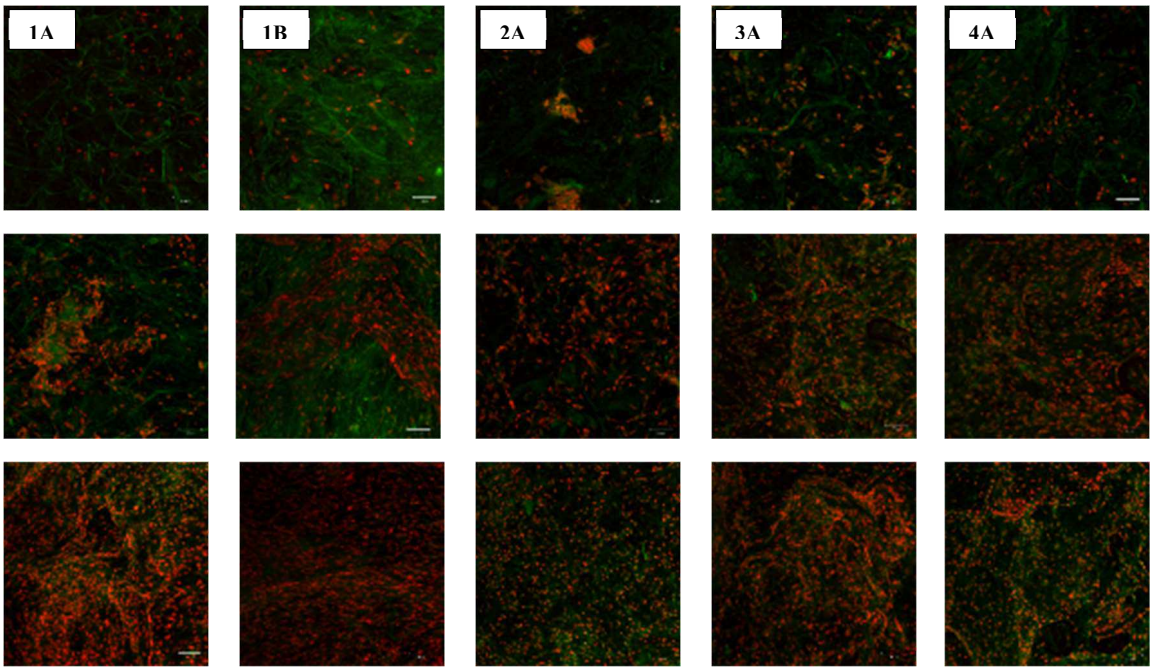

Fig. 27: Images from fluorescence microscope of cells (DiOC/PI dyeing) on the pure collagen scaffolds and the collagen/HAp/β-TCP/α-TCP composite scaffolds, nuclea of cells are red and cytoplasm is green; upper row – after 1 day, middle row – after 14 days, bottom row – after 21 days.

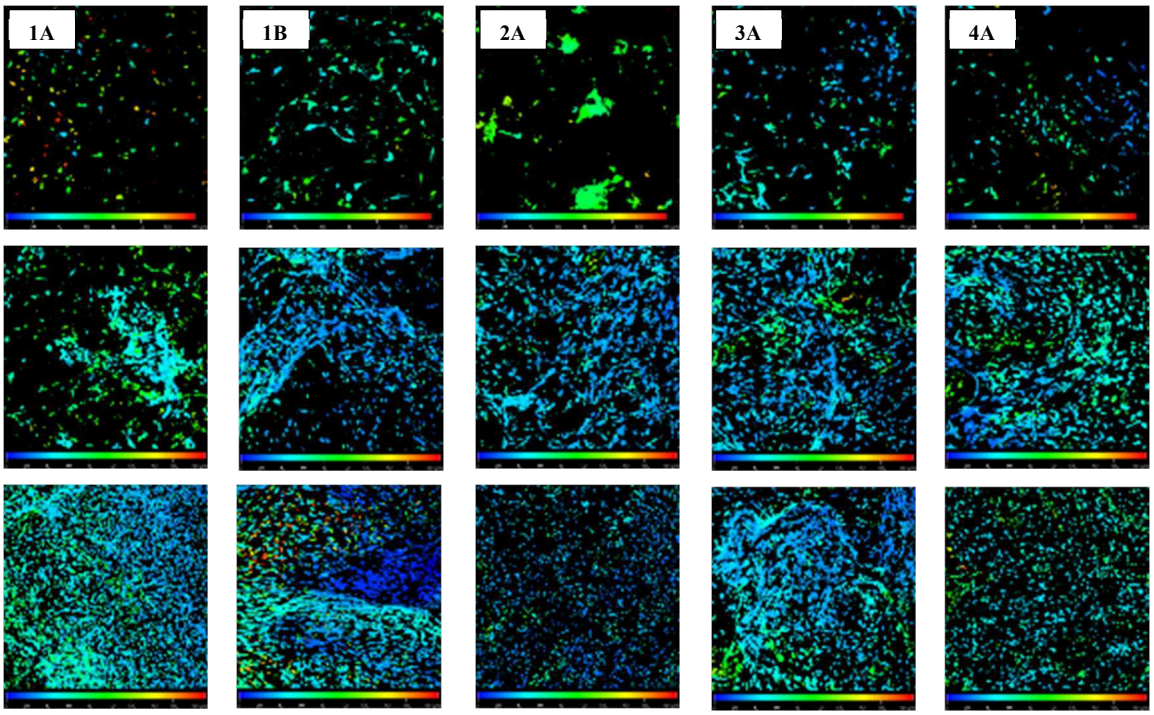

Fig. 28: Images of depth projection of cell penetration into the pure collagen scaffolds and the collagen/HAp/β-TCP/α-TCP composite scaffolds; upper row – after 1 day, max depth 150 μm, middle row – after 14 days, max depth 200 μm, bottom row – after 21 days, max depth 200 μm; the red coloured is the deepest.

Addition of HAp and TCPs particles to the collagen matrix in ratio 1 : 1 (sample 2A) enhanced cell adhesion and cell proliferation sufficiently and even better after 7 and 14 days compared to the bovine collagen scaffolds (1A). TCPs particles that were more soluble and resorbable than HAp promoted mainly cell adhesion and proliferation at beginning (2A, 3A and 4A) as shown in Fig. 27 and Fig. 28. On the other hand, insoluble and hardly absorbable HAp particles should particularly support cell differentiation in late phases of experiment. As shown in Fig. 26 the samples with the predominance of HAp (4A) had the least appropriate environment for cell living from all composite scaffolds because they did not create environment attractive enough for cells at beginning of the experiment. The samples with predominance of β-TCP (3A) provided a suitable environment for cell adhesion and proliferation, but after 14 days there were lack of HAp particles which normally should ensure following cell differentiation.

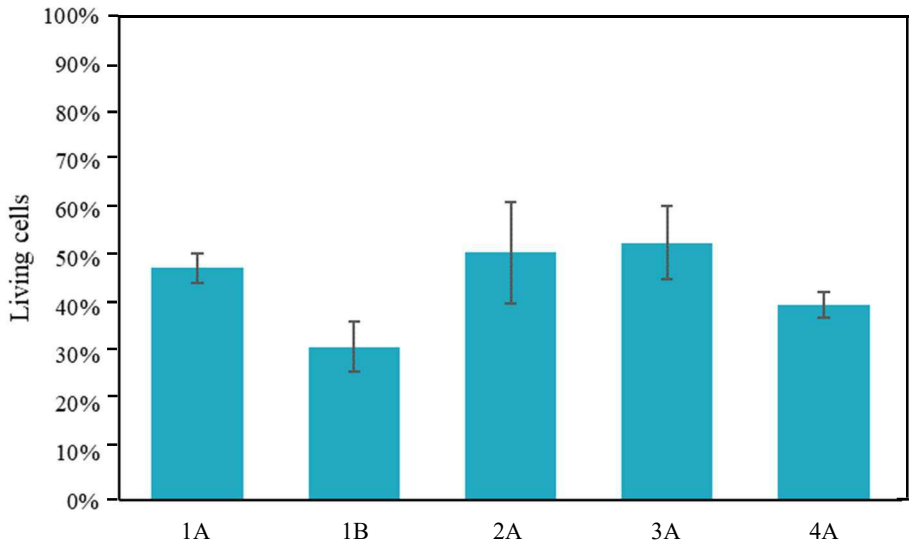

Fig. 29: Percentage of living cells on the pure collagen scaffolds and the collagen/HAp/β-TCP/α-TCP composite scaffolds after 24 days.

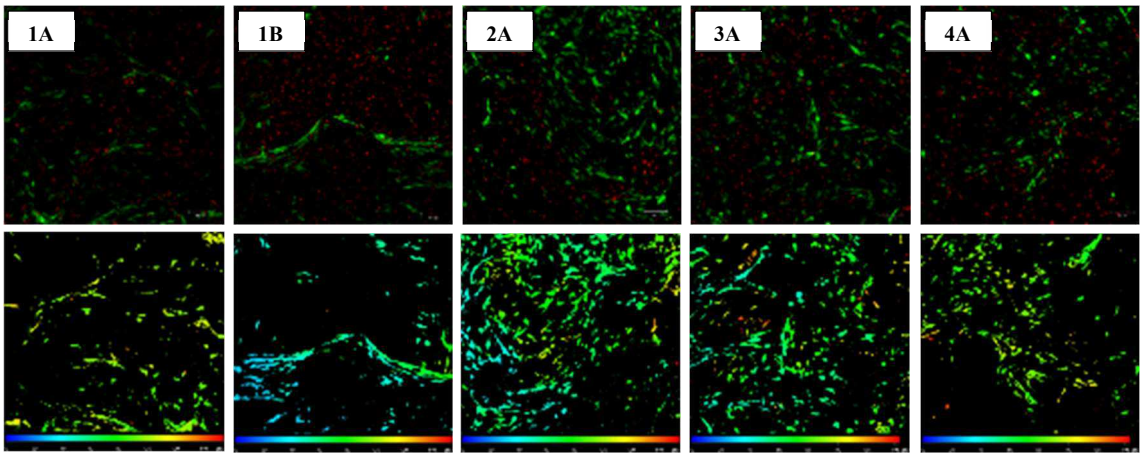

Fig. 30: Images from fluorescence microscope of dead and living cells after 24 days on the pure collagen scaffolds and the collagen/HAp/β-TCP/α-TCP composite scaffolds; upper row – nuclei of dead cells are red and nuclei of living cells are green; bottom row – depth projection of cell penetration, max depth 150 μm, the red coloured is the deepest.

As demonstrated in Fig. 29 and Fig. 30, which represented number of living cells and their depth projection on the pure collagen scaffolds and the collagen/HAp/β-TCP/α-TCP composite scaffolds after 24 days of the experiment, addition of HAp and TCPs particles in ratio 1 : 1 (sample 2A) significantly enhanced environment for cell proliferation and differentiation compared to other composite scaffolds and even to the bovine collagen scaffolds (1A). These results also correlated with the rate of induction of osteogenic differentiation as reported in Fig. 31. The best induction of osteogenic differentiation provided the samples 1A, 2A and 3A. In contrast, the sample with the predominance of Hap (4A), which should enhance particularly osteogenic differentiation had the worst result due to lack of TCPs from the beginning.

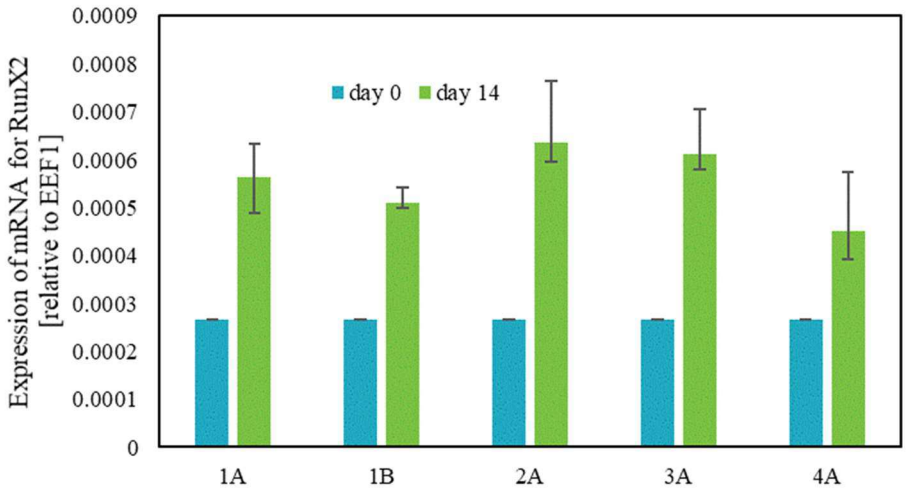

Fig. 31: Relative expression of mRNA (qPCR) for the transcription factor RunX2 (Runt-related transcription factor 2) on the pure collagen scaffolds and the collagen/HAp/β-TCP/α-TCP composite scaffolds after 0 and 14 days.

6 CONCLUSION

Using the freeze-drying fabrication method, 3D porous pure collagen scaffolds and collagen/HAp/β-TCP/α-TCP composite scaffolds for potential application in regenerative bone medicine were prepared. The effect of mixtures of the individual bioceramic components (HAp, β-TCP, α-TCP) on morphology, physical, biomechanical and the biological properties of the prepared composite scaffolds was observed.

The morphological properties of all scaffolds investigated by means of SEM showed highly porous 3D structure with high degree of interconnectivity. The pure bovine collagen scaffolds (1A) had the most regular and complex structure of all samples. Samples 1A also achieved optimal pore size (407 ± 142 μm) for cell adhesion and proliferation and at the same time the narrowest pore size distribution of all. Contrary, the porcine collagen scaffolds (1B) appeared highly structurally irregular, thus with the greatest pore size (568 ± 252 μm) and the widest pore size distribution, which could not be entirely suitable for cell proliferation and differentiation. The bioceramic particles made the scaffolds (2A, 3A and 4A) less regular than the pure bovine collagen scaffolds (1A). Especially, the content of TCPs particles influenced the structure of the pore walls which then appeared more fibrillar and relaxed. The addition of bioceramic particles no matter the type also decreased the pore size approx. by 20 % (100 μm) and widened the pore size distribution.

All samples were highly porous showed similar values of porosity (96–97%). The porcine collagen scaffolds (1B) achieved the lowest porosity (96 %) of all which could be explained on molecular difference between collagens from each source. Mixture of bioceramic particles slightly increased (by 1 %) the porosity of the scaffolds (2A, 3A and 4A) because they limited the collagen in self-assembly process.

The pore size and porosity corresponded to the ability of the pure collagen scaffolds (1A and 1B) to absorb water. The porcine collagen scaffold (1B) reached the highest value of the swelling ratio (~1.6). The bovine collagen scaffolds (1A), though with smaller pore size, but with higher porosity achieved little lower value of the swelling ratio (~1.5). However, the content of bioceramic particles decreased hydrophilicity of the collagen matrix and thereby significantly decreased the swelling ratio of the samples 2A (~0.75), 3A (~1.0) and 4A (~0.7). The greatest influence on lowering the hydrophilic characteristics had the content of HAp particles.

The in vitro enzymatic degradation was also related to decreasing hydrophilicity with the content of bioceramic particles, especially HAp particles. The bioceramic particles apparently stabilized the scaffolds (2A, 3A and 4A) against the collagenase activity. The mass loss of the composite scaffolds (2A, 3A and 4A) was lower by approx. 15 % compared to the pure collagen scaffolds (1A and 1B). The collagenase in PBS solution could not get to collagen matrix and peptide bonds so easily as in pure collagen scaffolds (1A and 1B).

Infrared analysis of the pure collagen scaffolds (1A and 1B) showed typical bands of type I collagen but also bands related improperly washed out products from crosslinking process. Spectra of the collagen/HAp/β-TCP/α-TCP composite scaffolds showed typical bands of type I collagen and also bands that corresponded to the content of the bioceramic particles. There were some shifts of the typical collagen bands that were caused by the bonds of the bioceramic particles to the collagen matrix.

The biomechanical properties of the pure collagen scaffolds and the collagen/HAp/β-TCP/α-TCP composite scaffolds were tested under in dry and also hydrated state which should mimic the physiological environment. In dry state, the pure bovine collagen scaffolds (1A) achieved the highest compressive strength (4931 ± 368 Pa). The pure porcine collagen scaffolds (1B) achieved the lowest compressive strength (2327 ± 252 Pa) mainly because of his irregular inner structure. The addition of the bioceramic particles made the scaffolds (2A, 3A and 4A) more brittle (average compressive strength decreased approx. by 20 %) no matter type of the bioceramic particles and they were not as rigid in compression as the pure bovine collagen scaffolds (1A). After hydration, the compressive strength of all samples decreased 100×. On the other hand, the bioceramic particles demonstrated the reinforcing effect, especially HAp particles, and the composite scaffolds (2A, 3A and 4A) reached higher values of compressive strength (by approx. 25 %) than the pure bovine collagen scaffolds (1A). They decreased the hydrophilicity of the collagen matrix and prevent the normal saline solution to weak it. Energy absorption efficiency did not change much after hydration which meant there were only small changes in the inner structure of the scaffolds following hydration.

None of the tested scaffolds were cytotoxic and cells in all samples proliferated during whole experiment, indicating sufficient mechanical stimulation by their environment. According to the quantification of cellular DNA on the samples and fluorescence microscopy, the most preferable environment for cell adhesion and proliferation was in the pure bovine collagen scaffolds (1A) and also in the composite scaffolds 2A (HAp : β-TCP : 1 : 1). The pure porcine collagen scaffolds thank large pores were settled by many cells, but they did not have enough stimuli to proliferate more. The predominance of β-TCPs in the samples 3A enhanced cell proliferation at beginning but then was lack of HAp particles for cell differentiation. The predominance of HAp particles (sample 4A) did not ensure sufficiently cell adhesion and proliferation at beginning. These results also correlated with the rate of induction of osteogenic differentiation.

Based on the found properties, all tested scaffolds could fairly imitate the environment for cell adhesion, proliferation and differentiation in bone tissue engineering. The pure bovine collagen scaffolds (1A) itself provided superior properties unlike the pure porcine collagen scaffolds (1B). The addition of bioceramic particles and also their ratio changed the inner morphology, decreased the hydrophilicity of the collagen matrix and influenced the cell adhesion, proliferation and differentiation. Overall, as the best ratio of the bioceramic particles appeared HAp : β-TCP : 1 : 1 (sample 2A) that provided to scaffolds highly suitable properties for bone tissue engineering.

7 LITERATURE

[1] LANGER, R a J. VACANTI. Tissue engineering. *Science* [online]. 1993, **260**(5110), 920-926 [cit. 2018-02-05]. DOI: 10.1126/science.8493529. ISSN 0036-8075. Dostupné z: http://www.sciencemag.org/cgi/doi/10.1126/science.8493529

[2] MACARTHUR, Ben a Richard OREFFO. Bridging the gap. *Nature* [online]. 2005, **433**(7021), 19-19 [cit. 2018-02-05]. DOI: 10.1038/433019a. ISSN 00280836.

[3] ZIPPEL, Nina, Margit SCHULZE a Edda TOBIASCH. Biomaterials and Mesenchymal Stem Cells for Regenerative Medicine. *Recent Patents on Biotechnology* [online]. 2010, **4**(1), 1-22 [cit. 2018-02-05]. DOI: 10.2174/187220810790069497. ISSN 18722083.

[4] RAEISDASTEH HOKMABAD, Vahideh, Soodabeh DAVARAN, Ali RAMAZANI a Roya SALEHI. Design and fabrication of porous biodegradable scaffolds: a strategy for tissue engineering. *Journal of Biomaterials Science, Polymer Edition* [online]. 2017, **28**(16), 1797-1825 [cit. 2018-02-05]. DOI: 10.1080/09205063.2017.1354674. ISSN 0920-5063. Dostupné z: https://www.tandfonline.com/doi/full/10.1080/09205063.2017.1354674

[5] MARTIN, Ivan, David WENDT a Michael HEBERER. The role of bioreactors in tissue engineering. *Trends in Biotechnology* [online]. 2004, **22**(2), 80-86 [cit. 2018-02-05]. DOI: 10.1016/j.tibtech.2003.12.001. ISSN 01677799. Dostupné z: http://linkinghub.elsevier.com/retrieve/pii/S0167779903003184

[6] KHAN, Ferdous, Masaru TANAKA a Sheikh AHMAD. Fabrication of polymeric biomaterials: a strategy for tissue engineering and medical devices. *Journal of Materials Chemistry B* [online]. 2015, **3**(42), 8224-8249 [cit. 2018-02-03]. DOI: 10.1039/C5TB01370D. ISSN 2050-750x. Dostupné z: http://xlink.rsc.org/?DOI=C5TB01370D

[7] CHERIAN, Eapen., G. NANDHINI a Anil. KURIAN. *Stem cells*. New Delhi: Jaypee Brothers Medical Publishers (P) Ltd., 2011. ISBN 93-502-5060-8.

[8] TRAN, N., Y. LI, S. BERTRAND, S. BANGRATZ, J. CARTEAUX, J. STOLTZ a J. VILLEMOT. Autologous cell transplantation and cardiac tissue engineering: potential applications in heart failure. *Biorheology*. 2003, **40**(1-3), 411-415.

[9] PHILIPS, Deepa, Nymphea PANDIT a Rajvir MALIK. *Tissue engineering: A new vista in periodontal regeneration* [online]. 2011 [cit. 2018-02-10]. DOI: 10.4103/0972-124X.92564. Dostupné z: http://www.jisponline.com/text.asp?2011/15/4/328/92564

[10] LI, Song, Nicholas L'HEUREUX a Jennifer ELISSEEFF. *Stem cell and tissue engineering* [online]. Hackensack, NJ [u.a.]: World Scientific, 2011 [cit. 2018-02-10]. ISBN 9781613441008.

[11] KIM, K. a G. EVANS. Tissue Engineering: The Future of Stem Cells. *Topics in Tissue Engineering* [online]. 2. Eds. N. Ashammakhi & R.L. Reis, 2005 [cit. 2018-02-10].

[12] SCHLOSSMANN, Jens. Editorial of the Special Issue: Signaling Molecules and Signal Transduction in Cells. *International Journal of Molecular Sciences* [online]. 2013, **14**(12), 11438-11443 [cit. 2018-02-10]. DOI: 10.3390/ijms140611438. ISSN 1422-0067. Dostupné z: http://www.mdpi.com/1422-0067/14/6/11438

[13] SUN, Xiaoqiang, Jing SU, Jiguang BAO, Tao PENG, Le ZHANG, Yuanyuan ZHANG, Yunzhi YANG a Xiaobo ZHOU. Cytokine combination therapy prediction for bone remodeling in tissue engineering based on the intracellular signaling pathway. *Biomaterials* [online]. 2012, **33**(33), 8265-8276 [cit. 2018-02-10]. DOI: 10.1016/j.biomaterials.2012.07.041. ISSN 01429612. Dostupné z: http://linkinghub.elsevier.com/retrieve/pii/S0142961212008368

[14] CHEN, Fa-Ming, Min ZHANG a Zhi-Fen WU. Toward delivery of multiple growth factors in tissue engineering. *Biomaterials* [online]. 2010, **31**(24), 6279-6308 [cit. 2018-02-10]. DOI: 10.1016/j.biomaterials.2010.04.053. ISSN 01429612. Dostupné z: http://linkinghub.elsevier.com/retrieve/pii/S0142961210005697

[15] TAYALIA, Prakriti a David MOONEY. Controlled Growth Factor Delivery for Tissue Engineering. *Advanced Materials* [online]. 2009, **21**(32-33), 3269-3285 [cit. 2018-02-10]. DOI: 10.1002/adma.200900241. ISSN 09359648. Dostupné z: http://doi.wiley.com/10.1002/adma.200900241

[16] BARRIENTOS, Stephan, Olivera STOJADINOVIC, Michael GOLINKO, Harold BREM a Marjana TOMIC-CANIC. Growth factors and cytokines in wound healing. *Wound Repair and Regeneration* [online]. 2008, **16**(5), 585-601 [cit. 2018-02-10]. DOI: 10.1111/j.1524-475X.2008.00410.x. ISSN 10671927. Dostupné z: http://doi.wiley.com/10.1111/j.1524-475X.2008.00410.x

[17] CHEN, Liang, Wei JIANG, Jiayi HUANG et al. Insulin-like growth factor 2 (IGF-2) potentiates BMP-9-induced osteogenic differentiation and bone formation. *Journal of Bone and Mineral Research* [online]. 2010, **25**(11), 2447-2459 [cit. 2018-02-10]. DOI: 10.1002/jbmr.133. ISSN 08840431. Dostupné z: http://doi.wiley.com/10.1002/jbmr.133

[18] ZHANG, Jun-Ming a Jianxiong AN. Cytokines, Inflammation, and Pain. *International Anesthesiology Clinics* [online]. 2007, **45**(2), 27-37 [cit. 2018-02-10]. DOI: 10.1097/AIA.0b013e318034194e. ISSN 0020-5907. Dostupné z: https://insights.ovid.com/crossref?an=00004311-200704520-00004

[19] DIMITRIOU, Rozalia, Eleftherios TSIRIDIS a Peter GIANNOUDIS. Current concepts of molecular aspects of bone healing. *Injury* [online]. 2005, **36**(12), 1392-1404 [cit. 2018-02-10]. DOI: 10.1016/j.injury.2005.07.019. ISSN 00201383. Dostupné z: http://linkinghub.elsevier.com/retrieve/pii/S0020138305002767

[20] KARAGEORGIOU, V a D KAPLAN. Porosity of 3D biomaterial scaffolds and osteogenesis. *Biomaterials* [online]. 2005, **26**(27), 5474-5491 [cit. 2018-01-25]. DOI: 10.1016/j.biomaterials.2005.02.002. ISSN 01429612. Dostupné z: http://linkinghub.elsevier.com/retrieve/pii/S0142961205001511

[21] HUTMACHER, Dietmar. Scaffold design and fabrication technologies for engineering tissues — state of the art and future perspectives. *Journal of Biomaterials Science, Polymer Edition* [online]. 2001, **12**(1), 107-124 [cit. 2018-01-24]. DOI: 10.1163/156856201744489. ISSN 0920-5063. Dostupné z: http://www.tandfonline.com/doi/abs/10.1163/156856201744489

[22] KWEON, H. A novel degradable polycaprolactone networks for tissue engineering. *Biomaterials* [online]. 2003, **24**(5), 801-808 [cit. 2018-01-25]. DOI: 10.1016/S0142-9612(02)00370-8. ISSN 01429612. Dostupné z: http://linkinghub.elsevier.com/retrieve/pii/S0142961202003708

[23] CIMA, L., J. VACANTI, C. VACANTI, D. INGBER, D. MOONEY a R. LANGER. Tissue Engineering by Cell Transplantation Using Degradable Polymer Substrates. *Journal of Biomechanical Engineering* [online]. 1991, **113**(2), 143- [cit. 2018-01-25]. DOI: 10.1016/S0142-9612(02)00370-8. ISSN 01480731. Dostupné z: http://Biomechanical.asmedigitalcollection.asme.org/article.aspx?articleid=1398574

[24] HUTMACHER, Dietmar. Scaffolds in tissue engineering bone and cartilage. *Biomaterials* [online]. 2000, **21**(24), 2529-2543 [cit. 2018-01-25]. DOI: 10.1016/S0142-9612(00)00121-6. ISSN 01429612. Dostupné z: http://linkinghub.elsevier.com/retrieve/pii/S0142961200001216

[25] MANDAL, Biman a Subhas KUNDU. Non-Bioengineered Silk Fibroin Protein 3D Scaffolds for Potential Biotechnological and Tissue Engineering Applications. *Macromolecular Bioscience* [online]. 2008, **8**(9), 807-818 [cit. 2018-01-25]. DOI: 10.1002/mabi.200800113. ISSN 16165187. Dostupné z: http://doi.wiley.com/10.1002/mabi.200800113

[26] MANDAL, Biman a Subhas KUNDU. Cell proliferation and migration in silk fibroin 3D scaffolds. *Biomaterials* [online]. 2009, **30**(15), 2956-2965 [cit. 2018-01-25]. DOI: 10.1016/j.biomaterials.2009.02.006. ISSN 01429612. Dostupné z: http://linkinghub.elsevier.com/retrieve/pii/S014296120900129X

[27] ZHOU, Hongjian a Jaebeom LEE. Nanoscale hydroxyapatite particles for bone tissue engineering. *Acta Biomaterialia* [online]. 2011, **7**(7), 2769-2781 [cit. 2018-01-25]. DOI: 10.1016/j.actbio.2011.03.019. ISSN 17427061. Dostupné z: http://linkinghub.elsevier.com/retrieve/pii/S1742706111001310

[28] CAUSA, Filippo, Paolo NETTI a Luigi AMBROSIO. A multi-functional scaffold for tissue regeneration: The need to engineer a tissue analogue. *Biomaterials* [online]. 2007, **28**(34), 5093-5099 [cit. 2018-01-25]. DOI: 10.1016/j.biomaterials.2007.07.030. ISSN 01429612. Dostupné z: http://linkinghub.elsevier.com/retrieve/pii/S0142961207005595

[29] LOH, Qiu a Cleo CHOONG. Three-Dimensional Scaffolds for Tissue Engineering Applications: Role of Porosity and Pore Size. *Tissue Engineering Part B: Reviews* [online]. 2013, **19**(6), 485-502 [cit. 2018-01-25]. DOI: 10.1089/ten.teb.2012.0437. ISSN 1937-3368. Dostupné z: http://online.liebertpub.com/doi/abs/10.1089/ten.teb.2012.0437

[30] DUTTA, Ranjna, Madhuri DEY, Aroop DUTTA a Bikramjit BASU. Competent processing techniques for scaffolds in tissue engineering. *Biotechnology Advances* [online]. 2017, **35**(2), 240-250 [cit. 2018-02-08]. DOI: 10.1016/j.biotechadv.2017.01.001. ISSN 07349750. Dostupné z: http://linkinghub.elsevier.com/retrieve/pii/S0734975017300010

[31] MEYER, Ulrich, Thomas MEYER, Jörg HANDSCHEL a Hans WIESMANN. *Fundamentals of tissue engineering and regenerative medicine* [online]. Berlin: Springer, 2009, s. 541-545 [cit. 2018-01-25]. ISBN 978-3-540-77755-7.

[32] LU, Lichun, Xun ZHU, Richard VALENZUELA, Bradford CURRIER a Michael YASZEMSKI. Biodegradable Polymer Scaffolds for Cartilage Tissue Engineering. *Clinical Orthopaedics and Related Research* [online]. 2001, **391**, 251-270 [cit. 2018-01-25]. DOI: 10.1097/00003086-200110001-00024. ISSN 0009-921x. Dostupné z: https://insights.ovid.com/crossref?an=00003086-200110001-00024

[33] CHUNG, Hyun Jung a Tae Gwan PARK. Surface engineered and drug releasing pre-fabricated scaffolds for tissue engineering. *Advanced Drug Delivery Reviews* [online]. 2007, **59**(4-5), 249-262 [cit. 2018-04-06]. DOI: 10.1016/j.addr.2007.03.015. ISSN 0169409X. Dostupné z: http://linkinghub.elsevier.com/retrieve/pii/S0169409X07000270

[34] GARG, Tarun, Onkar SINGH, Saahil ARORA a R. MURTHY. Scaffold: A Novel Carrier for Cell and Drug Delivery. *Critical Reviews™ in Therapeutic Drug Carrier Systems* [online]. 2012, **29**(1), 1-63 [cit. 2018-01-26]. DOI: 10.1615/CritRevTherDrugCarrierSyst.v29.i1.10. ISSN 0743-4863. Dostupné z: http://www.dl.begellhouse.com/journals/3667c4ae6e8fd136,2ccd8f8553046ba4,54eb9b5a0d45ccd7.html

[35] FRANTZ, C., K. STEWART a V. WEAVER. The extracellular matrix at a glance. *Journal of Cell Science* [online]. 2010, **123**(24), 4195-4200 [cit. 2017-12-26]. DOI: 10.1242/jcs.023820. ISSN 0021-9533. Dostupné z: http://jcs.biologists.org/cgi/doi/10.1242/jcs.023820

[36] CLAUSE, Kelly a Thomas BARKER. Extracellular matrix signaling in morphogenesis and repair. *Current Opinion in Biotechnology* [online]. 2013, **24**(5), 830-833 [cit. 2017-12-26]. DOI: 10.1016/j.copbio.2013.04.011. ISSN 09581669. Dostupné z: http://linkinghub.elsevier.com/retrieve/pii/S0958166913001092

[37] AAMODT, Joseph a David GRAINGER. Extracellular matrix-based biomaterial scaffolds and the host response. *Biomaterials* [online]. 2016, **86**, 68-82 [cit. 2017-12-26]. DOI: 10.1016/j.biomaterials.2016.02.003. ISSN 01429612. Dostupné z: http://linkinghub.elsevier.com/retrieve/pii/S0142961216001009

[38] Extracellular Matrix and Cell Adhesion Molecules. In: *British Society for Cell Biology* [online]. London: British Society for Cell Biology, 1965 [cit. 2017-12-26]. Dostupné z: http://bscb.org/learning-resources/softcell-e-learning/extracellular-matrix-and-cell-adhesion-molecules/

[39] ROZARIO, Tania a Douglas DESIMONE. The extracellular matrix in development and morphogenesis: A dynamic view. *Developmental Biology* [online]. 2010, **341**(1), 126-140 [cit. 2017-12-26]. DOI: 10.1016/j.ydbio.2009.10.026. ISSN 00121606. Dostupné z: http://linkinghub.elsevier.com/retrieve/pii/S0012160609012858

[40] WISE, Steven a Anthony WEISS. *Tropoelastin* [online]. 2009, **41**(3), 494-497 [cit. 2017-12-26]. DOI: 10.1016/j.biocel.2008.03.017. ISSN 13572725. Dostupné z: http://linkinghub.elsevier.com/retrieve/pii/S1357272508001453

[41] LUCERO, H. a H. KAGAN. Lysyl oxidase: an oxidative enzyme and effector of cell function. *Cellular and Molecular Life Sciences* [online]. 2006, **63**(19-20), 2304-2316 [cit. 2017-12-26]. DOI: 10.1007/s00018-006-6149-9. ISSN 1420-682x. Dostupné z: http://link.springer.com/10.1007/s00018-006-6149-9

[42] ALBERTS, Bruce, Alexander JOHNSON a Julian LEWIS. The Extracellular Matrix of Animals. *Molecular biology of the cell*. 4th ed. New York: Garland Science, 2002. ISBN 978-0815332183.

[43] WAGENSEIL, Jessica a Robert MECHAM. New insights into elastic fiber assembly. *Birth Defects Research Part C: Embryo Today: Reviews* [online]. 2007, **81**(4), 229-240 [cit. 2017-12-26]. DOI: 10.1002/bdrc.20111. ISSN 1542975x. Dostupné z: http://doi.wiley.com/10.1002/bdrc.20111

[44] SCHWARZBAUER, J. a D. DESIMONE. Fibronectins, Their Fibrillogenesis, and In Vivo Functions. *Cold Spring Harbor Perspectives in Biology* [online]. 2011, **3**(7), 005041-005041 [cit. 2017-12-26]. DOI: 10.1101/cshperspect.a005041. ISSN 1943-0264. Dostupné z: http://cshperspectives.cshlp.org/lookup/doi/10.1101/cshperspect.a005041

[45] ASTROF, Sophie a Richard HYNES. Fibronectins in vascular morphogenesis. *Angiogenesis* [online]. 2009, **12**(2), 165-175 [cit. 2017-12-26]. DOI: 10.1007/s10456-009-9136-6. ISSN 0969-6970. Dostupné z: http://link.springer.com/10.1007/s10456-009-9136-6

[46] THEOCHARIS, Achilleas, Spyros SKANDALIS, Chrysostomi GIALELI a Nikos KARAMANOS. Extracellular matrix structure. *Advanced Drug Delivery Reviews* [online]. 2016, **97**, 4-27 [cit. 2017-12-26]. DOI: 10.1016/j.addr.2015.11.001. ISSN 0169409x. Dostupné z: http://linkinghub.elsevier.com/retrieve/pii/S0169409X15002574

[47] YURCHENCO, P. Basement Membranes: Cell Scaffoldings and Signaling Platforms. *Cold Spring Harbor Perspectives in Biology* [online]. 2011, **3**(2), 004911-004911 [cit. 2017-12-26]. DOI: 10.1101/cshperspect.a004911. ISSN 1943-0264. Dostupné z: http://cshperspectives.cshlp.org/lookup/doi/10.1101/cshperspect.a004911

[48] SCHAEFER, Liliana a Roland SCHAEFER. Proteoglycans: from structural compounds to signaling molecules. *Cell and Tissue Research* [online]. 2010, **339**(1), 237-246 [cit. 2017-12-26]. DOI: 10.1007/s00441-009-0821-y. ISSN 0302-766x. Dostupné z: http://link.springer.com/10.1007/s00441-009-0821-y

[49] IOZZO, Renato a Liliana SCHAEFER. Proteoglycan form and function: A comprehensive nomenclature of proteoglycans. *Matrix Biology* [online]. 2015, **42**, 11-55 [cit. 2017-12-26]. DOI: 10.1016/j.matbio.2015.02.003. ISSN 0945053x. Dostupné z: http://linkinghub.elsevier.com/retrieve/pii/S0945053X15000402

[50] YANG, Shoufeng, Kah-Fai LEONG, Zhaohui DU a Chee-Kai CHUA. The Design of Scaffolds for Use in Tissue Engineering. Part I. Traditional Factors. *Tissue Engineering* [online]. 2001, **7**(6), 679-689 [cit. 2018-02-08]. DOI: 10.1089/107632701753337645. ISSN 1076-3279. Dostupné z: http://www.liebertonline.com/doi/abs/10.1089/107632701753337645

[51] SEOL, Young-Joon, Tae-Yun KANG a Dong-Woo CHO. Solid freeform fabrication technology applied to tissue engineering with various biomaterials. *Soft Matter* [online]. 2012, **8**(6), 1730-1735 [cit. 2018-02-08]. DOI: 10.1039/C1SM06863F. ISSN 1744-683x. Dostupné z: http://xlink.rsc.org/?DOI=C1SM06863F

[52] LU, Lichun a Antonios MIKOS. The Importance of New Processing Techniques in Tissue Engineering. *MRS Bulletin* [online]. 1996, **21**(11), 28-32 [cit. 2018-02-08]. DOI: 10.1557/S088376940003181X. ISSN 0883-7694. Dostupné z: http://www.journals.cambridge.org/abstract_S088376940003181X

[53] *Method of fabricating emulsion freeze-dried scaffold bodies and resulting products*. 1998. United States of America. US5723508A. Uděleno 1996-01-25. Zapsáno 1998-03-03.

[54] VACANTI, Joseph, Martin MORSE, W. SALTZMAN, Abraham DOMB, Antonio PEREZ-ATAYDE a Robert LANGER. Selective cell transplantation using bioabsorbable artificial polymers as matrices. *Journal of Pediatric Surgery* [online]. 1988, **23**(1), 3-9 [cit. 2018-02-08]. DOI: 10.1016/S0022-3468(88)80529-3. ISSN 00223468. Dostupné z: http://linkinghub.elsevier.com/retrieve/pii/S0022346888805293

[55] PARK, Ann, BEN WU a Linda GRIFFITH. Integration of surface modification and 3D fabrication techniques to prepare patterned poly(L-lactide) substrates allowing regionally selective cell adhesion. *Journal of Biomaterials Science, Polymer Edition* [online]. 1998, **9**(2), 89-110 [cit. 2018-02-08]. DOI: 10.1163/156856298X00451. ISSN 0920-5063. Dostupné z: http://www.tandfonline.com/doi/abs/10.1163/156856298X00451

[56] LEONG, K, K PHUA, C CHUA, Z DU a K TEO. Fabrication of porous polymeric matrix drug delivery devices using the selective laser sintering technique. *Proceedings of the Institution of Mechanical Engineers, Part H: Journal of Engineering in Medicine* [online]. 2016, **215**(2), 191-192 [cit. 2018-02-08]. DOI: 10.1243/0954411011533751. ISSN 0954-4119. Dostupné z: http://journals.sagepub.com/doi/10.1243/0954411011533751

[57] LOW, K.H., K.F. LEONG, C.K. CHUA, Z.H. DU a C.M. CHEAH. Characterization of SLS parts for drug delivery devices. *Rapid Prototyping Journal* [online]. 2001, **7**(5), 262-268 [cit. 2018-02-08]. DOI: 10.1108/13552540110410468. ISSN 1355-2546. Dostupné z: http://www.emeraldinsight.com/doi/10.1108/13552540110410468

[58] CHEN, Qizhi, Chenghao ZHU a George THOUAS. Progress and challenges in biomaterials used for bone tissue engineering: bioactive glasses and elastomeric composites. *Progress in Biomaterials* [online]. 2012, **1**(1), 2- [cit. 2018-02-07]. DOI: 10.1186/2194-0517-1-2. ISSN 2194-0517. Dostupné z: http://www.progressbiomaterials.com/content/1/1/2

[59] O'BRIEN, Fergal. *Materials Today* [online]. 2011, **14**(3), 88-95 [cit. 2018-02-07]. DOI: 10.1016/S1369-7021(11)70058-X. ISSN 13697021. Dostupné z: http://linkinghub.elsevier.com/retrieve/pii/S136970211170058X

[60] DHANDAYUTHAPANI, Brahatheeswaran, Yasuhiko YOSHIDA, Toru MAEKAWA a D. KUMAR. Polymeric Scaffolds in Tissue Engineering Application: A Review. *International Journal of Polymer Science* [online]. 2011, **2011**, 1-19 [cit. 2018-02-07]. DOI: 10.1155/2011/290602. ISSN 1687-9422. Dostupné z: http://www.hindawi.com/journals/ijps/2011/290602/

[61] ZOU, Yuan, Lin ZHANG, Lei YANG, Fang ZHU, Mingming DING, Fei LIN, Zhao WANG a Yiwen LI. "Click" chemistry in polymeric scaffolds: Bioactive materials for tissue engineering. *Journal of Controlled Release* [online]. 2018, **273**, 160-179 [cit. 2017-12-23]. DOI: 10.1016/j.jconrel.2018.01.023. ISSN 01683659. Dostupné z: http://linkinghub.elsevier.com/retrieve/pii/S0168365918300397

[62] HELARY, Christophe a Abhay PANDIT. Collagen-Based Biomaterials for Regenerative Medicine. MANO, João F., ed., João MANO. *Biomimetic Approaches for Biomaterials Development* [online]. Weinheim, Germany: Wiley-VCH Verlag GmbH & Co., 2012, s. 55-74 [cit. 2018-02-10]. DOI: 10.1002/9783527652273.ch3. ISBN 9783527652273. Dostupné z: http://doi.wiley.com/10.1002/9783527652273.ch3

[63] MIENALTOWSKI, Michael a David BIRK. Structure, Physiology, and Biochemistry of Collagens. *Progress in Heritable Soft Connective Tissue Diseases* [online]. Dordrecht: Springer Netherlands, 2014, , 5-29 [cit. 2018-02-10]. Advances in Experimental Medicine and Biology. DOI: 10.1007/978-94-007-7893-1_2. ISBN 978-94-007-7892-4. Dostupné z: http://link.springer.com/10.1007/978-94-007-7893-1_2

[64] GORGIEVA, S. a V. KOKOL. Collagen- vs. Gelatine-Based Biomaterials and Their Biocompatibility: Review and Perspectives. *Biomaterials Applications for Nanomedicine* [online]. InTech, 2011, , 18-52 [cit. 2018-02-10]. DOI: 10.5772/1957. ISBN 978-953-307-661-4. Dostupné z: https://www.intechopen.com/books/biomaterials-applications-for-nanomedicine

[65] GELSE, K. Collagens—structure, function, and biosynthesis. *Advanced Drug Delivery Reviews* [online]. 2003, **55**(12), 1531-1546 [cit. 2018-02-10]. DOI: 10.1016/j.addr.2003.08.002. ISSN 0169409x. Dostupné z: http://linkinghub.elsevier.com/retrieve/pii/S0169409X03001820

[66] PIEZ, K.A. Molecular and aggregate structure of the collagens. *Extracellular Matrix Biology*. Amsterdam: Elsevier, 1984, , 1-39.

[67] HOFMANN, H., P.P. FIETZEK a K. KÜHN. The role of polar and hydrophobic interactions for the molecular packing of type I collagen: A three-dimensional

evaluation of the amino acid sequence. *Journal of Molecular Biology* [online]. 1978, **125**(2), 137-165 [cit. 2018-02-10]. DOI: 10.1016/0022-2836(78)90342-X. ISSN 00222836. Dostupné z: http://linkinghub.elsevier.com/retrieve/pii/002228367890342X

[68] FRASER, R.D.B., T.P. MACRAE a E. SUZUKI. Chain conformation in the collagen molecule. *Journal of Molecular Biology* [online]. 1979, **129**(3), 463-481 [cit. 2018-02-10]. DOI: 10.1016/0022-2836(79)90507-2. ISSN 00222836. Dostupné z: http://linkinghub.elsevier.com/retrieve/pii/0022283679905072

[69] GORDON, Marion a Rita HAHN. Collagens. *Cell and Tissue Research* [online]. 2010, **339**(1), 247-257 [cit. 2018-02-10]. DOI: 10.1007/s00441-009-0844-4. ISSN 0302-766x. Dostupné z: http://link.springer.com/10.1007/s00441-009-0844-4

[70] CANELÓN, Silvia P., Joseph M. WALLACE a Laurent KREPLAK. *β-Aminopropionitrile-Induced Reduction in Enzymatic Crosslinking Causes In Vitro Changes in Collagen Morphology and Molecular Composition* [online]. b.r. [cit. 2018-04-06]. DOI: 10.1371/journal.pone.0166392. Dostupné z: http://dx.plos.org/10.1371/journal.pone.0166392

[71] BATEMAN, J., S.R. LAMANDE a J. RAMSHAW. Collagen superfamily. *Molecular Components and Interactions*. Amsterdam: Harwood Academic Publishers, 1996, (2), 22-67.

[72] VON DER MARK, KLAUS. Structure, Biosynthesis and Gene Regulation of Collagens in Cartilage and Bone. *Dynamics of Bone and Cartilage Metabolism* [online]. Elsevier, 2006, , 3-40 [cit. 2018-02-10]. DOI: 10.1016/B978-012088562-6/50002-9. ISBN 9780120885626. Dostupné z: http://linkinghub.elsevier.com/retrieve/pii/B9780120885626500029

[73] PARENTEAU-BAREIL, Rémi, Robert GAUVIN a François BERTHOD. Collagen-Based Biomaterials for Tissue Engineering Applications. *Materials* [online]. 2010, **3**(12), 1863-1887 [cit. 2018-02-10]. DOI: 10.3390/ma3031863. ISSN 1996-1944. Dostupné z: http://www.mdpi.com/1996-1944/3/3/1863

[74] CORMAN, B., M. DURIEZ, P. POITEVIN, D. HEUDES, P. BRUNEVAL, A. TEDGUI a B.I. LEVY. Aminoguanidine prevents age-related arterial stiffening and cardiac hypertrophy. *Proceedings of the National Academy of Sciences of the United States of America* [online]. 1998, **95**(3), 1301-1306 [cit. 2018-02-17]. DOI: 10.1073/pnas.95.3.1301. ISSN 00278424.

[75] WAGNER, Diane, Karen REISER a Jeffrey LOTZ. Glycation increases human annulus fibrosus stiffness in both experimental measurements and theoretical predictions. *Journal of Biomechanics* [online]. Elsevier Ltd, 2006, **39**(6), 1021-1029 [cit. 2018-02-17]. DOI: 10.1016/j.jbiomech.2005.02.013. ISSN 0021-9290.

[76] BAILEY, Allen, Robert PAUL a Lynda KNOTT. Mechanisms of maturation and ageing of collagen. *Mechanisms of Ageing and Development* [online]. Elsevier Ireland Ltd, 1998, **106**(1), 1-56 [cit. 2018-02-17]. DOI: 10.1016/S0047-6374(98)00119-5. ISSN 0047-6374.

[77] JONI D MOTT, , RAJA G KHALIFAH, HIDEAKI NAGASE, CHARLES F SHIELD, JULIE K HUDSON a BILLY G HUDSON. Nonenzymatic glycation of type IV collagen and matrix metalloproteinase susceptibility. *Kidney International* [online]. Nature Publishing Group, 1997, **52**(5), 1302 [cit. 2018-02-17]. DOI: 10.1038/ki.1997.455. ISSN 0085-2538.

[78] VATER, C, E HARRIS a R SIEGEL. Native cross-links in collagen fibrils induce resistance to human synovial collagenase. *The Biochemical journal* [online]. 1979, **181**(3), 639 [cit. 2018-02-17]. DOI: 10.1042/bj1810639. ISSN 0264-6021.

[79] CANNON, D.J. a P.F. DAVISON. Cross-linking and aging in rat tendon collagen. *Experimental Gerontology*. 1973, **8**(1), 51-62. DOI: 10.1016/0531-5565(73)90051-X. ISSN 05315565. Dostupné také z: http://linkinghub.elsevier.com/retrieve/pii/053155657390051X

[80] EYRE, David a Jiann-Jiu WU. Collagen Cross-Links. *Collagen* [online]. Berlin, Heidelberg: Springer Berlin Heidelberg, 2005, , 207-229 [cit. 2018-02-17]. Topics in Current Chemistry. DOI: 10.1007/b103828. ISBN 978-3-540-23272-8. Dostupné z: http://link.springer.com/10.1007/b103828

[81] FIELDING, A.M. Preparation of neutral salt soluble collagen,. *The Methodology of Connective Tissue Research*. Oxford: Joynson– Bruvvers, 1976, , 9-12.

[82] TRELSTAD, R. Immunology of collagens. *Immunochemistry of the Extracellular Matrix*. Boca Raton: CRC Press, 1982, (1), 32–39.

[83] *Process for preparing macromolecular biologically active collagen*. b.r. US Patent. CA1147726A. Uděleno 1979-09-12.

[84] PIEZ, K.A. Molecular and aggregate structures of the collagens. *Extracellular Matrix Biochemistry*. New York: Elsevier, 1984, , 1-40.

[85] RÝGLOVÁ, Šárka, Martin BRAUN a Tomáš SUCHÝ. Collagen and Its Modifications-Crucial Aspects with Concern to Its Processing and Analysis. *Macromolecular Materials and Engineering* [online]. 2017, **302**(6), 1600460- [cit. 2018-02-10]. DOI: 10.1002/mame.201600460. ISSN 14387492. Dostupné z: http://doi.wiley.com/10.1002/mame.201600460

[86] SCHMITT, F.O., L. LEVINE, M.P. DRAKE, A.L. RUBIN, D. PFAHL a P.F. DAVISON. THE ANTIGENICITY OF TROPOCOLLAGEN. *Proc Natl Acad Sci U S A*. 1964, **51**(3), 493-497.

[87] DAVISON, P.F., L. LEVINE, M.P. DRAKE, A. RUBIN a S. BUMP. The serologic specificity of tropocollagen telopeptides. *J Exp Med*. 1967, **126**(2), 331-346.

[88] FURTHMAYR, H., W. BEIL a R. TIMPL. Different antigenic determinants in the polypeptide chains of human collagen. *FEBS Letters* [online]. 1971, **12**(6), 341-344 [cit. 2018-02-07]. DOI: 10.1016/0014-5793(71)80010-8. ISSN 00145793. Dostupné z: http://doi.wiley.com/10.1016/0014-5793(71)80010-8

[89] LINDSLEY, H. THE DISTRIBUTION OF ANTIGENIC DETERMINANTS IN RAT SKIN COLLAGEN. *Journal of Experimental Medicine* [online]. 1971, **133**(6), 1309-

1324 [cit. 2018-02-07]. DOI: 10.1084/jem.133.6.1309. ISSN 0022-1007. Dostupné z: http://www.jem.org/cgi/doi/10.1084/jem.133.6.1309

[90] WEADOCK, K, E MILLER, E KEUFFEL a M DUNN. Effect of physical crosslinking methods on collagen-fiber durability in proteolytic solutions. *Journal of biomedical materials research* [online]. 1996, **32**(2), 221 [cit. 2018-02-07]. DOI: 10.1002/(SICI)1097-4636(199610)32:2221::AID-JBM113.0.CO;2-M. ISSN 0021-9304.

[91] MIKŠÍK, Ivan, Pavla SEDLÁKOVÁ, Kateřina MIKULÍKOVÁ a Adam ECKHARDT. Capillary electromigration methods for the study of collagen. *Journal of Chromatography B* [online]. 2006, **841**(1-2), 3-13 [cit. 2018-02-10]. DOI: 10.1016/j.jchromb.2006.02.043. ISSN 15700232. Dostupné z: http://linkinghub.elsevier.com/retrieve/pii/S1570023206001383

[92] GOO, Hyun, Yu-Shik HWANG, Yon CHOI, Hyun CHO a Hwal SUH. Development of collagenase-resistant collagen and its interaction with adult human dermal fibroblasts. *Biomaterials* [online]. 2003, **24**(28), 5099-5113 [cit. 2018-02-10]. DOI: 10.1016/S0142-9612(03)00431-9. ISSN 01429612. Dostupné z: http://linkinghub.elsevier.com/retrieve/pii/S0142961203004319

[93] YANNAS, I., J. BURKE, D. ORGILL a E. SKRABUT. Wound tissue can utilize a polymeric template to synthesize a functional extension of skin. *Science* [online]. 1982, **215**(4529), 174-176 [cit. 2018-02-10]. DOI: 10.1126/science.7031899. ISSN 0036-8075. Dostupné z: http://www.sciencemag.org/cgi/doi/10.1126/science.7031899

[94] POSTLETHWAITE, A., J. SEYER a A. KANG. Chemotactic attraction of human fibroblasts to type I, II, and III collagens and collagen-derived peptides. *Proceedings of the National Academy of Sciences* [online]. 1978, **75**(2), 871-875 [cit. 2018-02-10]. DOI: 10.1073/pnas.75.2.871. ISSN 0027-8424. Dostupné z: http://www.pnas.org/cgi/doi/10.1073/pnas.75.2.871

[95] EDITED BY JOSEPH A. BUCKWALTER, a MARTIN LOTZ AND JEAN-FRANçOIS STOLTZ. *Osteoarthritis, inflammation, and degradation a continuum* [online]. Amsterdam: IOS Press, 2007 [cit. 2018-02-10]. ISBN 978-160-7502-654.

[96] STERNLICHT, Mark a Zena WERB. How Matrix Metalloproteinases Regulate Cell Behavior. *Annual Review of Cell and Developmental Biology* [online]. 2001, **17**(1), 463-516 [cit. 2018-02-10]. DOI: 10.1146/annurev.cellbio.17.1.463. ISSN 1081-0706. Dostupné z: http://www.annualreviews.org/doi/10.1146/annurev.cellbio.17.1.463

[97] FIGUEIRO, S, J GOES, R MOREIRA a A SOMBRA. On the physico-chemical and dielectric properties of glutaraldehyde crosslinked galactomannan–collagen films. *Carbohydrate Polymers* [online]. 2004, **56**(3), 313-320 [cit. 2018-02-10]. DOI: 10.1016/j.carbpol.2004.01.011. ISSN 01448617. Dostupné z: http://linkinghub.elsevier.com/retrieve/pii/S0144861704000608

[98] OLDE DAMINK, L.H.H., P.J. DIJKSTRA, M.J.A. VAN LUYN, P.B. VAN WACHEM, P. NIEUWENHUIS a J. FEIJEN. Cross-linking of dermal sheep collagen using a water-soluble carbodiimide. *Biomaterials* [online]. 1996, **17**(8), 765-773 [cit.

2018-02-10]. DOI: 10.1016/0142-9612(96)81413-X. ISSN 01429612. Dostupné z: http://linkinghub.elsevier.com/retrieve/pii/014296129681413X

[99] WEADOCK, Kevin, Edward MILLER, Lisa BELLINCAMPI, Joseph ZAWADSKY a Michael DUNN. Physical crosslinking of collagen fibers: Comparison of ultraviolet irradiation and dehydrothermal treatment. *Journal of Biomedical Materials Research* [online]. 1995, **29**(11), 1373-1379 [cit. 2018-02-10]. DOI: 10.1002/jbm.820291108. ISSN 0021-9304. Dostupné z: http://doi.wiley.com/10.1002/jbm.820291108

[100] RODRIGUES, Fabiana, Virginia MARTINS a Ana PLEPIS. Porcine skin as a source of biodegradable matrices: alkaline treatment and glutaraldehyde crosslinking. *Polímeros* [online]. 2010, **20**(2), 92-97 [cit. 2018-02-10]. DOI: 10.1590/S0104-14282010005000013. ISSN 0104-1428.

[101] ZEUGOLIS, Dimitrios, Gordon PAUL a Geoffrey ATTENBURROW. Cross-linking of extruded collagen fibers-A biomimetic three-dimensional scaffold for tissue engineering applications. *Journal of Biomedical Materials Research Part A* [online]. 2009, **89**(4), 895-908 [cit. 2018-02-10]. DOI: 10.1002/jbm.a.32031. ISSN 15493296. Dostupné z: http://doi.wiley.com/10.1002/jbm.a.32031

[102] BÜRCK, Jochen, Stefan HEISSLER, Udo GECKLE, Mohammad ARDAKANI, Reinhard SCHNEIDER, Anne ULRICH a Murat KAZANCI. Resemblance of Electrospun Collagen Nanofibers to Their Native Structure. *Langmuir* [online]. 2013, **29**(5), 1562-1572 [cit. 2018-02-10]. DOI: 10.1021/la3033258. ISSN 0743-7463. Dostupné z: http://pubs.acs.org/doi/10.1021/la3033258

[103] USHA, R a T RAMASAMI. Effect of crosslinking agents (basic chromium sulfate and formaldehyde) on the thermal and thermomechanical stability of rat tail tendon collagen fibre. *Thermochimica Acta* [online]. 2000, **356**(1-2), 59-66 [cit. 2018-02-10]. DOI: 10.1016/S0040-6031(00)00518-9. ISSN 00406031. Dostupné z: http://linkinghub.elsevier.com/retrieve/pii/S0040603100005189

[104] KUIJPERS, A., G. ENGBERS, J. FEIJEN et al. Characterization of the Network Structure of Carbodiimide Cross-Linked Gelatin Gels. *Macromolecules* [online]. 1999, **32**(10), 3325-3333 [cit. 2018-02-10]. DOI: 10.1021/ma981929v. ISSN 0024-9297. Dostupné z: http://pubs.acs.org/doi/abs/10.1021/ma981929v

[105] HUANG, Gloria, Shobana SHANMUGASUNDARAM, Pallavi MASIH, Deep PANDYA, Suwah AMARA, George COLLINS a Treena ARINZEH. An investigation of common crosslinking agents on the stability of electrospun collagen scaffolds. *Journal of Biomedical Materials Research Part A* [online]. 2015, **103**(2), 762-771 [cit. 2018-02-10]. DOI: 10.1002/jbm.a.35222. ISSN 15493296. Dostupné z: http://doi.wiley.com/10.1002/jbm.a.35222

[106] GARCIA, Yolanda, Naik HEMANTKUMAR, Russell COLLIGHAN, Martin GRIFFIN, Jose RODRIGUEZ-CABELLO a Abhay PANDIT. In Vitro Characterization of a Collagen Scaffold Enzymatically Cross-Linked with a Tailored Elastin-like Polymer. *Tissue Engineering Part A* [online]. 2009, **15**(4), 887-899 [cit. 2018-02-10]. DOI: 10.1089/ten.tea.2008.0104. ISSN 1937-3341. Dostupné z: http://www.liebertonline.com/doi/abs/10.1089/ten.tea.2008.0104

[107] MA, Lie, Changyou GAO, Zhengwei MAO, Jie ZHOU a Jiacong SHEN. Biodegradability and cell-mediated contraction of porous collagen scaffolds: The effect of lysine as a novel crosslinking bridge. *Journal of Biomedical Materials Research* [online]. 2004, **71**(2), 334-342 [cit. 2018-02-10]. DOI: 10.1002/jbm.a.30170. ISSN 0021-9304. Dostupné z: http://doi.wiley.com/10.1002/jbm.a.30170

[108] RAULT, I., V. FREI, D. HERBAGE, N. ABDUL-MALAK a A. HUC. Evaluation of different chemical methods for cros-linking collagen gel, films and sponges. *Journal of Materials Science: Materials in Medicine* [online]. 1996, **7**(4), 215-221 [cit. 2018-02-10]. DOI: 10.1007/BF00119733. ISSN 0957-4530. Dostupné z: http://link.springer.com/10.1007/BF00119733

[109] SACHLOS, E. Novel collagen scaffolds with predefined internal morphology made by solid freeform fabrication. *Biomaterials* [online]. 2003, **24**(8), 1487-1497 [cit. 2018-02-10]. DOI: 10.1016/S0142-9612(02)00528-8. ISSN 01429612. Dostupné z: http://linkinghub.elsevier.com/retrieve/pii/S0142961202005288

[110] CHEN, Li, Zhenxu WU, Yulai ZHOU, Linlong LI, Yu WANG, Zongliang WANG, Yue CHEN a Peibiao ZHANG. Biomimetic porous collagen/hydroxyapatite scaffold for bone tissue engineering. *Journal of Applied Polymer Science* [online]. 2017, **134**(37), 45271- [cit. 2018-02-10]. DOI: 10.1002/app.45271. ISSN 00218995. Dostupné z: http://doi.wiley.com/10.1002/app.45271

[111] ZHONG, Shao, Wee TEO, Xiao ZHU, Roger BEUERMAN, Seeram RAMAKRISHNA a Lin YUNG. *Development of a novel collagen–GAG nanofibrous scaffold via electrospinning* [online]. 2007 [cit. 2018-02-10]. DOI: 10.1016/j.msec.2006.05.010. Dostupné z: http://linkinghub.elsevier.com/retrieve/pii/S0928493106000762

[112] INZANA, Jason, Diana OLVERA, Seth FULLER, James KELLY, Olivia GRAEVE, Edward SCHWARZ, Stephen KATES a Hani AWAD. 3D printing of composite calcium phosphate and collagen scaffolds for bone regeneration. *Biomaterials* [online]. 2014, **35**(13), 4026-4034 [cit. 2018-02-10]. DOI: 10.1016/j.biomaterials.2014.01.064. ISSN 01429612. Dostupné z: http://linkinghub.elsevier.com/retrieve/pii/S0142961214000945

[113] LOWE, Christopher, Ian REUCROFT, Matthew GROTA a David SHREIBER. *Production of Highly Aligned Collagen Scaffolds by Freeze-drying of Self-assembled, Fibrillar Collagen Gels* [online]. 2016, **2**(4), 643-651 [cit. 2018-02-10]. DOI: 10.1021/acsbiomaterials.6b00036. ISSN 2373-9878. Dostupné z: http://pubs.acs.org/doi/10.1021/acsbiomaterials.6b00036

[114] ROSETI, Livia, Valentina PARISI, Mauro PETRETTA, Carola CAVALLO, Giovanna DESANDO, Isabella BARTOLOTTI a Brunella GRIGOLO. Scaffolds for Bone Tissue Engineering: State of the art and new perspectives. *Materials Science and Engineering: C* [online]. 2017, **78**, 1246-1262 [cit. 2018-02-10]. DOI: 10.1016/j.msec.2017.05.017. ISSN 09284931. Dostupné z: http://linkinghub.elsevier.com/retrieve/pii/S0928493117317228

[115] WHANG, K., C.H. THOMAS, K.E. HEALY a G. NUBER. A novel method to fabricate bioabsorbable scaffolds. *Polymer* [online]. 1995, **36**(4), 837-842 [cit. 2018-02-10]. DOI: 10.1016/0032-3861(95)93115-3. ISSN 00323861. Dostupné z: http://linkinghub.elsevier.com/retrieve/pii/0032386195931153

[116] GRINBERG, Orly, Itzhak BINDERMAN, Hila BAHAR a Meital ZILBERMAN. Highly porous bioresorbable scaffolds with controlled release of bioactive agents for tissue-regeneration applications. *Acta Biomaterialia* [online]. 2010, **6**(4), 1278-1287 [cit. 2018-02-10]. DOI: 10.1016/j.actbio.2009.10.047. ISSN 17427061. Dostupné z: http://linkinghub.elsevier.com/retrieve/pii/S1742706109004826

[117] BOLAND, E.D., P.G. ESPY a G.L. BOWLIN. Tissue engineering scaffolds. *Encyclopedia of biomaterials and biomedical engineering*. 2004, , 1630-1638.

[118] BAJAJ, Piyush, Ryan SCHWELLER, Ali KHADEMHOSSEINI, Jennifer WEST a Rashid BASHIR. 3D Biofabrication Strategies for Tissue Engineering and Regenerative Medicine. *Annual Review of Biomedical Engineering* [online]. 2014, **16**(1), 247-276 [cit. 2018-02-10]. DOI: 10.1146/annurev-bioeng-071813-105155. ISSN 1523-9829. Dostupné z: http://www.annualreviews.org/doi/10.1146/annurev-bioeng-071813-105155

[119] ZHU, Ning a Xiongbiao CHE. Biofabrication of Tissue Scaffolds. *Advances in Biomaterials Science and Biomedical Applications* [online]. InTech, 2013 [cit. 2018-02-10]. DOI: 10.5772/54125. ISBN 978-953-51-1051-4. Dostupné z: http://www.intechopen.com/books/advances-in-biomaterials-science-and-biomedical-applications/biofabrication-of-tissue-scaffolds

[120] SUBIA, B., J. KUNDU a S. C. Biomaterial Scaffold Fabrication Techniques for Potential Tissue Engineering Applications. *Tissue Engineering* [online]. InTech, 2010 [cit. 2018-02-10]. DOI: 10.5772/8581. ISBN 978-953-307-079-7. Dostupné z: http://www.intechopen.com/books/tissue-engineering/biomaterial-scaffold-fabrication-techniques-for-potential-tissue-engineering-applications

[121] LI, Long, Guangliang ZHOU, Yi WANG, Guang YANG, Shan DING a Shaobing ZHOU. Controlled dual delivery of BMP-2 and dexamethasone by nanoparticle-embedded electrospun nanofibers for the efficient repair of critical-sized rat calvarial defect. *Biomaterials* [online]. 2015, **37**, 218-229 [cit. 2018-02-10]. DOI: 10.1016/j.biomaterials.2014.10.015. ISSN 01429612. Dostupné z: http://linkinghub.elsevier.com/retrieve/pii/S014296121401062X

[122] WU, Benjamin, Scott BORLAND, Russell GIORDANO, Linda CIMA, Emanuel SACHS a Michael CIMA. Solid free-form fabrication of drug delivery devices. *Journal of Controlled Release* [online]. 1996, **40**(1-2), 77-87 [cit. 2018]. DOI: 10.1016/0168-3659(95)00173-5. ISSN 01683659. Dostupné z: http://linkinghub.elsevier.com/retrieve/pii/0168365995001735

[123] CIMA, M.J., E. SACHS, L.G. CIMA a J. YOO. Computer-Derived Microstructures by 3D Printing: Bio- and Structural Materials. *SOLD FREEFORM FABRICATION - CONFERENCE-*. University of Texas, 1994, , 181-190.

[124] CHIA, Helena a Benjamin WU. Recent advances in 3D printing of biomaterials. *Journal of Biological Engineering* [online]. 2015, **9**(1), - [cit. 2018-02-10]. DOI: 10.1186/s13036-015-0001-4. ISSN 1754-1611. Dostupné z: http://www.jbioleng.org/content/9/1/4

[125] CASTRO, Nathan, Joseph O'BRIEN a Lijie ZHANG. Integrating biologically inspired nanomaterials and table-top stereolithography for 3D printed biomimetic osteochondral scaffolds. *Nanoscale* [online]. 2015, **7**(33), 14010-14022 [cit. 2018-02-10]. DOI: 10.1039/C5NR03425F. ISSN 2040-3364. Dostupné z: http://xlink.rsc.org/?DOI=C5NR03425F

[126] ZHANG, Shuguang, Fabrizio GELAIN a Xiaojun ZHAO. Designer self-assembling peptide nanofiber scaffolds for 3D tissue cell cultures. *Seminars in Cancer Biology* [online]. 2005, **15**(5), 413-420 [cit. 2018-02-10]. DOI: 10.1016/j.semcancer.2005.05.007. ISSN 1044579x. Dostupné z: http://linkinghub.elsevier.com/retrieve/pii/S1044579X05000325

[127] MA, Peter. Biomimetic materials for tissue engineering. *Advanced Drug Delivery Reviews* [online]. 2008, **60**(2), 184-198 [cit. 2018-02-10]. DOI: 10.1016/j.addr.2007.08.041. ISSN 0169409x. Dostupné z: http://linkinghub.elsevier.com/retrieve/pii/S0169409X07002979

[128] STUPP, Samuel. Self-Assembly and Biomaterials. *Nano Letters* [online]. 2010, **10**(12), 4783-4786 [cit. 2018-02-10]. DOI: 10.1021/nl103567y. ISSN 1530-6984. Dostupné z: http://pubs.acs.org/doi/abs/10.1021/nl103567y

[129] HARTGERINK, J. Self-Assembly and Mineralization of Peptide-Amphiphile Nanofibers. *Science* [online]. 2002, **294**(5547), 1684-1688 [cit. 2018-02-10]. DOI: 10.1126/science.1063187. ISSN 00368075. Dostupné z: http://www.sciencemag.org/cgi/doi/10.1126/science.1063187

[130] KYLE, Stuart, Amalia AGGELI, Eileen INGHAM a Michael MCPHERSON. Production of self-assembling biomaterials for tissue engineering. *Trends in Biotechnology* [online]. 2009, **27**(7), 423-433 [cit. 2018-02-10]. DOI: 10.1016/j.tibtech.2009.04.002. ISSN 01677799. Dostupné z: http://linkinghub.elsevier.com/retrieve/pii/S0167779909000936

[131] GEIGER, M. Collagen sponges for bone regeneration with rhBMP-2. *Advanced Drug Delivery Reviews* [online]. 2003, **55**(12), 1613-1629 [cit. 2017-12-01]. DOI: 10.1016/j.addr.2003.08.010. ISSN 0169409x. Dostupné z: http://linkinghub.elsevier.com/retrieve/pii/S0169409X03001856

[132] YUNUS BASHA, Rubaiya, Sampath T.S. a Mukesh DOBLE. Design of biocomposite materials for bone tissue regeneration. *Materials Science and Engineering: C* [online]. 2015, **57**, 452-463 [cit. 2017-12-01]. DOI: 10.1016/j.msec.2015.07.016. ISSN 09284931. Dostupné z: http://linkinghub.elsevier.com/retrieve/pii/S0928493115302010

[133] BAINO, Francesco, Giorgia NOVAJRA, Valentina MIGUEZ-PACHECO, Aldo BOCCACCINI a Chiara VITALE-BROVARONE. Bioactive glasses: Special

applications outside the skeletal system. *Journal of Non-Crystalline Solids* [online]. 2016, **432**, 15-30 [cit. 2017-12-01]. DOI: 10.1016/j.jnoncrysol.2015.02.015. ISSN 00223093. Dostupné z: http://linkinghub.elsevier.com/retrieve/pii/S0022309315000733

[134] MIGUEZ-PACHECO, Valentina, Larry HENCH a Aldo BOCCACCINI. Bioactive glasses beyond bone and teeth: Emerging applications in contact with soft tissues. *Acta Biomaterialia* [online]. 2015, **13**, 1-15 [cit. 2017-12-01]. DOI: 10.1016/j.actbio.2014.11.004. ISSN 17427061. Dostupné z: http://linkinghub.elsevier.com/retrieve/pii/S1742706114004966

[135] ANDRONESCU, E., G. VOICU, M. FICAI, I. MOHORA, R. TRUSCA a A. FICAI. Collagen/hydroxyapatite composite materials with desired ceramic properties. *Journal of Electron Microscopy* [online]. 2011, **60**(3), 253-259 [cit. 2017-11-10]. DOI: 10.1093/jmicro/dfr010. ISSN 0022-0744. Dostupné z: https://academic.oup.com/jmicro/article-lookup/doi/10.1093/jmicro/dfr010

[136] LICKORISH, David, John RAMSHAW, Jerome WERKMEISTER, Veronica GLATTAUER a C. HOWLETT. Collagen-hydroxyapatite composite prepared by biomimetic process. *Journal of Biomedical Materials Research* [online]. 2004, **68**(1), 19-27 [cit. 2017-11-10]. DOI: 10.1002/jbm.a.20031. ISSN 0021-9304. Dostupné z: http://doi.wiley.com/10.1002/jbm.a.20031

[137] Hydroxyapatite Ca5(OH)(PO4)3. In: *ChemTub3D* [online]. Liverpool: The University of Liverpool, b.r. [cit. 2017-12-09]. Dostupné z: http://www.chemtube3d.com/solidstate/SShydroxyapatite.htm

[138] RHO, Jae-Young, Liisa KUHN-SPEARING a Peter ZIOUPOS. Mechanical properties and the hierarchical structure of bone. *Medical Engineering & Physics* [online]. 1998, **20**(2), 92-102 [cit. 2017-11-10]. DOI: 10.1016/S1350-4533(98)00007-1. ISSN 13504533. Dostupné z: http://linkinghub.elsevier.com/retrieve/pii/S1350453398000071

[139] KANTHARIA, Nidhi, Sonali NAIK, Sanjay APTE, Mohit KHEUR, Supriya KHEUR a Bharat KALE. Nano-hydroxyapatite and its contemporary applications. *Journal of Dental Research and Scientific Development* [online]. 2014, **1**(1), 15- [cit. 2018-04-06]. DOI: 10.4103/2348-3407.126135. ISSN 2348-3407. Dostupné z: http://www.iadrsd.org/wp-content/journal/JDRSD_9_13R2.pdf

[140] WEGST, Ulrike, Hao BAI, Eduardo SAIZ, Antoni TOMSIA a Robert RITCHIE. Bioinspired structural materials. *Nature Materials* [online]. 2014, **14**(1), 23-36 [cit. 2017-12-10]. DOI: 10.1038/nmat4089. ISSN 1476-1122. Dostupné z: http://www.nature.com/doifinder/10.1038/nmat4089

[141] WEINER, S. a H. WAGNER. THE MATERIAL BONE: Structure-Mechanical Function Relations. *Annual Review of Materials Science* [online]. 1998, **28**(1), 271-298 [cit. 2017-11-10]. DOI: 10.1146/annurev.matsci.28.1.271. ISSN 0084-6600. Dostupné z: http://www.annualreviews.org/doi/10.1146/annurev.matsci.28.1.271

[142] HASSENKAM, Tue, Georg FANTNER, Jacqueline CUTRONI, James WEAVER, Daniel MORSE a Paul HANSMA. High-resolution AFM imaging of intact and fractured trabecular bone. *Bone* [online]. 2004, **35**(1), 4-10 [cit. 2017-11-10]. DOI: 10.1016/j.bone.2004.02.024. ISSN 87563282. Dostupné z: http://linkinghub.elsevier.com/retrieve/pii/S8756328204000869

[143] KE, Peng, Xiao-Ning JIAO, Xiao-Hui GE, Wei-Min XIAO a Bin YU. From macro to micro: structural biomimetic materials by electrospinning. *RSC Adv* [online]. 2014, **4**(75), 39704-39724 [cit. 2017-11-10]. DOI: 10.1039/C4RA05098C. ISSN 2046-2069. Dostupné z: http://xlink.rsc.org/?DOI=C4RA05098C

[144] PROSECKÁ, E., M. RAMPICHOVÁ, L. PLENCNER et al. Optimized conditions for mesenchymal stem cells to differentiate into osteoblasts on a collagen/hydroxyapatite matrix. *Journal of Biomedical Materials Research - Part A* [online]. 2011, **99**(2), 307-315 [cit. 2018-05-05]. DOI: 10.1002/jbm.a.33189. ISSN 15493296.

[145] PROSECKÁ, E., M. RAMPICHOVÁ, A. LITVINEC et al. Collagen/hydroxyapatite scaffold enriched with polycaprolactone nanofibers, thrombocyte-rich solution and mesenchymal stem cells promotes regeneration in large bone defect in vivo. *Journal of Biomedical Materials Research Part A* [online]. 2015, **103**(2), 671-682 [cit. 2018-05-05]. DOI: 10.1002/jbm.a.35216. ISSN 1549-3296.

[146] CALABRESE, Giovanna, Raffaella GIUFFRIDA, Claudia FABBI et al. Collagen-Hydroxyapatite Scaffolds Induce Human Adipose Derived Stem Cells Osteogenic Differentiation In Vitro. *PLOS ONE* [online]. 2016, **11**(3), 0151181- [cit. 2017-11-10]. DOI: 10.1371/journal.pone.0151181. ISSN 1932-6203. Dostupné z: http://dx.plos.org/10.1371/journal.pone.0151181

[147] KUNZLER, Tobias, Tanja DROBEK, Martin SCHULER a Nicholas SPENCER. Systematic study of osteoblast and fibroblast response to roughness by means of surface-morphology gradients. *Biomaterials* [online]. 2007, **28**(13), 2175-2182 [cit. 2017-11-10]. DOI: 10.1016/j.biomaterials.2007.01.019. ISSN 01429612. Dostupné z: http://linkinghub.elsevier.com/retrieve/pii/S0142961207000518

[148] SHEN, Xinyu, Li CHEN, Xuan CAI, Tong TONG, Hua TONG a Jiming HU. A novel method for the fabrication of homogeneous hydroxyapatite/collagen nanocomposite and nanocomposite scaffold with hierarchical porosity. *Journal of Materials Science: Materials in Medicine* [online]. 2011, **22**(2), 299-305 [cit. 2017-11-10]. DOI: 10.1007/s10856-010-4199-x. ISSN 0957-4530. Dostupné z: http://link.springer.com/10.1007/s10856-010-4199-x

[149] YUNOKI, S., T. IKOMA, A. MONKAWA, K. OHTA, M. KIKUCHI, S. SOTOME, K. SHINOMIYA a J. TANAKA. Control of pore structure and mechanical property in hydroxyapatite/collagen composite using unidirectional ice growth. *Materials Letters* [online]. 2006, **60**(8), 999-1002 [cit. 2017-11-25]. DOI: 10.1016/j.matlet.2005.10.064. ISSN 0167577x. Dostupné z: http://linkinghub.elsevier.com/retrieve/pii/S0167577X05010499

[150] CHAUHAN, Vijendra, Sansar SHARMA, Rajesh MAHESHWARI, Anil JUYAL, Shailendra RAGHUVANSHI a Sanjay BANSAL. Evaluation of hydroxyapatite and

beta-tricalcium phosphate mixed with bone marrow aspirate as a bone graft substitute for posterolateral spinal fusion. *Indian Journal of Orthopaedics* [online]. 2009, **43**(3), 234- [cit. 2017-11-25]. DOI: 10.4103/0019-5413.49387. ISSN 0019-5413. Dostupné z: http://www.ijoonline.com/text.asp?2009/43/3/234/49387

[151] HIRATA, M., H. MURATA, H. TAKESHITA, T. SAKABE, Y. TSUJI a T. KUBO. Use of purified beta-tricalcium phosphate for filling defects after curettage of benign bone tumours. *International Orthopaedics* [online]. 2006, **30**(6), 510-513 [cit. 2017-11-25]. DOI: 10.1007/s00264-006-0156-1. ISSN 0341-2695. Dostupné z: http://link.springer.com/10.1007/s00264-006-0156-1

[152] ARAHIRA, Takaaki a Mitsugu TODO. Effects of Proliferation and Differentiation of Mesenchymal Stem Cells on Compressive Mechanical Behavior of Collagen/β-TCP Composite Scaffold. *Journal of the Mechanical Behavior of Biomedical Materials* [online]. 2014, **39**, 218-230 [cit. 2017-11-25]. DOI: 10.1016/j.jmbbm.2014.07.013. ISSN 17516161. Dostupné z: http://linkinghub.elsevier.com/retrieve/pii/S1751616114002069

[153] MURAKAMI, Shusuke, Hirofumi MIYAJI, Erika NISHIDA et al. Dose effects of beta-tricalcium phosphate nanoparticles on biocompatibility and bone conductive ability of three-dimensional collagen scaffolds. *Dental Materials Journal* [online]. 2017, **36**(5), 573-583 [cit. 2017-11-25]. DOI: 10.4012/dmj.2016-295. ISSN 0287-4547. Dostupné z: https://www.jstage.jst.go.jp/article/dmj/36/5/36_2016-295/_article

[154] ELLIOTT, J. *Structure and chemistry of the apatites and other calcium orthophosphates*. New York: Elsevier, 1994. ISBN 9780444815828.

[155] ZHANG, Ming-Xing a Patrick KELLY. Crystallographic features of phase transformations in solids. *Progress in Materials Science* [online]. 2009, **54**(8), 1101-1170 [cit. 2017-11-20]. DOI: 10.1016/j.pmatsci.2009.06.001. ISSN 00796425. Dostupné z: http://linkinghub.elsevier.com/retrieve/pii/S0079642509000589

[156] BOHNER, M. Calcium orthophosphates in medicine: from ceramics to calcium phosphate cements. *Injury* [online]. 2000, **31**, 37-47 [cit. 2017-11-20]. DOI: 10.1016/S0020-1383(00)80022-4. ISSN 00201383. Dostupné z: http://linkinghub.elsevier.com/retrieve/pii/S0020138300800224

[157] DOROZHKIN, Sergey. Calcium orthophosphate cements for biomedical application. *Journal of Materials Science* [online]. 2008, **43**(9), 3028-3057 [cit. 2017-11-20]. DOI: 10.1007/s10853-008-2527-z. ISSN 0022-2461. Dostupné z: http://link.springer.com/10.1007/s10853-008-2527-z

[158] EHARA, A. Effects of α-TCP and TetCP on MC3T3-E1 proliferation, differentiation and mineralization. *Biomaterials* [online]. 2003, **24**(5), 831-836 [cit. 2017-12-10]. DOI: 10.1016/S0142-9612(02)00411-8. ISSN 01429612. Dostupné z: http://linkinghub.elsevier.com/retrieve/pii/S0142961202004118

[159] TAMAI, Masato, Ryusuke NAKAOKA a Toshie TSUCHIYA. Cytotoxicity of Various Calcium Phosphate Ceramics. *Key Engineering Materials* [online]. 2006, **309-311**,

263-266 [cit. 2017-11-20]. DOI: 10.4028/www.scientific.net/KEM.309-311.263. ISSN 1662-9795. Dostupné z: http://www.scientific.net/KEM.309-311.263

[160] YOO, Jeong, Kang LEE a Soo LEE. The Analysis of Osteoconducting Ability of Alpha-Tricalcium Phosphate-Based Bone Filler Powder. *Key Engineering Materials* [online]. 2006, **309-311**, 259-262 [cit. 2017-11-20]. DOI: 10.4028/www.scientific.net/KEM.309-311.259. ISSN 1662-9795. Dostupné z: http://www.scientific.net/KEM.309-311.259

[161] WILTFANG, J., H. MERTEN, K. SCHLEGEL, S. SCHULTZE-MOSGAU, F. KLOSS, S. RUPPRECHT a P. KESSLER. Degradation characteristics of ? and ? tri-calcium-phosphate (TCP) in minipigs. *Journal of Biomedical Materials Research* [online]. 2002, **63**(2), 115-121 [cit. 2017-11-20]. DOI: 10.1002/jbm.10084. ISSN 0021-9304. Dostupné z: http://doi.wiley.com/10.1002/jbm.10084

[162] SLOVIKOVÁ, Alexandra, Lucy VOJTOVÁ a Josef JANČAŘ. Preparation and modification of collagen-based porous scaffold for tissue engineering. *Chemical Papers* [online]. Heidelberg: SP Versita, 2008, **62**(4), 417-422 [cit. 2018-05-05]. DOI: 10.2478/s11696-008-0045-8. ISSN 0366-6352.

[163] SANG, Lin, Dongmei LUO, Songmei XU, Xiaoliang WANG a Xudong LI. Fabrication and evaluation of biomimetic scaffolds by using collagen–alginate fibrillar gels for potential tissue engineering applications. *Materials Science and Engineering: C* [online]. 2011, **31**(2), 262-271 [cit. 2018-04-13]. DOI: 10.1016/j.msec.2010.09.008. ISSN 09284931. Dostupné z: http://linkinghub.elsevier.com/retrieve/pii/S0928493110002262

[164] Phosphate-buffered saline (PBS). *Cold Spring Harbor Protocols* [online]. 2010, **2006**(1), 8247- [cit. 2018-04-13]. DOI: 10.1101/pdb.rec8247. ISSN 1940-3402. Dostupné z: http://www.cshprotocols.org/lookup/doi/10.1101/pdb.rec8247

[165] BAUER, E. A., T. W. COOPER, J. S. HUANG, J. ALTMAN a T. F. DEUEL. Stimulation of in vitro Human Skin Collagenase Expression by Platelet-Derived Growth Factor. *Proceedings of the National Academy of Sciences of the United States of America* [online]. National Academy of Sciences of the United States of America, 1985, **82**(12), 4132-4136 [cit. 2018-04-13]. DOI: 10.1073/pnas.82.12.4132. ISSN 00278424.

[166] CLARK, I. M., L. K. POWELL, S. RAMSEY, B. L. HAZLEMAN a T. E. CAWSTON. *The measurement of collagenase, tissue inhibitor of metalloproteinases (timp), and collagenase—timp complex in synovial fluids from patients with osteoarthritis and rheumatoid arthritis* [online]. 1993, **36**(3), 372-379 [cit. 2018-04-13]. ISSN 00043591. Dostupné z: http://doi.wiley.com/10.1002/art.1780360313

[167] TIHAN, Graţiela Teodora, Ileana RăU, Roxana Gabriela ZGâRIAN a Mihaela Violeta GHICA. Collagen-based biomaterials for ibuprofen delivery. *Comptes Rendus Chimie* [online]. 2016, **19**(3), 390-394 [cit. 2018-04-13]. DOI: 10.1016/j.crci.2015.09.008. ISSN 16310748. Dostupné z: http://linkinghub.elsevier.com/retrieve/pii/S1631074815002398

[168] ISO 13314. *Mechanical testing of metals - Ductility testing - Compression test for porous and cellular metals*. 1. London: IHS, 2011.

[169] AMIN YAVARI, S., R. WAUTHLE, J. VAN DER STOK et al. Fatigue behavior of porous biomaterials manufactured using selective laser melting. *Materials Science & Engineering C* [online]. Elsevier B.V, 2013, **33**(8), 4849-4858 [cit. 2018-04-12]. DOI: 10.1016/j.msec.2013.08.006. ISSN 0928-4931.

[170] AHMADI, S.M., G. CAMPOLI, S. AMIN YAVARI, B. SAJADI, R. WAUTHLE, J. SCHROOTEN, H. WEINANS a A.A. ZADPOOR. Mechanical behavior of regular open-cell porous biomaterials made of diamond lattice unit cells. *Journal of the Mechanical Behavior of Biomedical Materials* [online]. Elsevier Ltd, 2014, **34**(), 106-115 [cit. 2018-04-12]. DOI: 10.1016/j.jmbbm.2014.02.003. ISSN 1751-6161.

[171] LIN, Yung Kai a Deng Cheng LIU. Comparison of physical–chemical properties of type I collagen from different species. *Food Chemistry* [online]. Elsevier Ltd, 2006, **99**(2), 244-251 [cit. 2018-04-19]. DOI: 10.1016/j.foodchem.2005.06.053. ISSN 0308-8146.

[172] MURPHY, Ciara M., Matthew G. HAUGH a O. The effect of mean pore size on cell attachment, proliferation and migration in collagen–glycosaminoglycan scaffolds for bone tissue engineering. *Biomaterials* [online]. Elsevier Ltd, 2010, **31**(3), 461-466 [cit. 2018-04-20]. DOI: 10.1016/j.biomaterials.2009.09.063. ISSN 0142-9612.

[173] KEAVENY, T.M., E.F. MORGAN, G.L. NIEBUR a O.C. YEH. Biomechanics of trabecular bone. *Annual Review of Biomedical Engineering* [online]. 2001, **3**(1), 307-333 [cit. 2018-04-21]. DOI: 10.1146/annurev.bioeng.3.1.307. ISSN 15239829.

[174] VENUGOPAL, J, Sharon LOW, Aw CHOON, A KUMAR a S RAMAKRISHNA. Electrospun-modified nanofibrous scaffolds for the mineralization of osteoblast cells. *Journal of Biomedical Materials Research Part A* [online]. 2008, **85**(2), 408-417 [cit. 2018-04-25]. DOI: 10.1002/jbm.a.31538. ISSN 1549-3296.

[175] RIZK, Moustafa A. a Nasser Y. MOSTAFA. Extraction and Characterization of Collagen from Buffalo Skin for Biomedical Applications. *Oriental Journal of Chemistry* [online]. 2016, **32**(3), 1601-1609 [cit. 2018-04-25]. DOI: 10.13005/ojc/320336. ISSN 0970020X. Dostupné z: http://www.orientjchem.org/vol32no3/extraction-and-characterization-of-collagen-from-buffalo-skin-for-biomedical-applications/

[176] KOZŁOWSKA, J. a A. SIONKOWSKA. Effects of different crosslinking methods on the properties of collagen–calcium phosphate composite materials. *International Journal of Biological Macromolecules* [online]. Elsevier B.V, 2015, **74**, 397-403 [cit. 2018-04-25]. DOI: 10.1016/j.ijbiomac.2014.12.023. ISSN 0141-8130.

[177] PANDA, Niladri Nath, Sriramakamal JONNALAGADDA a Krishna PRAMANIK. Development and evaluation of cross-linked collagen-hydroxyapatite scaffolds for tissue engineering. *Journal of Biomaterials Science, Polymer Edition* [online]. Routledge, 2013, , 1-14 [cit. 2018-04-25]. DOI: 10.1080/09205063.2013.822247. ISSN 0920-5063.

[178] Infračervená spektrometrie: Infračervená spektrometrie - Tabulky. In: *Ústav analytické chemie VŠCHT Praha* [online]. Praha: VŠCHT Praha, b.r. Dostupné také z: http://old.vscht.cz/anl/dolensky/uvodstrukturyleciva/soubory/05_UvDoStAnFaLa_IR_Tabulky.pdf

[179] BERZINA-CIMDINA, Liga a Natalija BORODAJENKO. Research of Calcium Phosphates Using Fourier Transform Infrared Spectroscopy. *Infrared spectroscopy - materials science, engineering and technology* [online]. Rijeka: InTech, 2012, s. 123-148. ISBN 9789535105374.

[180] ANTONIAC, I., M. D. VRANCEANU, A. ANTONIAC a M. G. ALBU. The influence of the ceramic phase on the structure of resorbable biocomposites based on collagen. In: *E-Health and Bioengineering Conference (EHB), 2011* [online]. IEEE Publishing, 2011, s. 1-4 [cit. 2018-04-24]. ISBN 978-1-4577-0292-1.

[181] REUSCH, William. Infrared Spectroscopy. *Michigan State University* [online]. Michigan: Michigan State University, b.r. Dostupné také z: https://www2.chemistry.msu.edu/faculty/reusch/virttxtjml/spectrpy/infrared/infrared.htm

[182] SALIMI, Esmael a Jafar JAVADPOUR. Synthesis and Characterization of Nanoporous Monetite Which Can Be Applicable for Drug Carrier. *Journal of Nanomaterials* [online]. 2012, **2012**, 1-5. DOI: 10.1155/2012/931492. ISSN 1687-4110. Dostupné také z: http://www.hindawi.com/journals/jnm/2012/931492/

8 List of Figures

9 LIST OF TABLES

10 List of Abbreviations

3D	three-dimensional
3DP	three-dimensional printing
AGEs	advanced glycation end-products
ATR-FTIR	atenuated total reflection infrared spectroscopy
BCP	biphasic calcium phosphate
BMP2	bone morphogenetic protein 2
CAD	computed-aided design
DHT	dehydrothermal treatment
DS	dermatan sulphate
dsDNA	double stranded deoxyribonucleic acid
ECM	extracellular matrix
EDC	N-ethyl-N′-[3–dimethylaminopropyl] carbodiimide chloride
EMS	embryonic stem cells
FACITs	fibril-associated collagens with interrupted triple helices
FBS	fetal bovine serum
FGF-2	fibroblast growth factor 2
GAG	glycosaminoglycan
GFs	growth factors
HA	hyaluronic acid
HAp	hydroxyapatite
Hep	heparin
HS	heparan sulphate
iPS	induced pluripotent cells
KS	keratan sulphate
MACITs	membrane-associated collagens with interrupted triple helices
mRNA	messenger ribonucleic acid
MSCs	mesenchymal stem cells
MULTIPLEXINs	multiple triple-helix domains and interruptions
nano-HAp	nano-hydroxyapatite
NHS	N-hydroxy succinimide
NS	normal saline solution
OCP	octacalcium phosphate
PBS	phosphate-buffered saline
RunX2	runt-related transcription factor 2
SBF	simulated body fluid
SEM	scanning electron microscope
s-HA	high temperature sintered hydroxyapatite
TCPs	tricalcium phosphates
TE	tissue engineering
TGFβ	transforming growth factor beta
TTCP	tetracalcium phosphate
u-HA	high temperature sintered hydroxyapatite

UV	ultra-violet wavelengths
W	energy of absorption
W_e	energy absorption efficiency
α-MEM	alpha-minimal essential medium
α-TCP	α-tricalcium phosphate
β-TCP	β-tricalcium phosphate
ε	compressive strain
ε_0	upper limit of the compressive strain
σ	compressive stress
σ_0	upper limit of the compressive stress
σ_{pl}	plateau stress